Chem Soc Rev

REVIEW ARTICLE

View Article Online
View Journal | View Issue

Cite this: *Chem. Soc. Rev.*, 2025, **54**, 8345

Advances in the bioapplications of ionic pillararenes

Ziyan Shen, †[a] Shuang Chao, †[ac] Luling Wu, [b] Huanyu Liu,[a] Yuxin Pei, *[a] Tony D. James *[bd] and Zhichao Pei *[ac]

The biological arena provides a wide range of challenges requiring cutting-edge developments, from the exploration of complex mechanisms within organisms, to the interactions between organisms and the environment, as well as the detection and analysis of bioactive substances, early disease diagnosis and precision treatment, and the research, development, and application of biomaterials. Solving these problems is of great significance for improving public health standards and promoting the innovation of medical technologies. Supramolecular chemistry, as an emerging interdisciplinary discipline, provides unique perspectives and research methods for overcoming these challenges. Ionic pillararenes (IPAs), as an emerging supramolecular tool, possess unique advantages due to their ionic properties. This enables them to show great potential in solving problems in the biological field, such as deciphering the mechanisms of transmembrane transport, precisely recognizing and sensing biomolecules, and achieving efficient disease diagnosis and treatment. This review article summarizes the application progress of IPAs in the biological field, providing a theoretical basis for the further development of novel biological application technologies and the design of more efficient biological solutions. This review also delves deeply into the challenges and opportunities faced by IPAs for biological applications. As well as offering comprehensive and in-depth insights into IPAs, that we hope will encourage researchers in related fields to conduct innovative and practical research using IPAs.

Received 11th March 2025

DOI: 10.1039/d4cs00458b

rsc.li/chem-soc-rev

[a] College of Chemistry & Pharmacy, Northwest A&F University, Yangling, Shaanxi 712100, P. R. China. E-mail: peiyx@nwafu.edu.cn, peizc@nwafu.edu.cn
[b] Department of Chemistry, University of Bath, Bath, BA2 7AY, UK. E-mail: t.d.james@bath.ac.uk
[c] College of Plant protection, Northwest A&F University, Yangling, Shaanxi 712100, P. R. China
[d] School of Chemistry and Chemical Engineering, Henan Normal University, Xinxiang, 453007, P. R. China
† These authors contributed equally to this work.

1. Introduction

The biological domain represents a vast expanse replete with challenges and opportunities, housing a multitude of critical issues demanding urgent resolution. These issues span not only the exploration of intricate mechanisms within organisms, such as fundamental biological processes including cell signalling, gene expression regulation, protein folding, and function,

Ziyan Shen

Ziyan Shen is a postdoctoral research fellow at Northwest A&F University. She received her BS degree from Nanjing Normal University in 2017, and MS degree and PhD degree from Northwest A&F University in 2020 and 2025, respectively. Her current research interests are in designing and synthesizing novel ionic pillararenes, preparation and bioactivity evaluation of supramolecular nanomedicines.

Shuang Chao

Shuang Chao is a postdoctoral research fellow at Northwest A&F University. He obtained his PhD degree and BS degree from Northwest A&F University in 2022 and 2018, respectively. His research interests include the synthesis and assembly of functionalized pillararenes, host–guest chemistry, and targeted drug delivery.

but also encompass the complex interplay between organisms and their environment, including the responses and metabolic adaptations of organisms to environmental pollution, as well as the profound influence of environmental factors on biodiversity.[1–4] Additionally, current research frontiers include the detection and analysis of bioactive substances, early-stage disease diagnosis and precision therapeutics, and the research, development, and application of biomaterials.[5–9] Advancements in these areas hold great importance for enhancing public health standards and propelling the innovation of medical technologies. In the face of these complex problems, there is an acute need for innovative research tools and methodologies to offer novel perspectives and solutions.

Supramolecular chemistry, an emerging interdisciplinary discipline, furnishes unique research vantage points and approaches for surmounting these challenges.[10–14] Originating from in-depth investigations into weak intermolecular interactions, the concept of supramolecular chemistry was first introduced by Jean-Marie Lehn.[15,16] This breakthrough shattered the traditional chemical paradigm that solely focused on covalent bonds, thereby inaugurating the study of complex systems formed through non-covalent intermolecular interactions, such as hydrogen bonds, van der Waals forces, and electrostatic interactions.[17–21] The development of supramolecular chemistry is intricately intertwined with that of macrocyclic compounds, including crown ethers,[22–24] cyclodextrins,[25–28] calixarenes,[29–32] cucurbiturils,[33–35] and pillararenes.[36–38] These compounds provide a rich foundational framework for constructing functional supramolecular systems, not only expanding the frontiers of materials science but also proffering novel solutions to the problems encountered in the biological domain.[39–45]

Pillararenes, as a new generation of macrocyclic molecules in the field of supramolecular chemistry, have attracted much attention due to their unique advantages in structural design and functional expansion.[37,46–48] The molecular skeleton of pillararenes is symmetrically connected by repeated 1,4-dimethoxybenzene units through methylene bridges at the 2,5 positions, forming a regular rigid columnar structure.[49–52] This structural characteristic endows pillararenes with two core

Luling Wu

Luling Wu is an incoming tenure-track assistant professor at Nanjing University. From 2023 to 2025, he was an EPSRC postdoctoral research fellow at the University of Bath, and from 2022 to 2023 he served as a postdoctoral research fellow at Westlake University. He earned his PhD in 2021 with support from the China Scholarship Council and the University of Bath.

Huanyu Liu

Huanyu Liu is pursuing her MS degree at Northwest A&F University. She obtained her BS degree from Baoji University of Arts and Sciences in 2023. Her research interests include multifunctional supramolecular assembly, supramolecular chemistry, and targeted drug delivery.

Yuxin Pei

Yuxin Pei did her PhD in 1998 in materials science at China Textile University (Donghua University at present) in Shanghai. After a two-year postdoctoral training at Zhejiang University, she moved to Europe and worked as a postdoctoral fellow at Lund University, Royal Institute of Technology, Technical University of Denmark, and Heidelberg University. Since 2010, she has been a professor of Chemistry at the College of Science (College of Chemistry and Pharmacy at present), Northwest A&F University. Her current research interests are functional supramolecular nanomaterials for biological and medicinal applications.

Tony D. James

Tony D. James is a professor at the University of Bath and Fellow of the Royal Society of Chemistry. He was a Royal Society University Research Fellow (1995–2000), Wolfson Research Merit Award holder (2017–2022) and was awarded the Daiwa-Adrian Prize (2013), the CASE Prize (2015), the MSMLG Czarnik Award (2018) and Frontiers in Chemistry Diversity Award. (2020). His research interests include many aspects of Supramolecular chemistry, including probes for redox imbalance and theranostic systems. His h-index is 99 (Google Scholar) and has been listed as a highly cited researcher in chemistry since 2022.

features: firstly, the ability to precisely regulate the cavity. By adjusting the number of benzene ring units (such as pillar[5]arene, pillar[6]arene, pillar[7]arene, *etc.*), the rigid electron-rich cavity can achieve dynamic adjustment of the pore size. Moreover, it can realize efficient recognition of various guests through cation–π interactions, π–π stacking, and hydrophobic effects, providing a structural basis for the precise construction of complex host–guest systems.[53–57] Secondly, it contains appropriate modification sites enabling efficient modular design. The upper-rim and lower-rim of pillararenes act as the main modification sites. Without the need for complex protecting group strategies, targeted ligands (such as glycosyl groups and peptides) or responsive groups (such as pH-sensitive carboxylic acids and photo-responsive azobenzenes) can be introduced in one step through reactions such as click chemistry or condensation reactions. The precise utilization of these symmetric sites makes the functionalization process both simple and controllable.[58–61] These characteristics, of structural tunability and functional integration, establish a link between molecular recognition and material construction, offering novel approaches for the innovative design of supramolecular systems in areas such as intelligent diagnosis and treatment vectors, as well as for environmentally-responsive materials.

Among the numerous pillararene derivatives, ionic pillararenes (IPAs) distinguish themselves by their unique properties. By incorporating charged groups, such as positively charged imidazolium salts, ammonium salts, and guanidinium salts, as well as negatively charged carboxylates, phosphates, and sulfonates, onto the rims of pillararenes, a series of anionic, cationic, and zwitterionic pillararenes can be synthesized (Fig. 1). The introduction of ionic groups confers several advantages to IPAs: (I) Solubility: the incorporation of ionic groups substantially enhances the solubility of IPAs in polar solvents, such as water.[62–64] (II) Dispersibility: ionic groups increase the electrostatic repulsion between molecules, thereby reducing the tendency for aggregation in solution and facilitating the formation of stable nanostructures.[65] (III) Biocompatibility: through rational design of the ionic groups, IPAs can exhibit low cytotoxicity and favorable biocompatibility.[66] (IV) Amphiphilicity: the amphiphilic nature of IPAs, characterized by both hydrophilic and hydrophobic moieties, enables them to adapt to complex biological environments. This property allows them to exist stably in both aqueous and lipid-based environments and interact with biomolecules with diverse properties.[67–71] (V) Self-assembly ability: owing to the presence of ionic groups, IPAs can self-assemble into various nanostructures, such as micelles and vesicles, in solution through multiple interactions, including electrostatic forces, van der Waals forces, and hydrogen bonds.[36,70,72,73] (VI) Host–guest recognition ability: ionic groups can participate in the host–guest recognition process *via* electrostatic interactions, forming strong electrostatic attractions with guest molecules of opposite charge. This significantly broadens the range of recognizable guests, enabling IPAs to recognize not only neutral molecules but also ionic guests selectively.[74–80] (VII) High controllability: the structure and properties of IPAs can be precisely tailored by modulating the type, number, and position of the ionic groups, as well as through the modification of other functional groups. This confers IPAs with enhanced selectivity towards guest molecules of different sizes, shapes, and charges, rendering them suitable for the separation and detection of specific ions or molecules. (VIII) Stability: the addition of ion–ion, ion–dipole, and other interactions significantly increases the binding constant between the host and guest, thereby enhancing the stability of the formed host–guest complexes. (IX) Stimuli-responsiveness: IPAs exhibit sensitivity to environmental stimuli, such as pH and ionic strength, with their structure or function undergoing changes under specific environmental conditions. This property is advantageous for the development of tumor-targeted drug delivery systems and intelligent sensing platforms.[81–86] (X) Ion conductivity: the ionic groups in IPAs allow their assemblies to form ion-conducting channels, which significantly improve the specificity and sensitivity of IPA-based electrochemical biosensors for target analyte detection.[87–89] (XI) Biological activity: certain cationic pillararenes exhibit strong electrostatic interactions with cell membranes, bacterial cell membranes, or bacterial biofilms, and do not induce drug resistance. These properties endow them with unique biological activities in anti-cancer and anti-bacterial applications.[90,91] (XII) Multifunctionality: IPAs possess a remarkable ability to integrate multiple functions, making them ideal components for constructing intelligent responsive materials and high-performance detection and sensing platforms.[92–96]

In recent years, an increasing number of researchers have recognized the structural advantages of IPAs and employed them as vital molecular tools to address a series of complex and pivotal issues in biological fields. These include the elucidation of the mechanisms underlying transmembrane transport, the investigation of biomolecular interactions, the recognition and sensing of bioactive substances, disease diagnosis and

Zhichao Pei

Prof. Zhichao Pei obtained his PhD degree in Chemistry from the KTH Royal Institute of Technology (Sweden) in 2006 under the supervision of Prof. Olof Ramstrom. From 2007 to 2010, he was a senior researcher and R&D manager of biochip at Attana AB in Sweden. Since 2010, he has been a chair professor at College of Chemistry and Pharmacy (Former College of Science), Northwest A&F University. He was selected as a specialist of "Hundred-talent Program" of Shaanxi Province, China in 2012. His current research interests include organic supramolecular chemistry, organic–inorganic hybrid nanomaterials, drug delivery and biosensors.

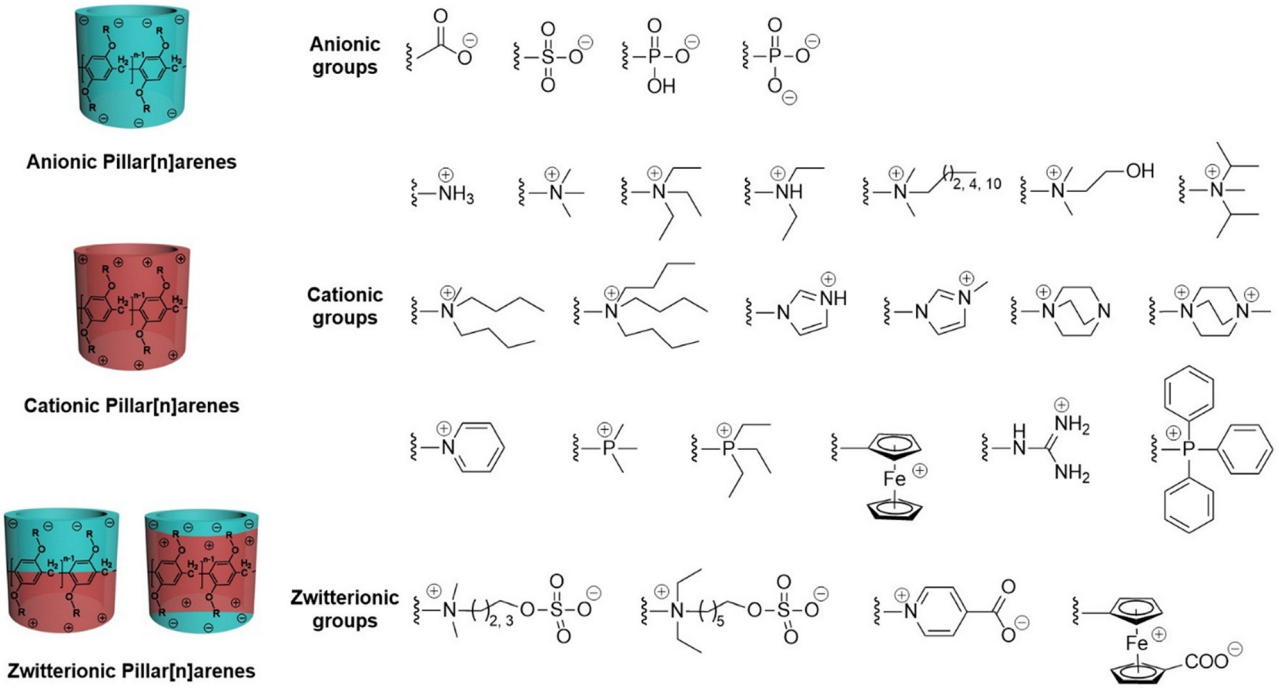

Fig. 1 The schematic of various types of IPAs and structures of typical anionic, cationic, and zwitterionic functional groups.

treatment, precise bioimaging, the control of drug-resistant bacteria, as well as environmental monitoring and pollutant remediation. To date, numerous review articles have been published regarding the biological applications of pillararenes.[97–104] However, a systematic review comprehensively detailing the significance of IPAs in biological applications remains lacking. Given the unparalleled advantages of IPAs in biological applications, there is an urgent need to conduct a comprehensive review of the research progress which was our inspiration for this review. We anticipate that this review will provide guidance for future drug development, the design of precision treatment strategies, and the innovation of biotechnologies, thereby facilitating the development of more efficient and personalized application outcomes. Additionally, we anticipate that our review will inspire and stimulate extensive and in-depth applications of high-performance supramolecular structures, such as IPAs, as powerful molecular tools in biological research and other interdisciplinary fields. In this review, we will also elaborate on how IPAs, as molecular tools, address life-science problems, with a focus on artificial channels, electrochemical biosensors, fluorescent sensing and bioimaging, supramolecular antidotes, antimicrobial activity, cancer treatment, and other aspects, including nucleic acid/protein transport, protein adsorption and separation, artificial enzymes, treatment of diseases such as Alzheimer's and diabetes, cell fusion, and communication. Furthermore, we will delve into the challenges faced by IPAs in biological applications and provide insights into future research directions. It's our hope that this review will offer valuable perspectives for the further development of IPAs into more potent molecular tools, thereby promoting their widespread application and far-reaching impact in the fields of human health, food safety, and ecological conservation.

2. Artificial channels from IPAs

Lipid bilayer membranes function as an important natural barrier separating living cells from the outside environment. Membrane proteins are responsible for processing the input and output of ions or molecules, sensing stimuli and transmitting signals, and performing important roles in the transfer of substances and exchange of information inside and outside the cell. Dysregulation in the functionality of these transmembrane transport proteins is closely associated with various diseases commonly referred to as channelopathies. Inspired by the diverse functions of membrane proteins, chemists have dedicated substantial effort to construct synthetic mimics, aiming to comprehend their transport mechanisms, produce materials for separation, and advance therapeutic drug development.

In natural biological systems, the efficient realization of transmembrane channels is based on the precise coupling of structure and function: (I) ion channels require a strict match between the pore diameter and the ionic radius, and an electrostatic screening layer is constructed through the directional enrichment of negatively charged groups (such as carboxylic acid and phosphate groups) to achieve the selective permeation of ions; (II) aquaporins (AQPs) rely on the synergistic effect between the hydrophilic inner wall of the pore (where the main chain carbonyl groups form a hydrogen bond network) and the nanoscale confined space. With the help of the "proton insulation" structure constructed by the aromatic ring

array, they can achieve rapid transmembrane transport of water molecules and repel ionic interferences; (III) molecular/protein channels depend on the specific recognition function of the modified groups, and at the same time, they mediate the binding-release process of substrates through the conformational dynamic regulation of the flexible domains. The functional mechanisms of the above biological channels requires three core elements to be present in the design of artificial channels: a rigid framework to support and stabilize the pore conformation, tunable functional groups to respond to substrate properties, and environmentally sensitive sites to achieve transport regulation.

With extensive development of supramolecular chemistry, multi-molecular self-assembly or single-molecule strategies based on macrocyclic molecules have made remarkable progress in the construction of artificial transmembrane channels. Following on from crown ethers, cyclodextrins, calixarenes, and cucurbiturils, pillararenes, with their highly symmetric rigid columnar framework (providing stable support for the pore structure) and para-modular modification sites (which can introduce ionic coordination groups, hydrophilic functional segments, or stimuli-responsive units), have unique advantages in simulating the precise transport functions of natural channels. Especially IPAs, due to their inherent charge characteristics and tunable cavity structure, have become an ideal molecular platform for mimicking charged ion channel proteins, achieving specific substance transport, or for the construction of controllable gated nanoscale channels. This section will systematically elaborate on the molecular design strategies for IPA-based biomimetic channels and explore their application in key scientific issues such as ion selective transport and responsive gating mechanisms.

2.1. Tubular unimolecular channels

Tubular unimolecular transmembrane channels are transmembrane channels formed by tubular molecules directly inserted into the cellular phospholipid bilayer. The tubular-styled structural feature of pillararenes, along with tunable side chains, promotes the formation of artificial channels. These channels facilitate the transport of small molecules and ions, enabling a better understanding of transport mechanisms. Recently, multiple new pillar[*n*]arene derivatives have been successfully applied as unimolecular channels for the selective transport of ions and water. In particular, IPAs-based unimolecular channels enable selective transmembrane transport of specific ions due to their high selectivity for ions.

2.1.1. Tubular unimolecular ion channels. Hou's group reported an anionic pillar[5]arene modified with dihydrogen phosphate groups, which can ionize to produce negative charges under physiological conditions. Meanwhile, the molecular length of 3.5 nm and the alternating design of D-Phe and L-Trp on the side chain ensures that the molecule can be inserted into a phospholipid bilayer stably and accurately. The results of the study indicate that the artificial channels can effectively incorporate into the lipid bilayer under low concentration conditions. The channel is highly NH_4^+/K^+ selective due to electrostatic and hydrogen bonding interactions between NH_4^+ and the terminal dihydrogen phosphate group.[105]

Transmembrane potential is responsible for performing a variety of important metabolic and signalling functions in biological systems. The natural K^+ channel is a typical voltage-gated ion channel that possesses a unique transmembrane segment, the S4 domain, which contains four to eight positively charged Arg units. Under an electric field, the S4 domain can move across the cell membranes, leading to the switching on and off of channels. On this basis, Hou's group introduced positively charged L-Arg into different positions of the side chains of the previously reported pillararene-based transmembrane channels (1a) to prepare cationic artificial channels (Fig. 2a). The results of patch-clamp experiments indicated that 1b could be inserted into a bilayer in the presence of different negative potentials. Simultaneously, the channel molecule 1b was dragged-out from the bilayer as the positive potential gradually increased. This study successfully demonstrates a voltage-driven reversible insertion/extraction mechanism of cationic channel compounds into/out of lipid bilayers, enabling precise control over transmembrane ion transport in artificial channels. Notably, one designed molecule exhibits antibacterial activity against *Bacillus subtilis* with an IC_{50} value comparable to natural channel-forming peptides, highlighting its potential as a novel antimicrobial agent.[106] Alamethicin, a dipolar naturally occurring peptide, can flip and arrange itself in bilayers driven by voltage, resulting in voltage-gating behavior of its channels. Hou's group constructed an amphipathic ion artificial transmembrane channel by mimicking the alamethicin channel. The channel molecules can flip in the lipid bilayer driven by voltage to form a directional arrangement (Fig. 2b). The aligned channel molecules produce rectification behavior and mediate directed ion transport. Such research provides paradigms for designing artificial biomimetic voltage-gated ion channels based on IPAs.[107]

Gramicidin A (GA), a lipophilic pentadecapeptide composed of alternating D- and L-amino acids, has been shown to form a β-helical cation channel within membranes. Xin and colleagues modified GA on pillar[5]arene and replaced the D-leucine residue of GA with either a D-arginine or D-aspartic acid residue, resulting in two types of ionic IPAs. Experiments indicated that the charge status of the peptide modules of these channels has a significant impact on their membrane incorporation ability and transport properties. The GA-based pillararene with D-aspartic acid residue exhibited stronger K^+ transport efficiency.[108]

2.1.2. Tubular unimolecular water channels. AQPs are critical membrane proteins responsible for regulating cellular osmotic pressure through selective water transport. Loss-of-function mutations in AQPs have been linked to severe diseases including congenital cataracts and nephrogenic diabetes insipidus. Inspired by the cationic selectivity filter of AQP1, Hou's group designed a cationic pillar[5]arene-based channel 1 featuring positively charged amino groups at both termini. To systematically evaluate the impact of charge distribution on

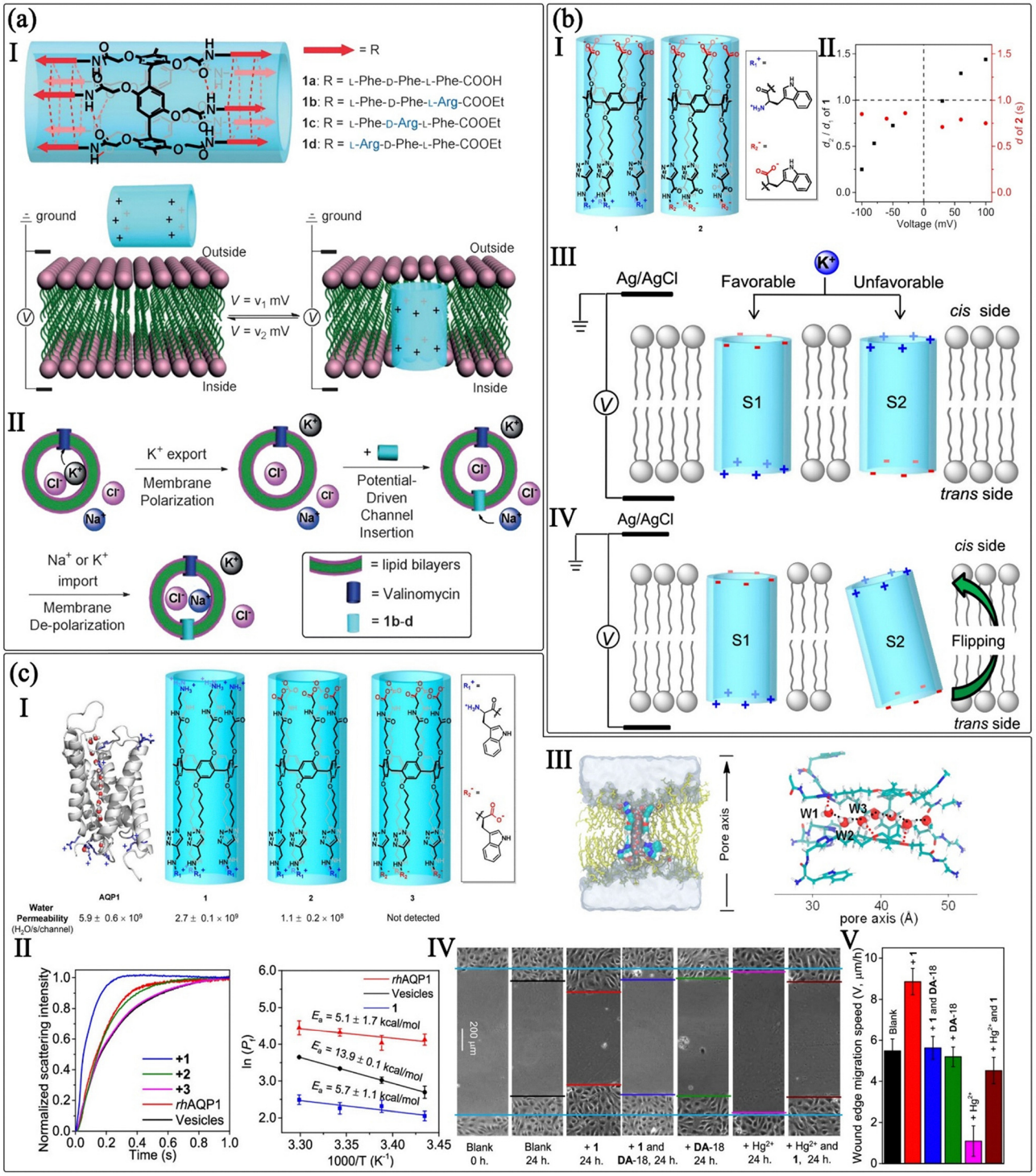

Fig. 2 Tubular unimolecular ion channels and water channels based on IPAs. (a) Structure of channels 1a–d and the schematic presentation for the voltage-driven channel inserting into and leaving lipid bilayer (I). The schematic presentation of the membrane polarization induced by the valinomycin mediated K^+ exportation and subsequent depolarization induced by the potential-driven 1a–d insertion into the bilayer (II) (Reproduced with permission from ref. 106. Copyright 2014, John Wiley & Sons, Inc.). (b) Chemical structures of channels 1 and 2 (I). Analysis of opening durations of channels 1 (black squares) and 2 (red dots) under various voltages (II). The schematic presentation of voltage-driven K^+ flowing through channel 1 with different orientations (III). The schematic presentation of the voltage-driven flipping of channel molecules in the bilayer (IV) (Reproduced with permission from ref. 107. Copyright 2021, American Chemical Society). (c) Structures and water permeability of natural aquaporin (AQP1, PDB#: 1J4N) and artificial channels 1–3 (I). SFLS traces performed with lipid vesicles in the presence of 1–3 (0.5%, molar ratio relative to lipid (mRL)) and *rh*AQP1 (1% w/w, protein to lipid) after exposure to a hypertonic solution containing 100 mM KCl, and Arrhenius plots for the determination of E_a of 1 and *rh*AQP1 (II). MD simulations of water transport through 1 (III). Wound healing analysis of HUVECs monolayers. Representative images of the cell assays showing wound edges (solid lines) at 0 h and 24 h in the presence of 1(1.0 μM), DA-18 (5.0 μM) and Hg^{2+} (10 μM) (IV) and the wound edge migration speed (V) (Reproduced with permission from ref. 109. Copyright 2020, American Chemical Society).

water permeability, zwitterionic channel 2 and anionic channel 3 were synthesized as control compounds. Tryptophan (Trp) residues were incorporated into the channel structure to facilitate spontaneous membrane insertion, as confirmed by fluorescence microscopy. Functional studies revealed that channel 1 exhibits water permeability (1.2×10^{10} H_2O per s per channel) and ion exclusion efficiency comparable to human AQP1 (Fig. 2c). Meanwhile, channel 1 restored wound healing in AQP-deficient cells by re-establishing osmotically driven water transport, providing a novel therapeutic strategy for AQP-related disorders.[109]

Andrei *et al.* designed several pillar[5]arenes with different structures, including rim-differentiated peralkyl-carboxylate-pillar[5]arene (A), peralkylamino-substituted pillar[5]arene (B), percarboxylate-pillar[5]arene (C) and peralkene-carboxylate-pillar[5]arene (D). They studied the water permeation properties of these pillar[5]arenes and found that the water permeability of structures C and D when inserted into bilayer membranes was 3–4 times higher than that of A and B, and they could transport about 10^7–10^8 water molecules per s per channel, indicating that they had similar functions to natural AQPs. Meanwhile, they also verified the ion transport properties of these pillar[5]arenes and found that they had a complete rejection of Na^+ and K^+ and extremely low proton transport. These research results indicate that these pillar[5]arenes and their mixtures could be assembled into artificial channels suitable for transporting water and protons, and their combinatorial self-assembly could synergistically increase water permeability while preventing the transport of hydrated alkali metal cations. In addition, they studied the water permeation behavior of binary combinations of pillar[5]arenes with different molar ratios and found that they could exhibit different behavior such as independent (linear ABA), recessive (inhibition AB, AC, DB, ACA) or dominant (amplification, DBD). The study reveals a new paradigm that compounds may exhibit dominant synergistic water transport activity in the presence of other co-active components, providing a theoretical basis for constructing industrially-related membranes for desalination.[110]

Recently, Wang, Hou and colleagues carried out in-depth research on the influence of four artificial water channels (symmetric positively-charged channel s-Ch^+, symmetric negatively-charged channel s-Ch^-, asymmetric positively-charged channel a-Ch^+, and asymmetric negatively-charged channel a-Ch^-) based on pillar[5]arene on the transport rate of water molecules. They also used molecular dynamics simulations to explain the influence of the charge distribution and structural characteristics at the channel entrance on water permeability.[111] Their research indicates that the water permeability of positively-charged channels (s-Ch^+, a-Ch^+) is significantly higher than that of negatively-charged channels (s-Ch^-, a-Ch^-). The root cause is that the hydrogen-bond lifetimes of water molecules in the positively-charged entrance region are shorter (a-Ch^+ 1.8 ± 0.4 ps, s-Ch^+ 1.8 ± 0.2 ps, a-Ch^- 3.5 ± 1.0 ps, s-Ch^- 4.4 ± 1.5 ps, respectively) and the rotational dynamics are faster. This is closely related to the fact that the hydrogen-bond stability of the NH_3^+ group with water is lower than that of the COO^- group, and the K^+ ions enriched at the entrance of the negatively-charged channels hinder the rotation of water more strongly than the Cl^- ions at the entrance of the positively-charged channels. This study not only reveals the regulatory mechanism of the charge nature and symmetry at the channel entrance on water transport dynamics, but also proves at the molecular level that artificial water channels can optimize the water permeation efficiency through precise design of charge distribution and structural modules (such as the hydrophilicity and hydrophobicity of functional groups at both ends, and charge density). It provides a key basis for the design of high-performance artificial water channels and lays a theoretical foundation for membrane separation technology and the treatment of AQP-related diseases.

As stated above, the structural characteristics of tubular unimolecular channels based on IPAs, including molecular modification, length, side chain design, and charge distribution, *etc.*, have a crucial impact on the performance of ion and water channels such as selectivity, permeability, and gating behavior. The channels formed by molecules with special structures are of great significance for understanding the transport mechanisms of small molecules and ions, and provide a basis for designing artificial channels for the selective transport of various substances and the voltage-gated transport of ions.

2.2. Artificial nanochannels

Distinguishable from tubular unimolecular transmembrane channels, IPAs-based artificial nanochannels are usually nanoscale channels constructed from several IPA molecules through electrostatic interactions, host–guest interactions, or covalent bonding. Meanwhile, the precise structural design of the IPAs and guest molecules can result in the opening and closing of nanochannels through stimulation by light, pH, redox, temperature, gaseous molecules, and ions, thus enabling the recognition and controlled transport of ions, proteins, and other substances. In this section, we will introduce the design concepts of different IPA-based stimulus-responsive nanochannels and their applications in the controlled transmembrane transport of ions, protons, molecules, proteins, *etc*.

2.2.1. Ion/proton nanochannels. Channelrhodopsins (ChR), light-gated ion channels serving as sensory photoreceptors, function as a signal transmission medium to uphold the normal functions of organisms. Through photoinduced conformational changes, natural ChR can be converted into chloride-conducting anion channels using the depolarization and hyperpolarization process. Inspired by ChR, Li's group reported a facile non-covalent approach towards light-responsive biomimetic ChR nanochannels using host–guest interactions between a negative pillar[6]arene host and a positive azobenzene guest (Fig. 3a). By switching between threading and dethreading states with alternating visible and UV light irradiation, the functional channels can regulate the inner surface charge of the channels, which facilitates different forms of ion transport, for instance, cation-selective transport and

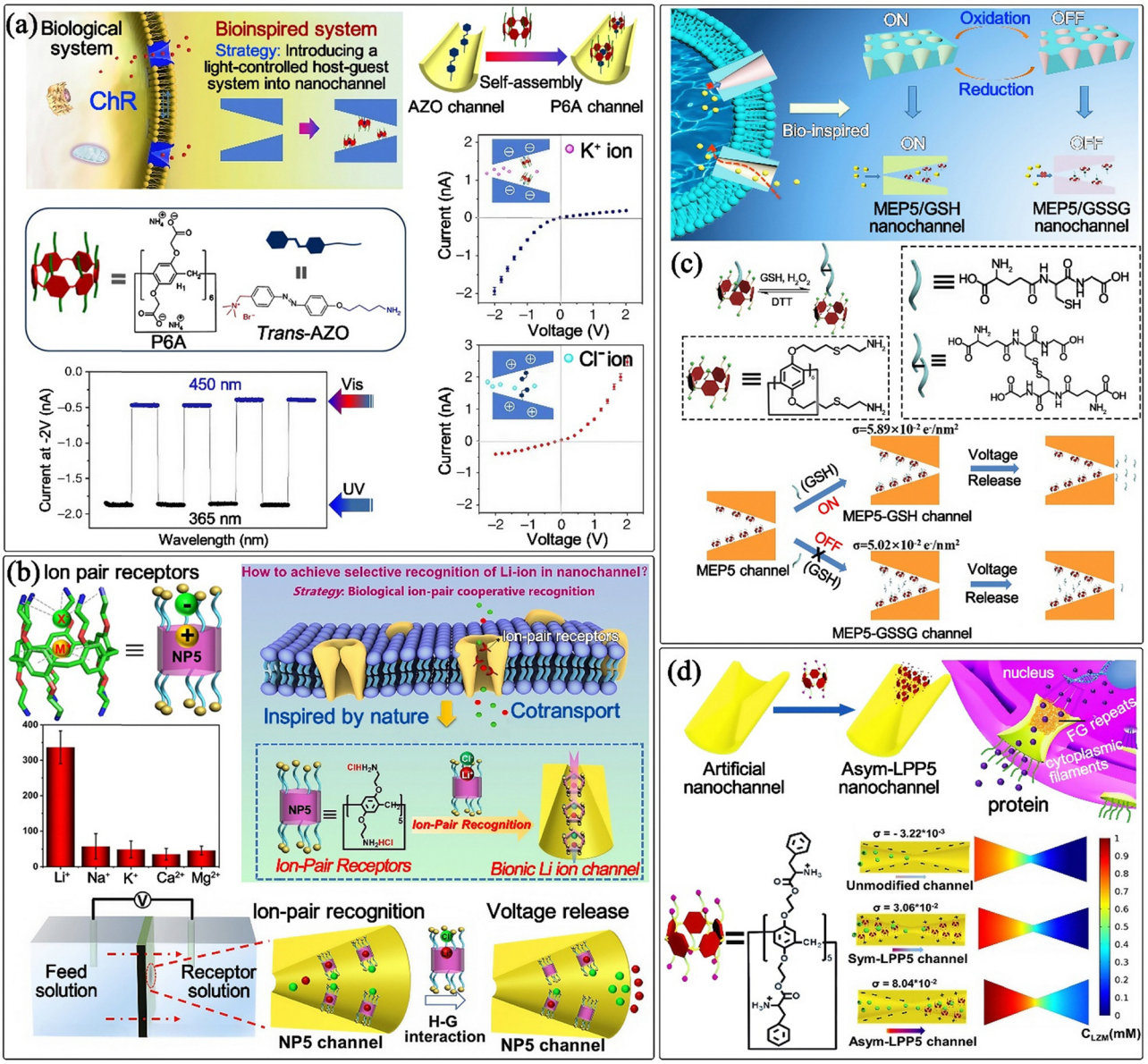

Fig. 3 Artificial nanochannels based on IPAs are used for ion/proton, molecule, and protein transmembrane transport research. (a) The schematic of the light-regulated host–guest-based nanochannel system inspired by ChR protein, including the design of biomimetic light-activated nanochannels using host–guest systems, the structures of host P6A and guest *trans*-azobenzene (*trans*-AZO), the UV-Vis spectra of an equimolar solution of P6A and AZO with absorbance changes at 345 nm under alternating UV and visible light irradiation, the construction process of light-controlled nanochannels *via* the host–guest system, and the ion selectivity and reusability of UV-regulated nanochannels demonstrated by current change detection (Reproduced with permission from ref. 112. Copyright 2017, Springer Nature). (b) The schematic of the highly selective transport and enrichment of lithium ions through bionic ion pair receptor nanochannels, including the ion pair recognition model between NP5 and metal ion pairs, the association constants of NP5 with LiCl, NaCl, KCl, $CaCl_2$, and $MgCl_2$ determined by ^1H NMR titration, the schematic of NP5 modification onto the PET membrane, and the device schematics for ionic transport experiments of different alkali chloride solutions (1×10^{-3} M) in the NP5 channel, which demonstrate the highly specific Li^+ recognition capability of the NP5 channel. (Reproduced with permission from ref. 117. Copyright 2023, American Chemical Society). (c) The schematic of the redox-driven channel designed for precise regulation of nanoconfined GSH recognition and transport, including the supramolecular nanobionic channel diagram, the molecular structure of host molecule MEP5 and its host–guest assembly/disassembly mechanism with GSH and oxidized GSH (GSSG), and the schematic of the possible mechanism for GSH transport mediated by the MEP5 channel (Reproduced with permission from ref. 119. Copyright 2021, American Chemical Society). (d) The schematic of the high-throughput protein transport channel inspired by nuclear pore complex, including the design diagram of biomimetic asymmetric LPP5-modified hourglass-shaped nanochannel for high-throughput protein transport and the schematic of the possible mechanism for lysozyme transport (Reproduced with permission from ref. 125. Copyright 2021, John Wiley & Sons, Inc.).

anion-selective transport.[112] Subsequently, they proposed an efficient ionic gating nanosensor based on this strategy. The carboxyl pillar[6]arene-functionalized AuNPs can easily regulate the azobenzene (AZO)-modified nanosensor, with an excellent ion rectification ratio (~22.2) and gating efficiency (~89.5). More importantly, this gating nanosensor system also exhibits

good stability and recyclability under the conditions of alternating irradiation of visible and ultraviolet light. These excellent research results will help to expand the application of artificial nanosensors in controllable drug delivery and as biosensors.[113] Temperature-sensitive ion channels are natural structures that can respond to specific temperature stimuli and are widely distributed in the peripheral and central nervous systems, playing a crucial role in many cellular processes such as maintaining the intracellular cation balance and achieving *in vivo* temperature information transmission. Li's group imitated the temperature-sensitive channels in organisms and designed a temperature-sensitive artificial channel structure based on the host–guest interaction between pillar[5]arene (P5A) and suitable ionic liquid (IL) guest molecules. Under temperature stimulation, this structure can regulate ion transport by controlling the degree of binding between P5A and IL. When the temperature rises from 25 °C to 55 °C, the interaction between P5A and IL weakens, P5A is released, and the inner surface charge of the channel changes, thus realizing the transition of ion transport from cations to anions. It paves a new way for better understanding the mechanism of temperature-sensitive biological channels and has great application prospects in biomedical research.[114] Carbon dioxide-sensitive ion channels are natural structures that can respond to carbon dioxide stimulation and play a crucial role in physiological processes such as plant photosynthesis and the olfactory perception of some insects. Cheng *et al.* imitated such natural channels and designed a carbon dioxide-activated ion nanochannel structure based on pillar[5]arene (P5N). This structure utilizes the fact that P5N can be converted into a water-soluble P5C containing cationic quaternary ammonium salt groups after absorbing carbon dioxide, and then P5C interacts with the nanochannel wall through host–guest interactions. This structure has good ion transport regulation characteristics. Under carbon dioxide stimulation, the ion transport rate changes. For example, in the P5N nanochannel, the ion transport rate of K^+ is 1.66×10^{-4} mol h^{-1} m^{-2} in a carbon dioxide environment and 7.98×10^{-4} mol h^{-1} m^{-2} in a nitrogen environment, and there is no significant change in the ion current after eight cycles, demonstrating good stability and recyclability. This research provides new ideas and methods for understanding the mechanism of carbon dioxide-sensitive biological channels and for applications in the biomedical and materials science fields.[115]

Mercury ion-sensitive ion channels are natural structures that can respond to mercury ion stimulation and play a crucial role in physiological processes such as the binding of mercury ions to potassium ion channels leading to toxicity *in vivo*. Zhang *et al.* imitated such natural channels and designed a mercury ion-regulated nanochannel structure based on mercaptoacetic acid-based pillar[5]arene (MAP5). This structure utilizes the binding characteristics of mercury ions with thiol-containing molecules and, through a host–guest competition mechanism, realizes the reversible switching of potassium ion transport between "on" and "off" in the presence or absence of mercury ions. The structure exhibits good mercury ion recognition and selective regulation characteristics, and can effectively distinguish Hg^{2+} from other metal ions and thus is applicable for the detection of Hg^{2+}. In addition, it provides a new approach to understand the physiological phenomenon of mercury toxicity.[116] Li's group designed a bionic nanochannel structure for the selective transport and enrichment of lithium ions based on amino pillar[5]arene (NP5). This structure utilizes the strong host–guest interaction of NP5 with the LiCl ion pair at the molecular level and, through the ion pair cooperative recognition mechanism, realizes the highly selective recognition, transport, and enrichment of lithium ions. The *I–V* test indicates that the NP5 channel has a highly selective recognition for lithium ions. Transmembrane transport and COMSOL simulation experiments prove that it can achieve the transport and enrichment of lithium ions. Moreover, the receptor solution obtained after 3-hour transmembrane transport of 1 mM LiCl through the NP5 channel significantly promoted wheat seedling growth, achieving a 75% increase in plant height (10.2 cm *vs.* 5.8 cm for control) after 7 days, providing a new method for practical applications such as metal ion extraction, enrichment, and recycling (Fig. 3b).[117]

Proton transport channels are natural structures capable of selective unidirectional transport of protons and play a crucial role in many biological processes such as virus replication and enzymatic catalysis. Qu *et al.* imitated the proton transport channels in organisms and designed a sub-nanoporous proton transport membrane structure based on amino pillar[5]arene NH_3^+-P5 and carboxyl pillar[5]arene COO^--P5. This structure utilizes the layer-by-layer assembly of the two pillar[5]arenes and, through the size effect of sub-nanopores as such the asymmetric structure, achieves good selectivity and unidirectional transport of protons. The selectivity for protons is superior to other ions such as Li^+, Na^+ and K^+, and the proton transport capacity is 459 μM m^{-2} h^{-1}, providing new ideas and methods for understanding the relationship between sub-nanostructure and function and for applications in fields such as nanofluidic ionic diodes.[118]

2.2.2. Molecular nanochannels. Inspired by the transmembrane transport of GSH, Li's group constructed a redox-reactive artificial nanochannel based on the host–guest chemical strategy between mercaptoethylamine-modified pillar[5]arene (MEP5) and GSH. The current of GSH in this nanochannel decreased significantly with time, and the gating ratio was higher than that of other analytes, demonstrating high selectivity and high efficiency. Meanwhile, this channel has good reversibility and recyclability, and can switch between the "ON" and "OFF" states through redox reactions, with stable switching performance under alternating oxidation/reduction conditions. At the same time, the average transport flux of GSH in the MEP5/GSH channel (reducing environment) is 22 times that of the MEP5/GSSG channel (oxidizing environment) (Fig. 3c).[119] The dopamine (DA) transporter achieves specific recognition of DA through a ring-shaped interaction mechanism, where the indole ring of tryptophan residues in the DA transporter forms π–π stacking and hydrophobic interactions with the catechol ring of DA. This structural complementarity ensures

high-affinity binding and directional transport of DA. Inspired by the DA transporter, they further modified the D-Tryptophan-pillar[5]arene (D-Trp-P5) molecule on a PET membrane through host–guest interactions to construct a functionalized conical nanochannel. The D-Trp-P5 functionalized nanochannel achieves specific wettability recognition of DA molecules through synergistic π–π stacking and hydrogen bonding interactions, as evidenced by a 55.1° contact angle decrease and 4.675×10^3 M^{-1} binding constant. This enables voltage-controlled fast DA transport with a maximum flux of 499.73 nmol cm^{-2} h^{-1} at −6 V, 16.88 times higher than under positive voltages.[120] Furthermore, they performed layer-by-layer self-assembly through the electrostatic interaction between mercaptoethylamine-based pillar[6]arene and mercaptoacetic acid-based pillar[6]arene, constructing a sub-nanochannel. The natural retinal chromophore with visible light-responsive properties was covalently immobilized onto the upper rim of amine-functionalized pillar[6]arene *via* Schiff-base reaction, forming a light-gated sub-nanochannel. This photoactive pillar[6]arene layer was then incorporated into a poly(methyl methacrylate) (PMMA) matrix through layer-by-layer self-assembly, followed by HF etching to fabricate a freestanding membrane. The resulting retinal-modified pillar[6]arene (ReP6) sub-nanochannel membrane exhibited reversible visible light-induced conformational switching of the retinal chromophore between all-trans and 11-*cis* isomers, enabling precise control over ATP transport across the sub-nanometer confinement. This supramolecular nanochannel has good ionic conductivity and has a selective regulation effect on the transport of ATP. Under visible light irradiation, the isomerization of the retinal chromaphore induces the closure of the channel and inhibits the transport of ATP, while in the absence of visible light irradiation, ATP can achieve selective transport in the sub-nanochannel.[121]

2.2.3. Protein nanochannels. Regulating the selective translocation of proteins is a crucial process, which has great potential in simulating and understanding complex biological activities. Li's group designed and prepared a switchable nanochannel based on a pillar[5]arene-based host–guest system. This channel employs pillar[5]arene as a "gatekeeper" and forms a special structure through host–guest assembly, enabling effective regulation of histone transport under different pH conditions. Under neutral conditions, the channel is in the "on" state, facilitating histone transport; when the pH = 4.5, the channel is in the "off" state, inhibiting histone transport, and this "on–off" state can be reversibly switched multiple times.[122] They also designed and prepared an artificial nanochannel modified with pillar[5]arene (P5) driven by GSH/GSSG for controllable protein transport. This channel can be reversibly converted between the P5–GSH channel and the P5–GSSG channel in different redox environments. The research indicated that hemoglobin (Hb) can selectively and effectively pass through the GSH-driven P5-modified nanochannel, and it has a higher rectification ratio, ion conductivity, and more hydrophilic characteristics compared with other related channels.[123] Furthermore, Li's group utilized the classic light-controlled assembly and disassembly characteristics of pillar[6]arene and azobenzene to design a nanochannel for protein transport regulated by ultraviolet/visible light. Through host–guest interactions, this nanochannel enables the light-controlled distribution of L-Phe-P6 within the channel, which in turn leads to differences in the surface charges of the nanochannel and simultaneously alters its electrical properties. Under different irradiation conditions of ultraviolet and visible light, this nanochannel can exhibit a significant regulatory ability for protein transport. Using bovine serum albumin (BSA) as a model protein, this nanochannel achieves efficient control of the transport flux of BSA under specific light conditions.[124] To achieve high-flux protein transport inspired by the nuclear pore complex, the researchers designed and synthesized L-phenylalanine-functionalized pillar[5]arene (LPP5), which was then asymmetrically immobilized onto one side of a polyethylene terephthalate (PET) nanochannel with an hourglass geometry. This novel biomimetic architecture, termed the asym-LPP5 channel, emulates the asymmetric phenyl alanine-glycine repeats (FG repeats) distribution of nuclear pores to enable directional protein translocation through host–guest interactions and electrostatic driving forces. Protein transport experiments were carried out with lysozyme, and the results indicated that the transport capacity of the asym-LPP5 channel was stronger than that of the unmodified and symmetrically modified channels. Electroosmotic flow (EOF) evaluation indicated that the specific binding of lysozyme to the asym-LPP5 channel led to an increase in surface charge density, which was 2.87 times that of the symmetrically modified channel and 37.48 times that of the unmodified channel. This was not only due to the interaction between LPP5 and lysozyme, but also related to the asymmetric modification of the channel. The special electrochemical potential generated by this asymmetry was one of the driving forces for protein transport (Fig. 3d).[125]

In conclusion, IPAs-based artificial nanochannels constructed through strategies such as electrostatic interaction, host–guest recognition, and covalent bonding exhibit the ability to precisely regulate the transmembrane transport of ions, molecules, and proteins. The core advantage of these channels lies in the structural programmability of IPAs. Their rigid columnar skeletons can serve as modular platforms. By modifying light-responsive groups, pH-sensitive units, and specific recognition sites, the channels are endowed with response characteristics to various stimuli such as light, temperature, gaseous molecules, and ions. From a mechanistic perspective, the design of IPA-based artificial nanochannels reveals two key scientific principles: (i) the synergy of intermolecular interactions. For example, the combination of host–guest recognition and electrostatic effects can break through the limitations of a single interaction mode and achieve highly selective transport; (ii) the confined space effect at the nanoscale. By precisely regulating the channel pore size and the surface chemical environment, it is possible to inhibit non-specific adsorption while maintaining high permeability efficiency. These findings provide new insights into solving the contradiction between

"selectivity and flux" for traditional nanochannels. In future research, if the relationship between structure and function can be further quantified (such as the correlation between molecular modification density and transport rate), and the stability bottleneck in practical applications can be overcome, IPA-based nanochannels are expected to exhibit significant application potential in fields such as precision medicine and environmental remediation.

3. IPA-based electrochemical biosensors

In recent years, with the continuous progress of science and technology and the increasing demand for biological detection, electrochemical biosensors have stood out due to their high sensitivity, good selectivity, rapid and accurate analysis, and other advantages. With the design of electrochemical biosensors, the core challenges lie in interfacial electron transfer efficiency, biomolecule recognition specificity, sensor stability, and anti-interference ability. Traditional electrode materials often face issues like low biomolecule adsorption efficiency, background signal interference from non-specific binding, and difficulties in selectively recognizing target analytes in complex samples. Additionally, achieving signal amplification, lowering detection limits, and maintaining long-term stability in harsh environments remain critical technical bottlenecks.

IPAs offer an ideal solution through their unique molecular structure: their rigid columnar skeletons serve as multifunctional platforms. By introducing charged groups (*e.g.*, carboxylic acids, quaternary ammonium salts) or biorecognition moieties (*e.g.*, peptides, aptamers), IPAs represent highly specific capture interfaces on electrodes. Charge complementarity enhances directional adsorption of charged biomolecules (*e.g.*, DNA, enzymes), minimizing non-specific protein adsorption, while their porous cavities create enrichment microenvironments to boost detection sensitivity. The water solubility and tunable amphiphilicity of IPAs optimize electrode wettability, accelerating electron transfer and resolving interfacial impedance issues common for hydrophobic materials. Furthermore, IPAs' electroactive groups (such as conjugated π systems or redox-active sites) directly participate in electrical signal conversion or act as amplifiers when coupled with enzyme/nanoparticle labels, enabling multistage signal amplification overcomming trace-detection limits. In this section, we will introduce the construction of electrochemical biosensors based on IPAs and the research progress of their applications.

3.1. Recognition and sensing of bioactive substances

3.1.1. Electrochemical nucleic acids biosensors. The detection of hepatitis B virus (HBV) DNA is of great significance for the diagnosis, treatment, and disease monitoring of hepatitis B. Yang's group reported a IPAs-based sandwich-type electrochemical biosensor for the ultrasensitive detection of HBV DNA (Fig. 4a). Firstly, the water-soluble pillar[5]arene (WP5)–Pd/Reduced Graphene Oxide (RGO) nanocomposite and the hydroxylatopillar[5]arene (HP5)–Au/Cobalt Sulfide (CoS) nanobox were prepared. The WP5–Pd/RGO dispersion was dropped onto the surface of a glassy carbon electrode (GCE), and the DNA probe was immobilized through the host–guest interaction between WP5 and methylene blue-labeled DNA (MB-DNA). Then, the redundant active sites were blocked with BSA, and after the hybridization reaction with the tDNA solution, the HP5–Au/CoS-aDNA was added to construct the sensor. This sensor can detect HBV DNA, and under optimized conditions, the detection limit for the tDNA solution was 0.32 fmol L^{-1}. Compared with traditional detection methods, it exhibits high sensitivity and better stability, reproducibility, and specificity. Therefore, it provides a new method for the detection of HBV DNA, which has potential applications in clinical diagnosis and analysis.[126]

3.1.2. Electrochemical bioactive molecule based biosensors. Caffeic acid (CA) is a phenolic acid widely existing in many substances such as red wine and green tea. It has good pharmacological effects for clinical treatments and health care, such as preventing heart diseases and reducing inflammation. However, excessive use can cause side effects to the human body, including carcinogenic or genotoxic effects. Therefore, it is of great significance to detect it sensitively. Yao's group utilized the easy functionalization of pillar[5]arenes and gold nanoparticles (Au NPs) to construct a photoelectrochemical sensor (Fig. 4b). This sensor achieves the ultrasensitive detection of CA through the localized surface plasmon resonance effect of Au NPs and the host–guest interaction principle between water-soluble carboxylatopillar[5]arene ammonium salts (WP5) and CA. Under optimal conditions, the detection limit is 0.01 μM (S/N = 3), and the concentration linear range is from 0.025 μM to 370 μM.[127] 5-hydroxytryptamine (5-HT) is an important monoamine neurotransmitter, synthesized by tryptophan hydroxylase – I existing in the human central nervous system. Abnormal levels of 5-HT can lead to various diseases. Yao's group added bismuth oxyhalides (BiOX) to the above WP5-functionalized Au NPs to construct a photoelectrochemical sensor. This sensor achieves ultrasensitive detection of serotonin through the high redox ability, moderate bandgap and low impedance of BiOBr, the electrostatic adsorption and host–guest complexation between WP5 and positively charged 5-HT in acidic or neutral environments, and the localized surface plasmon resonance effect of Au NPs. The detection range is from 0.01 to 100 μM, and the detection limit is as low as 3 nM (S/N = 3). Compared with the previously constructed Au@WP5 sensor for CA detection, the addition of BiOX further improves the performance of the sensor, endowing it with improved stability and selectivity.[128] Amino acids are crucial as building blocks of proteins and in metabolic processes. Lysine (Lys), in particular, is important in protein synthesis and human growth, making its selective recognition vital. Li's group constructed a macroscopic responsive liquid quantum dot system for amino acid sensing and separation. They synthesized WP5 *via* a "thiol–ene" click reaction and introduced it onto the surface of PEG1810-modified quantum dots (QDs) through host–guest interactions to obtain

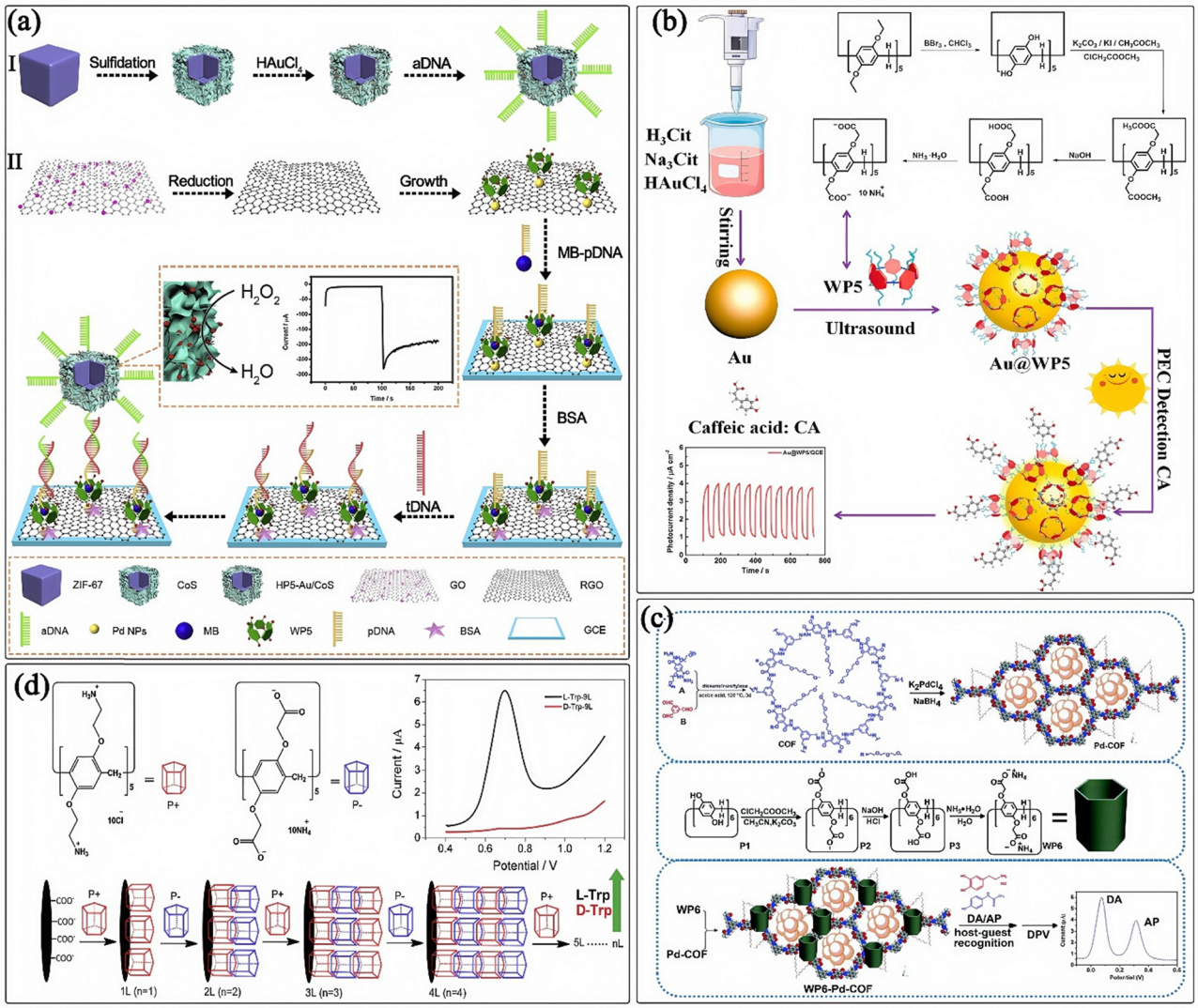

Fig. 4 Electrochemical biosensors based on IPAs are used to detect nucleic acids and bioactive molecules. (a) A robust host–guest interaction controlled probe immobilization strategy for the ultrasensitive detection of HBV DNA using hollow HP5–Au/CoS nanobox as biosensing platform: (I) the preparation process of HP5–Au/CoS-aDNA label. (II) Shows the preparation procedure of the constructed electrochemical sandwich-type DNA sensor (Reproduced with permission from ref. 126. Copyright 2020, Elsevier). (b) The schematic of the preparation of an enhanced photoelectrochemical sensor constructed from pillar[5]arene-functionalized Au NPss for ultrasensitive detection of CA (Reproduced with permission from ref. 127. Copyright 2022, Elsevier). (c) The schematic of the preparation of a nanocomposite based on water-soluble pillar[6]arene and ultrafine Pd nanoparticle-modified covalent organic framework, and the simultaneous determination of DA and acetaminophen (AP) by electrochemical sensing (Reproduced with permission from ref. 130. Copyright 2021, The Royal Society of Chemistry). (d) The schematic of the layer-by-layer assembly of anionic-/cationic-pillar[5]arenes multilayer films and their use as a chiral interface for the electrochemical recognition of tryptophan isomers (Reproduced with permission from ref. 133. Copyright 2018, Elsevier).

WP5-1810-QDs. This method takes advantage of the unique properties of pillar[5]arene. The principle is that the interaction between WP5 and Lys is stronger than that with PEG-1810. In the presence of Lys, WP5 is released from the QDs surface, causing macroscopic fluorescence quenching. Through NMR studies and experiments with different amino acids, the selectivity for Lys was confirmed. The system shows good reversibility, and the detection limit for Lys is 1.2 μM. The liquid WP5-1810-QDs obtained as a waxy solid retains fluorescent properties. It shows distinct fluorescence quenching for Lys in both solid and liquid states, and a significant selectivity for Lys was also shown by contact angle measurements.[129] In practical applications, biological samples or environmental samples are often complex mixtures. Electrochemical biosensors are of great significance for improving the analysis efficiency and accuracy when simultaneously determining multiple analytes. For example, the redox potentials of acetaminophen (AP), DA, and ascorbic acid (AA) are very close, leading to mutual interference and difficulty in distinguishing them from one another using electrochemical detection. Therefore, these three substances have become typical representatives for evaluating selective detection methods. If the selective detection problem

of these three substances can be solved, it will provide an important reference for developing highly selective electrochemical sensing methods. Tan *et al.* designed a WP6–Pd–COF nanocomposite using water-soluble pillar[6]arene (WP6), ultrafine Pd nanoparticles, and covalent organic framework (COF) (Fig. 4c). This composite material exhibits characteristics such as good thermal stability and appropriate microstructure. The experimental results show that the WP6–Pd–COF electrode can simultaneously detect AP and DA, and the detection limits reach 0.03 μM (AP) and 0.06 μM (DA) respectively, with high accuracy and precision, showing potential application in fields such as catalysis and sensing.[130]

In addition, there are also some electrochemically biosensors modified by cationic IPAs used for the detection of bioactive molecules. Duan *et al.* used a simple one-step pulsed electrodeposition technique to directly prepare electrochemically reduced graphene–cationic pillar[6]arene (ErGO–CP6) composite films on GCE from graphene oxide–cationic pillar[6]arene (GO–CP6) dispersions. The GO–CP6 composites and ErGO–CP6 films were characterized by multiple methods. The results indicated that CP6 was successfully grafted onto the GO surface and the films exhibited good properties. Electrochemical evaluation confirmed that the electrochemical response of the ErGO–CP6 films to theophylline (TP), AA, AP, and folic acid (FA) were significantly higher than those of the unmodified ErGO films and the bare GCE. This was attributed to the excellent electrical properties of graphene and the high inclusion complexation and enrichment capabilities of the CP6 molecules. Under optimal conditions, the detection limit for FA could reach 40 nM. Meanwhile, this electrode had good selectivity, stability, and reproducibility, and could be used for the determination of FA in real samples.[131] By employing a similar approach, Li's group synthesized CP5@RGO through the combination of cationic pillar[5]arene (CP5) and reduced graphene oxide (RGO). Subsequently, they prepared the PtPd–CP5@RGO nanocomposite loaded with PtPd bimetallic nanoparticles. Electrochemical evaluation indicated that the electrochemical response of the PtPd–CP5@RGO-modified GCE towards bisphenol A (BPA) was significantly higher than that of other relevant electrodes. This was ascribed to the excellent electrical conductivity of RGO, the efficient catalytic activity of PtPd nanoparticles, and the enrichment capacity of CP5 for BPA. Under the optimum conditions, the detection limit for BPA could reach 3.3 nM. At the same time, this electrode exhibited good selectivity, stability, and reproducibility, and could be used for the determination of BPA in real samples.[132]

The separation of chiral amino acids is of great importance in the fields of biochemistry, pharmaceutics and medical science. Zhao *et al.* successfully designed and prepared a chiral interface based on anionic/cationic pillar[5]arene multilayer films. The construction method is to assemble layer-by-layer the water-soluble anionic pillar[5]arene (WP5) and the cationic pillar[5]arene (CP5) on a GCE modified with carboxylated graphene (C-Gra) (Fig. 4d). Differential pulse voltammetry (DPV) was used to study the electrochemical recognition of tryptophan isomers (L-/D-Trp). The results indicate that as the number of layers of the assembled pillar[5]arene increases, the peak currents of both L-Trp and D-Trp exhibit a downward trend, while the difference in the peak current values between the two gradually increases. This phenomenon is mainly attributed to the fact that the stability constant of L-Trp with the host is higher than that of D-Trp, which means that L-Trp has a stronger host–guest interaction. In addition, the research also found that this electrochemical biosensor performs well in the detection of L-Trp. Its detection limit can reach 0.33 μM (S/N = 3), the linear response range is 1–300 μM, the recovery rate is between 99.6–101.5%, the relative standard deviation (RSDs) is 3.4–5.2%, and the interference of other amino acids in the recognition of L-Trp is negligible. This design provides a novel and effective method for the separation, storage of chiral molecules and the detection and analysis of L-Trp.[133]

3.1.3. Electrochemical bioactive protein biosensors. T4 polynucleotide kinase (T4 PNK) plays a crucial role in processes such as DNA recombination, replication, and damage repair. Its abnormal activity is associated with various diseases. Therefore, it is of great importance to develop a simple, rapid, accurate, and sensitive method for detecting T4 PNK activity. Luo *et al.* designed an electrochemical biosensor for the detection of T4 PNK activity using the host–guest interaction between phosphate pillar[5]arene (PP5) and methylene blue (MB). At first, DNA was modified on the surface of a gold electrode by chemically adsorbing thiol groups, and the T4 PNK to be tested and ATP were added. PP5 was connected to the phosphorylated DNA through TiO_2. MB is a molecule with electrochemical activity. It can undergo redox reactions on the electrode surface and produce detectable electrochemical signals. This electrochemical activity enables MB to be used as a signal reporting molecule. Due to the host–guest interaction between MB and PP5, MB molecules can be enriched on the electrode surface. When the activity of T4 PNK increases, more phosphorylated DNA links with PP5 through TiO_2, and then captures more MB molecules, resulting in a further enhancement of the electrochemical signal, achieving a signal amplification effect and improving the detection sensitivity and specificity. The research results indicate that the sensor exhibits a good linear range (2×10^{-4} to 5 U mL^{-1}), a low detection limit (1×10^{-4} U mL^{-1}), good selectivity and reproducibility when detecting T4 PNK activity, and also exhibits good performance in inhibition experiments and cell lysate detection.[134]

Utilizing the design concept of enhancing the detection signal based on the host–guest interaction between pillararenes and photosensitive molecules as described above, Yang *et al.* designed a series of sandwich – type electrochemical biosensors for the sensitive detection of immune-related proteins. For example, they designed a highly sensitive and robust sandwich-type electrochemical immunosensor for the detection of prostate-specific antigen (PSA) (Fig. 5a). First, HP5@AuNPs@g-C_3N_4 hybrid nanomaterials were prepared by reacting HP5 with $HAuCl_4$ and NaOH and then adding g-C_3N_4. Subsequently, MB linked to the surface of HP5@AuNPs@g-C_3N_4 through the host–guest interaction between the pillararenes on the surface, and then the secondary antibody (Ab_2) was

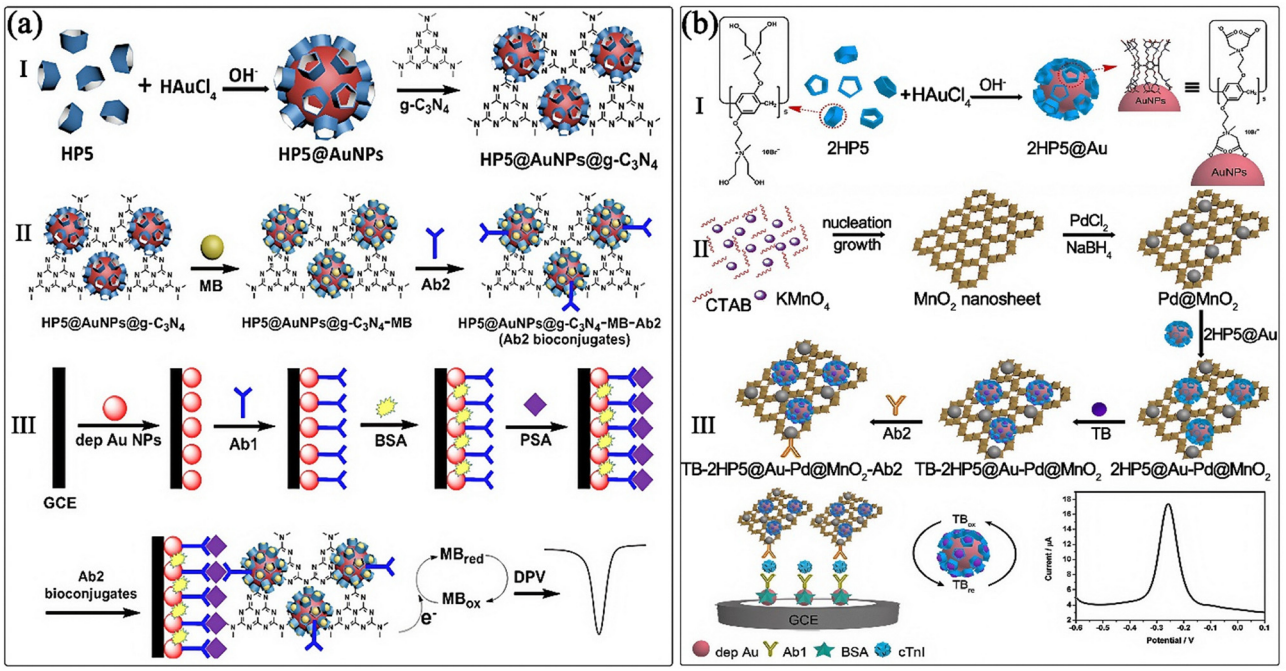

Fig. 5 Electrochemical biosensors based on IPAs are used to detect bioactive proteins. (a) A robust electrochemical immunosensor based on hydroxyl pillar[5]arene@AuNPs@g-C_3N_4 hybrid nanomaterial for ultrasensitive detection of prostate specific antigen: the illustrations for synthesis of the HP5@AuNPs@g-C_3N_4 hybrid nanomaterial (I), Ab_2 bioconjugates (II), and the fabrication process as well as sensing principle of the electrochemical immunosensor (III) (Reproduced with permission from ref. 135. Copyright 2018, Elsevier). (b) Facile and clean synthesis of dihydroxylatopillar[5]arene-stabilized Au NPs integrated Pd/MnO_2 nanocomposites for robust and ultrasensitive detection of cardiac troponin I: the preparation process of 2HP5@Au (I),2HP5@Au–Pd/MnOAb_2 bioconjugates (II) and sandwich-type immunosensor (III) (Reproduced with permission from ref. 138. Copyright 2019, Elsevier).

incubated to obtain Ab_2 bioconjugates. When constructing the sensor, AuNPs were first electrodeposited on the surface of a GCE and used to capture the primary antibody (Ab_1). Upon initial specific binding of PSA to Ab_1, Ab_2 bioconjugates are added and incubated, enabling the formation of an immune complex and subsequent signal amplification. Ultimately, highly sensitive detection of prostate-specific antigen is achieved by measuring the change in current. The detection range of this sensor is 0.0005–10.00 ng mL^{-1}, and the detection limit is 0.12 pg mL^{-1} (S/N = 3).[135]

Besides MB, host–guest complexes between pillararenes and other molecules such as thionine (Thi) and toluidine blue (TB) have also been used by Yang *et al.* in the design of this sandwich-type electrochemical biosensor to enhance the detection of immune-related antigens or proteins. For example, they prepared an ultrasensitive and robust sandwich-type electrochemical immunosensor for the quantitative determination of squamous cell carcinoma antigen (SCCA) in human serum. First, Ab_1 was immobilized using Au@TiO_2 nanosheets, and then the electrode was blocked with BSA to prevent non-specific adsorption during the subsequent reaction process. To achieve signal amplification and enhancement, they immobilized Thi on Pd/MoS_2 nanosheets through the host–guest interaction between pillararene WP5 and Thi, and after modifying Ab_2, obtained Thi@WP5–Pd/MoS_2–Ab_2 as a signal amplification label. This research indicated that the sensor exhibits good detection ability for SCCA, with high sensitivity and accuracy. When detecting SCCA, its linear range is 0.001–10 ng mL^{-1}, and the detection limit is as low as 0.14 pg mL^{-1}, which can meet the needs of clinical detection and provides a new and effective method for the detection of SCCA.[136] At the same time, they used pillararene HP6-modified Au NPs HP6@Au hybrid nanomaterial to construct an electrochemical biosensor for the highly sensitive detection of human epididymis protein 4 (HE4). Unlike previous designs, HP6@Au nanoparticles are strategically employed in a dual capacity: they are covalently conjugated to detection Ab_2 *via* Au–N bonds to form stable bioconjugates that securely encapsulate Thi through host–guest interactions, while simultaneously being anchored onto the electrode surface *via* carboxylate–Au coordination to enhance surface area and provide robust immobilization sites for Ab_1. This dual-functional design synergistically enhances both signal stability through host–guest complexation and immunosensor sensitivity *via* surface area expansion, resulting in a 3.8-fold increase in antibody loading capacity and a 76% improvement in mediator retention compared to single-functionalized systems.[137] Similarly, 2HP5@Au was used to immobilize TB on Pd-modified MnO_2 nanosheets to prepare Ab_2 bioconjugates. Meanwhile, Au nanoparticles were used to modify a GCE to enhance its surface area and thus increase the modification efficiency of Ab_1. This sandwich-type electrochemical bio-immunosensor was used for the robust and ultrasensitive detection of cardiac troponin I (cTnI), a significant biomarker of acute myocardial infarction. It shows a linear correspondence with the cTnI concentration in the range of 0.005–20 ng mL^{-1}, with a low detection limit of 2 pg mL^{-1}

(S/N = 3) (Fig. 5b).[138] They also constructed WP6 functionalized PdPt porous core–shell octahedral nanodendrites (PdPt PCONs) loaded with TB and Ab_2 to construct Ab_2 bioconjugates, which were combined with Ab_1-modified GCE for the highly sensitive detection of neuron-specific enolase (NSE). The experimental results indicate that the immunosensor can accurately detect NSE over a wide concentration range and exhibit a good linear relationship. The detection range is 0.0003–100.00 ng mL^{-1}, and the detection limit is as low as 0.095 pg mL^{-1}.[139]

For the electrochemical sensing and detection of bioactive substances, IPAs exhibit unique advantages due to the programmability of their molecular structures and their ability for functional integration. Their rigid columnar skeletons serve as modular platforms. By modifying charged groups, biorecognition sites, or coupling with nanoscale functional materials, multifunctional sensing interfaces can be constructed, which possess high-specificity, efficient signal amplification, and optimized interfacial electron transfer. The design based on charge complementarity can directionally capture charged biomolecules and inhibit non-specific adsorption. The porous cavity structure can enrich trace target substances to improve the detection sensitivity. Moreover, the introduction of electrochemically active groups or nanocomposites significantly enhances the signal conversion efficiency. Such designs have broken through the bottlenecks of traditional sensors, which include insufficient recognition accuracy in complex matrices and low sensitivity for the detection of trace substances. They provide universal solutions for the detection of bioactive substances at different dimensions, such as DNA, bioactive small molecules, and proteins.

3.2. Environmental monitoring

In recent years, the issue of pesticide residues, explosives, and toxic substances in the environment has become increasingly severe, leading to soil and water pollution and posing significant threats to the safety of humans and wildlife. The continuous accumulation of these harmful substances exacerbates ecosystem degradation and health risks. To address this growing environmental challenge, efficient, rapid, and accurate detection and control of these pollutants are urgently required. Electrochemical detection technology, with its unique advantages, has gained considerable attention. Particularly, the combination of electrochemical detection with pillararenes for host–guest recognition is pioneering a new era of high-sensitivity detection for harmful small molecules, providing novel solutions for environmental protection.

Paraquat (PQ) is an effective herbicide, and its chemical name is 1,1′-dimethyl-4,4′-bipyridinium dichloride. It kills weeds by inhibiting the photosynthesis of plants. It is widely used in the agricultural field and can effectively control the growth of weeds and increase the yield of crops. However, PQ exhibits serious harm to human health and the environment. After being in contact with or ingested by humans, it can lead to poisoning and can even endanger lives. Additionally, it can cause pollution to the environment such as the soil and water sources. Therefore, it is of great significance to conduct rapid, sensitive and selective detection of PQ Pillararenes have good host–guest recognition abilities and provide appropriate approaches for the detection of PQ. For example, Tan *et al.* prepared a WP6@Ag@COF composite material by assembling WP6-modified Ag nanoparticles (WP6@Ag) onto the surface of a covalent organic framework (COF), achieving electrochemical detection of PQ, with a detection range of 0.01–50 μM and a detection limit of 0.014 μM.[140] Xiong *et al.* modified carboxylatopillar[5]arenes (CP5) or carboxylated pillar[6]arene (CLP6) on nanopipettes and introduced Au NPs to prepare a nanopipette sensor, achieving highly sensitive detection of PQ. The CP5–Au NPs (3 nm)-modified nanopipette has a detection limit of 0.034 nM for PQ and exhibits higher sensitivity.[141] Zhao *et al.* used a similar method to modify phosphate pillar[6]arene (PP6) on single-walled carbon nanotubes (SWCNT) and *in situ* load silver nanoparticles (Ag NPs) to prepare Ag@PP6@SWCNT nanomaterials, achieving highly sensitive detection of PQ. The detection limit was 0.027 μM (S/N = 3). Meanwhile, compared with commercial Pd/C and Ag@SWCNT catalysts, Ag@PP6@SWCNT also exhibits higher catalytic efficiency for the reduction of 4-nitrobenzene (4-NP) and the degradation of MB (Fig. 6a).[142] Luo *et al.* ingeniously utilized naphthalene-derivated pillar[5]arene (NTP5) and cucurbit[10]uril (Q[10]) to successfully prepare a supramolecular complex for the detection of PQ. During the formation process of this complex, the host–guest interaction plays a crucial role. Q[10], with its unique large cavity structure, tightly binds with the 4-[2-(1-naphthyl)ethenyl]pyridine group of NTP5. This tight binding mode enhances the fluorescence performance of NTP5. When PQ is added to the solution containing this complex, the fluorescence of the solution changes significantly, quenching sharply from yellow to colorless. This obvious color change can be easily observed even with the naked eye. The detection limit reaches a relatively low level of 7.06×10^{-8} mol L^{-1}, providing an intuitive and effective method for the detection of PQ.[143]

Methyl parathion (MP) is a common organophosphorus pesticide with high toxicity. Tan *et al.* designed an electrochemical sensor based on a GCE (CP5–rGO/GCE) modified with a cationic water-soluble pillar[5]arene (CP5) and reduced graphene (rGO) nanocomposite for the trace detection of MP. The experimental results indicate that compared with the GCE (β-CD–rGO/GCE) modified with β-cyclodextrin (β-CD)-functionalized reduced graphene (rGO), the CP5–rGO/GCE sensor exhibits higher electrochemical catalytic activity, faster response rate, higher sensitivity, better reproducibility and anti-interference ability for MP. The linear range for detecting MP is 0.001–150 μM, and the detection limit is 0.0003 μM (S/N = 3) (Fig. 6b).[144] Based on the above method, Yang's group replaced the cationic water-soluble pillar[5]arene (CP5) with hydroxylatopillar[5]arene (HCP5) and replaced the chemically reduced graphene with electrochemically reduced graphene oxide (ERGO). The experimental results indicate that the detection range for methyl MP is 0.005–30 μM, and the detection limit is 0.001 μM.[145]

In addition to pesticide residues, the detection of some dangerous explosives in the environment is also crucial. TNT

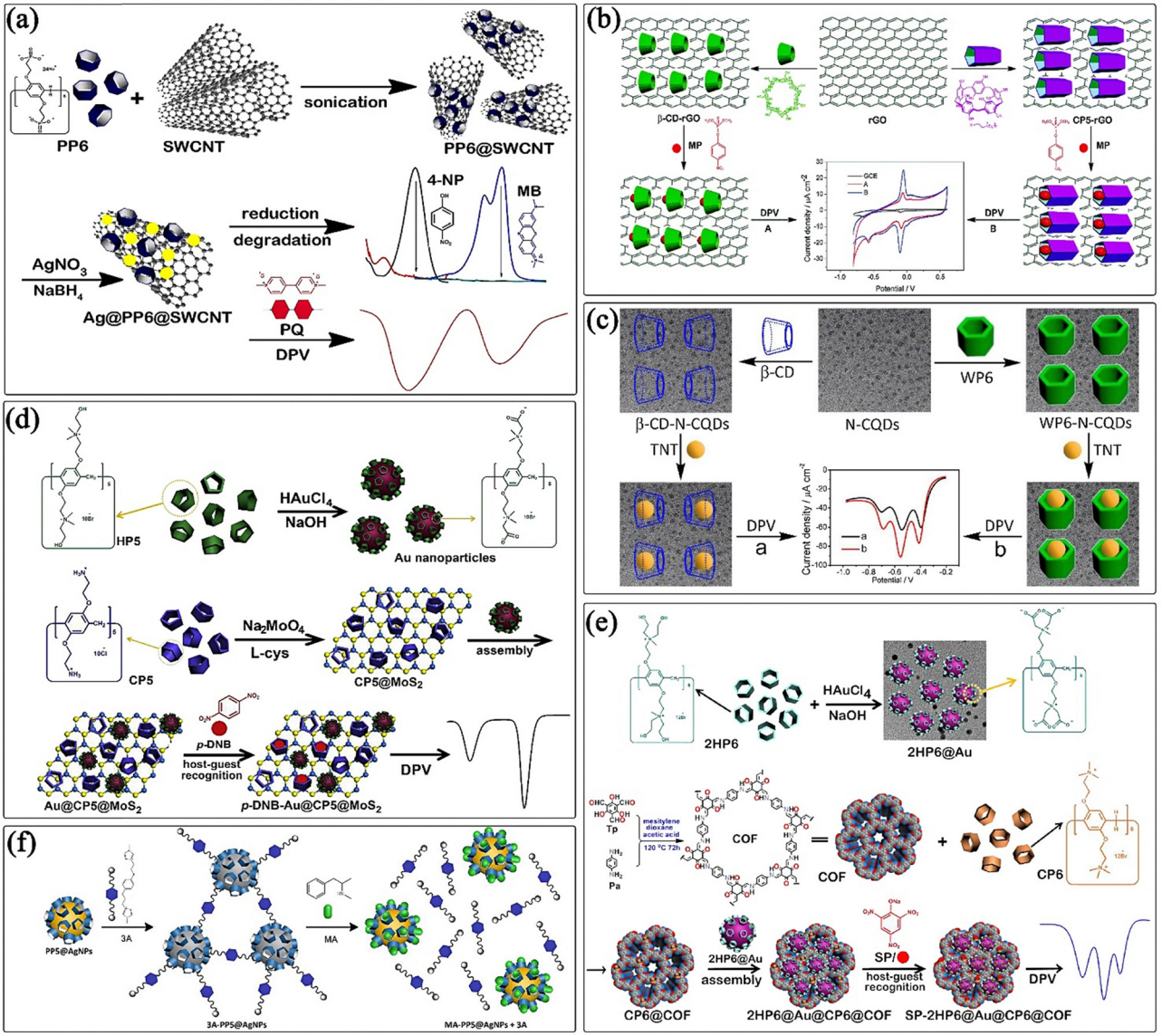

Fig. 6 Electrochemical biosensors based on IPAs are used for pesticide residues, explosives, and toxic substances in the environment. (a) The schematic of the controlled assembly of silver nanoparticles on the surface of phosphate pillar[6]arene-functionalized single-walled carbon nanotubes and their applications in the catalytic and electrochemical detection of PQ (Reproduced with permission from ref. 142. Copyright 2019, Elsevier). (b) The schematic of the ultrasensitive electrochemical detection of MP pesticide based on cationic water-soluble pillar[5]arene and reduced graphene nanocomposite (Reproduced with permission from ref. 144. Copyright 2019, The Royal Society of Chemistry). (c) The schematic of the water-soluble pillar[6]arene–functionalized nitrogen-doped carbon quantum dots (WP6–N-CQD) nanocomposites for the electrochemical sensing and recognition of TNT (Reproduced with permission from ref. 146. Copyright 2017, Elsevier). (d) The schematic of the process for preparing a multi-component functionalized nanomaterial (Au@CP5@MoS_2) by the controlled assembly of Au NPs on the surface of CP5@MoS_2 for the sensing detection and catalytic reduction of the toxic explosive *p*-dinitrobenzene (*p*-DNB) (Reproduced with permission from ref. 147. Copyright 2019, Elsevier). (e) The schematic of ultrasensitive and highly selective electrochemical sensing of sodium picrate based on dihydroxylatopillar[6]arene-modified Au NPs and cationic pillar[6]arene-functionalized covalent organic framework (Reproduced with permission from ref. 149. Copyright 2020, Elsevier). (f) The schematic of the principle of competitive molecular recognition of methamphetamine (MA) by the supramolecular sensor 3A/PP5@AgNP hybrid material (Reproduced with permission from ref. 150. Copyright 2023, Elsevier).

(2,4,6-trinitrotoluene) is a common explosive. Yang's group used WP6 and nitrogen-doped carbon quantum dots (N-CQDs) to prepare WP6–N-CQD composites for the detection of TNT. The experimental results indicate that the WP6–N-CQD composites exhibit a greater supramolecular recognition ability and electrochemical signal for TNT. Compared with β-CD–N-CQD composites, WP6 with stronger supramolecular recognition ability for TNT, generates a significantly higher reduction peak current on WP6–N-CQD-modified electrodes than on β-CD–N-CQD-modified electrodes. The linear range for detecting TNT is 0.001 μM–1.0 μM and 1.0 μM–20.0 μM, and the detection limit is 0.95 nM (S/N = 3). Compared with other electrochemical sensing materials, the WP6–N-CQD composites exhibits higher detection performance (Fig. 6c).[146]

p-Dinitrobenzene (*p*-DNB) is an important nitroaromatic compound, often used in the synthesis of the dye and plastics *etc.* However, its environmental toxicity and explosive nature make it of great significance to detect it with high sensitivity. Yang's group designed a multicomponent functionalized nanomaterial (Au@CP5@MoS_2) for the sensing and catalytic reduction of *p*-DNB by controlling the assembly of Au NPs on the surface of cationic pillar[5]arene (CP5)-functionalized MoS_2. This sensor can detect *p*-DNB with high sensitivity and selectivity, and in the presence of $NaBH_4$, it can reduce *p*-DNB to 1,4-diaminobenzene, reducing the explosive danger to some extent (Fig. 6d).[147] Borjigin *et al.* designed a composite material based on Au NPs (Au@HP5@SWCNT) loaded on single-walled carbon nanotubes (SWCNT) functionalized with hydroxyl pillar[5]arene (HP5) for the detection of *p*-DNB. The experimental results indicate that the composite material has a sensitive sensing performance for *p*-DNB. Its detection limit is 0.043 pM (S/N = 3).[148]

Sodium picrate (SP) and picric acid (PA) analogues are a class of substances with high toxicity and explosive nature. Their highly selective and rapid detection is crucial for protecting the environment and preventing terrorist threats. Tan *et al.* reduced and stabilized Au NPs using dihydroxylatopillar[6]arene (2HP6) to obtain 2HP6@Au, and then assembled it on the surface of a cationic pillar[6]arene (CP6)-functionalized covalent organic framework (COF) to obtain a 2D heterogeneous composite material (2HP6@Au@CP6@COF) for the rapid and sensitive detection of SP. The research indicated that this sensor can detect SP with high selectivity, with a detection range of 0.005–120 μM and a detection limit of 0.0017 μM (Fig. 6e).[149]

In addition to the environmental trace detection of toxic explosives, it is also crucial to achieve efficient detection of trace drugs at crime scenes. Yang's group has developed a handheld sensor based on phosphate pillar[5]arene@silver nanoparticles (PP5@AgNPs) and an inducing compound 3A, which can achieve rapid monitoring of methamphetamine (MA). The main principle is that the inducing compound 3A undergoes molecular recognition with PP5 in PP5@AgNPs, inducing the aggregation of AgNPs and changing the color of the solution from yellow to gray-black; after adding MA, MA has a stronger interaction with PP5, competitively replacing 3A, causing the AgNPs to depolymerize and the color of the solution to change back to yellow. By observing the characteristic peak at 410 nm using a mobile phone APP, it can be determined whether the sample contains MA (Fig. 6f).[150]

In the field of environmental pollutant detection, IPAs exhibit significant advantages owing to the structural adaptability of their molecules and the capacity for functional integration. Their rigid columnar skeletons serve as multifunctional platforms. By modifying recognition groups or coupling with nanocatalytic materials, detection interfaces that integrate high-selectivity capture, trace substance enrichment, and signal enhancement have been constructed: host–guest interactions can specifically recognize target pollutants, the porous cavity structure enables the efficient enrichment of trace molecules, and the introduction of nanocomposites significantly improves the electrochemical catalytic activity and signal conversion efficiency.

However, current research still faces the following key challenges: (i) anti-interference ability and compatibility in complex environments: complex components in real samples such as soil and water (including humic acids and metal ions) may interfere with the recognition process and affect the detection accuracy; (ii) capability of simultaneous detection of multiple pollutants: for multiple coexisting pollutants (such as mixed pesticides and explosive derivatives), sensors with existing single recognition mechanisms find it difficult to achieve simultaneous and efficient detection; (iii) engineering the implementation of detection technologies: the miniaturized design of portable devices (such as the stability of handheld sensors), the automation ability for processing large-scale samples, and the *in situ* degradation of pollutants after detection still need to be improved. In the future, it will be necessary to address the above issues to provide innovative solutions for the rapid and accurate detection of pesticide residues, explosives, and toxic substances.

4. IPA-based fluorescence sensing and bioimaging systems

In the fields of environmental monitoring and biomedicine, fluorescence detection and bioimaging technologies have emerged as core tools for analyzing complex biological systems and environmental pollutants, thanks to their precision in molecular recognition and intuitiveness in visual analysis. The efficient detection of trace heavy metal ions and phenolic compounds in the environment, as well as the early warning of abnormalities in biological molecules such as choline and spermine in the human body, rely on the specific capture and signal amplification of target substances by detection systems. For the precise imaging of the tumor microenvironment (TME) and the targeted visualization of organs like the kidneys, materials are urgently required to exhibit targeted enrichment, biocompatibility, and responsive regulation characteristics in the dynamic environment of living organisms. However, issues such as non-specific adsorption in complex matrices, insufficient detection sensitivity for low-concentration targets, poor biocompatibility of traditional materials, and difficulties in overcoming physiological barriers remain key bottlenecks in technological development.

In recent years, for environmental and biological detection, IPAs specifically bind to polar pollutants or charged biological molecules through electrostatic interactions. In conjunction with fluorescent probes, they have achieved highly sensitive detection. Additionally, the ionic groups of IPAs can reduce non-specific aggregation in complex matrices by improving water solubility, thereby enhancing the stability of detection. In the field of bioimaging, some ionic groups of IPAs not only endow the system with pH/charge responsiveness but also significantly improves biocompatibility by enhancing water

solubility and reduces the *in vivo* clearance rate. This enables IPA-based nanocomposites to efficiently accumulate in target organs, facilitating the controlled release of drugs and the enhancement of imaging signals. Moreover, the supramolecular assembly of IPAs allows them to synergize with various functional materials, enabling the construction of intelligent systems with targeted recognition, signal amplification, and multimodal imaging capabilities to meet the needs of precise positioning and dynamic monitoring in complex biological systems.

This section will focus on the applications of IPAs for the fluorescence sensing of environmental pollutants, highly sensitive detection of biological molecules, and targeted bioimaging.

4.1. Fluorescence based sensing of environmental pollutants

In complex environmental and biological systems, an imbalance in the concentrations of ions such as CN^-, Al^{3+}, Fe^{3+}, and F^- can pose a serious threat to the ecological environment, organism health, and numerous industrial production processes. Their highly efficient and sensitive detection is of crucial significance for environmental protection, human health monitoring, and industrial production quality control. Fluorescence detection technology has attracted significant attention in the field of ion detection due to its advantages such as high sensitivity, ease of operation, and the ability to achieve real-time detection. However, most organic fluorescent groups have poor water solubility, making it difficult to introduce signal groups and binding sites simultaneously. They are also easily interfered with by other ions. At the same time, the high hydration enthalpy of some ions hinders their effective binding to sensors, greatly limiting the accuracy and sensitivity of detection. IPAs, with their good water solubility, excellent molecular recognition ability, and controllable self-assembly properties, provide a new tool for constructing fluorescence imaging systems for the highly selective and sensitive detection of specific ions in aqueous solutions.

Lin and colleagues constructed a series of supramolecular complexes for the detection of multiple ions by means of host–guest assembly between IPAs and different photosensitive guest groups. They self-assembled water-soluble cationic pillar[5]arene (P5) with acid-functionalized naphthalene monoimide derivative (N2), *N*-(pyridinium-4-yl)naphthalimide derivative (B1), and aromatic acid derivative (N1) respectively, to obtain P5N2, P5B1, and P5N1. During the ion detection process, the detection is mainly determined using changes in fluorescence. When P5N2 interacts with Al^{3+}, its fluorescence is significantly enhanced, and the detection limit for Al^{3+} is 9.93×10^{-8} mol L^{-1}. P5B1 and P5N1 show fluorescence quenching when detecting Fe^{3+}, with detection limits of 5.01×10^{-7} mol L^{-1} and 8.24×10^{-7} mol L^{-1} respectively. After introducing Al^{3+} and Fe^{3+} to form P5N2Al, P5B1Fe, and P5N1Fe, when P5N2Al detects CN^-, a significant red-shift in fluorescence occurs, from λ_{em} = 390 nm to 470 nm, and the color changes from blue to blue-green, with a detection limit of 2.29×10^{-6} mol L^{-1}. When P5B1Fe and P5N1Fe detect F^-, both show a significant increase in fluorescence, with detection limits of 4.07×10^{-6} mol L^{-1} and 4.07×10^{-8} mol L^{-1} respectively.[151–153] These host–guest complexes take advantage of the good water solubility, excellent molecular recognition ability, and controllable self-assembly properties of IPAs, which is of great significance for achieving highly selective and sensitive detection of specific ions in aqueous solutions. Meanwhile, Yao *et al.* designed a supramolecular host–guest system based on WP5 and water-soluble quaternized perylene diimide derivative (G).[154] Morphological transformation was achieved by adding WP5 to an aqueous solution of G, and a fluorescence "turn-off" phenomenon was observed due to supramolecular photoinduced electron transfer (PeT). This system can act as a "turn-on" fluorescent probe for Fe^{3+} ion detection through interdicting the supramolecular PeT process. Experimental results indicate that Fe^{3+} ion detection exhibits specificity, ratiometric properties, and reversibility, with a detection limit of 2.13×10^{-7} M, where the hydrophobic effect and electrostatic interaction play important roles in the supramolecular process (Fig. 7a).

The fluorescence indicator displacement (FID) strategy is based on the principle of competitive binding between the host and the guest. It utilizes the fact that after a fluorescent indicator binds to a receptor, displacement occurs in the presence of the target analyte, leading to changes in the fluorescence signal suitable for monitoring the binding process. Huang's group developed a FID detection method based on pillar[5]arene-assisted dye deprotonation (Fig. 7b).[155] In this system, the pH-sensitive dye salicylaldehyde (SA) exists in the form of SA with weak fluorescence under neutral conditions. After adding cationic pillar[5]arene (AP5), due to the larger binding constant between AP5 and the deprotonated SA^- and the existence of an electrostatic driving force, SA undergoes deprotonation and transforms into SA^-, resulting in a significant enhancement of the solution's fluorescence. By using this fluorescence switch, phenolic pollutants can be detected by FID based on the different binding abilities of phenolic substances to AP5. Phenols with more chlorine substituents have stronger binding to AP5, leading to higher detection sensitivity. This study provides a new method for the detection of phenolic pollutants, and related FID systems have potential applications for the detection of biological and environmentally relevant anionic compounds.

4.2. Fluorescent detection of bioactive molecules

Spermine, an important polyamine in the body, is closely related to cell proliferation, cancer development, and other biological processes. Precise imaging of spermine is of great significance for understanding biological processes and diagnosing diseases. Ling and colleagues designed and synthesized a fluorescent conjugate based on pillar[6]arene, composed of fully carboxylated water-soluble pillar[6]arene and pyrene fluorophore with an alternating methylene bridge. The design strategy leverages the rigid structure and host–guest recognition properties of pillar[6]arene to specifically bind to spermine *via* host–guest interactions, triggering fluorescence changes in the pyrene fluorophore for spermine imaging. Pillar[6]arene

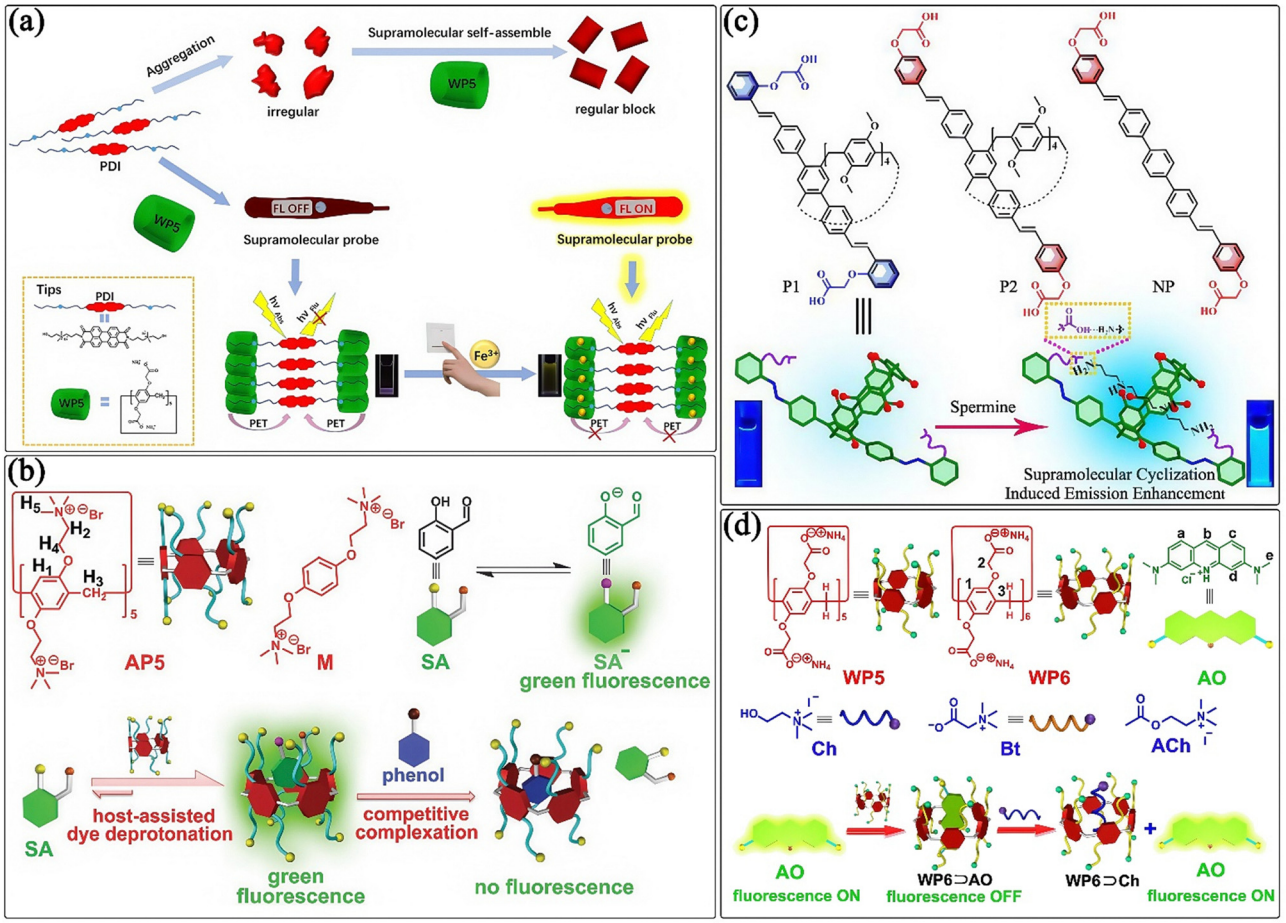

Fig. 7 IPAs are employed for fluorescence sensing of environmental pollutants and bioactive molecules. (a) The schematic of supramolecular host–guest system as ratiometric Fe^{3+} ion sensor based on water-soluble pillar[5]arene (Reproduced with permission from ref. 154. Copyright 2017, American Chemical Society). (b) The schematic of the mechanism for constructing a fluorescence switch *via* host–guest complexation between water-soluble cationic pillar[5]arene AP5 and salicylaldehyde SA, and detecting phenolic pollutants using fluorescence indicator displacement: AP5 induces deprotonation of SA to enhance fluorescence, while phenolic pollutants cause fluorescence quenching through competitive displacement of SA^- (Reproduced with permission from ref. 155. Copyright 2016, The Royal Society of Chemistry). (c) The schematic of the recognition mechanism for spermine using emission enhancement induced by supramolecular cyclization in a pillar[5]arene probe (Reproduced with permission from ref. 157. Copyright 2023, Elsevier). (d) The schematic of the host–guest complexation system constructed by anionic water-soluble pillar[6]arene and aromatic fluorescent dye acridine orange, and its mechanism for detecting choline compounds and monitoring enzyme reactions (Reproduced with permission from ref. 158. Copyright 2017, Elsevier).

plays a core role by not only providing a binding site for specific interaction with spermine but also enhancing water solubility through carboxylation, which is beneficial for applications in biological systems. Additionally, electrostatic interactions further strengthen the binding with spermine. The experimental results indicate that this conjugate exhibits high selectivity for spermine, with fluorescence intensity significantly increasing as the spermine concentration rises, successfully enabling the imaging of spermine in living cells. This approach provides a new pathway for visualizing spermine in biological systems.[156] Zhou and colleagues proposed a ''supramolecular cyclization-induced fluorescence enhancement'' strategy and designed a pillar[5]arene probe, P1, for spermine imaging. This design strategically arranges multiple spermine-binding sites on the pillar[5]arene, allowing it to form a cyclic host–guest complex with spermine, thereby restricting molecular motion and enhancing the fluorescence signals for imaging. The unique rigid cavity structure and well-designed binding site arrangement of pillar[5]arene are key elements for achieving specific recognition of spermine and supramolecular cyclization. Experimental results indicate that P1 has low detection limits and high selectivity for spermine, effectively detecting it in systems like acetonitrile and artificial urine. Notably, P1 demonstrates excellent performance in imaging, clearly presenting the distribution of spermine in relevant systems. This work provides a promising tool for the visual detection of spermine and early cancer diagnosis (Fig. 7c).[157]

Choline is an important neurotransmitter in the human body, closely related to nervous system functions and diseases such as Alzheimer's disease. Therefore, accurate detection of choline and monitoring of its enzymatic reactions are of critical significance in biomedical research. Hua *et al.* designed and

constructed a supramolecular host–guest fluorescent sensing system based on anionic WP6 and acridine orange (AO) (Fig. 7d).[158] The system utilizes the electron-rich rigid cavity of pillar[6]arene and its host–guest recognition properties to achieve response to choline compounds through the FID assay mechanism. When WP6 forms a complex with AO, charge-transfer interactions result in fluorescence quenching and a color change of the solution to red. Upon addition of choline compounds, these complexes displace AO through competitive binding, triggering ''turn-on'' fluorescence and yellow color change. Experimental results indicate that this system exhibits high selectivity for acetylcholine and choline. Additionally, they further constructed a supramolecular tandem enzyme assay that monitors the enzymatic reaction catalyzed by choline oxidase through the dual signals of fluorescence and color. By leveraging the binding affinity difference between the substrate (choline) and the product (betaine), this assay enables real-time tracking of the enzymatic reaction process. This method provides a new tool exhibiting both sensitivity and convenience for the visual detection of choline compounds and the monitoring of biological enzymatic reactions.

Given that ATP is a core energy molecule in life activities, its selective detection is crucial for cell metabolism research, disease diagnosis, and drug development. Bojtár *et al.* designed and constructed a supramolecular FID assay based on cationic water-soluble pillar[6]arene (AP6) and dapoxyl sodium sulfonate (DSS), realizing specific response and quantitative detection of ATP through host–guest recognition and competitive binding mechanisms.[159] Cationic AP6 forms a 1:1 complex with the anionic fluorescent dye DSS *via* electrostatic interactions. When DSS is partially embedded in the electron-rich cavity of AP6, intramolecular charge transfer is restricted, leading to significant fluorescence enhancement. Upon addition of ATP, its negatively charged triphosphate chain forms strong electrostatic interactions ($K_a = 4.45 \times 10^5$ M^{-1}) with the cationic sites of AP6, competitively displacing DSS. Solvation of free DSS after displacement results in fluorescence quenching, achieving a ''fluorescence turn-on to turn-off'' signal response. Furthermore, this system exhibits significantly higher selectivity for ATP over ADP, AMP, and GTP. As such, this method provides a sensitive and convenient supramolecular tool for the real-time monitoring of ATP-related diseases (such as cancer and neurodegenerative diseases).

Amino acids serve as fundamental molecules in life, and their precise detection is of critical significance in biomedical research, metabolic studies, and disease diagnosis. In particular the basic amino acids, arginine and lysine play pivotal roles in life, and their selective detection is essential for physiological function research, metabolic disease diagnosis, and biogenic amine monitoring. Bojtár *et al.* designed and constructed a supramolecular FID analysis system based on anionic water-soluble pillar[5]arene and aminonaphthalimide derivatives, achieving highly selective detection of arginine, lysine, and cadaverine through host–guest recognition and specific group regulation mechanisms.[160] Meanwhile, Wei *et al.* designed and synthesized a supramolecular fluorescent sensor BTAP5 based on functionalized pillar[5]arene, achieving highly selective and sensitive detection of L-tryptophan (L-Trp) through a mechanism of host–guest interaction forming an inclusion complex leading to fluorescence quenching.[161] Detection results indicate that BTAP5 has a detection limit as low as 2.83×10^{-7} mol L^{-1} for L-Trp in H_2O/DMSO (7:3, v/v) solution, with a binding constant of 9.69×10^3 M^{-1}. Significantly, among 20 natural amino acids, it only exhibited significant fluorescence response towards L-Trp without interference from other amino acids. They also used the cationic pillar[5]arene AWP5 as a supramolecular fluorescence based sensor to achieve highly selective and sensitive detection of L-methionine (L-Met) through a mechanism of host–guest interaction forming an inclusion complex leading to fluorescence enhancement.[162] The detection results indicate that the detection limit of AWP5 for L-Met in aqueous solution is as low as 5.46×10^{-7} mol L^{-1}, and among 20 natural amino acids, it only exhibits a significant fluorescence enhancement response towards L-Met without interference from other amino acids. The design of supramolecular sensors based on pillararenes using mechanisms such as host–guest recognition, anchoring group regulation, and fluorescence signal changes induced by inclusion complex formation, have resulted in highly selective and sensitive detection systems for different amino acids. Providing innovative tools and strategies for the precise detection of amino acids in biomedical research, metabolic analysis, and disease diagnosis.

4.3. Targeted bioimaging

The assessment and monitoring of kidney diseases are of great significance, but traditional imaging methods have obvious drawbacks, and ideal fluorescence imaging materials for kidneys are scarce. Yang and colleagues, using the rigid structure of pillar[5]arene, its simple synthesis, and ease of functionalization, developed a functionalized pillar[5]arene (P5DMP) with 10 positive charges for kidney-targeted imaging. The study found that P5DMP exhibits good photophysical properties, can self-assemble into a layered structure, be taken up by kidney-resident cells, and exhibits differential distribution across different cell types with high biocompatibility. The positive charge of the system enables it to specifically accumulate in the negatively charged glomerular filtration barrier (GFB), thereby achieving kidney-targeted imaging. *In vivo* imaging demonstrated that after intravenous injection, P5DMP accumulated specifically in the kidney, primarily concentrating in the glomeruli, with less accumulation in other kidney regions. In conclusion, P5DMP has excellent biocompatibility and strong kidney-targeted imaging capability, making it a promising material for kidney-targeted imaging, which could pave the way for early diagnosis of kidney diseases and holds potential for distinguishing different types of kidney lesions.[163]

In recent years, optimizing the performance of photosensitizer groups using IPAs to achieve high-efficiency tumor imaging has been a key research direction in the scientific community. The amphiphilic derivative of dicyanostilbene-

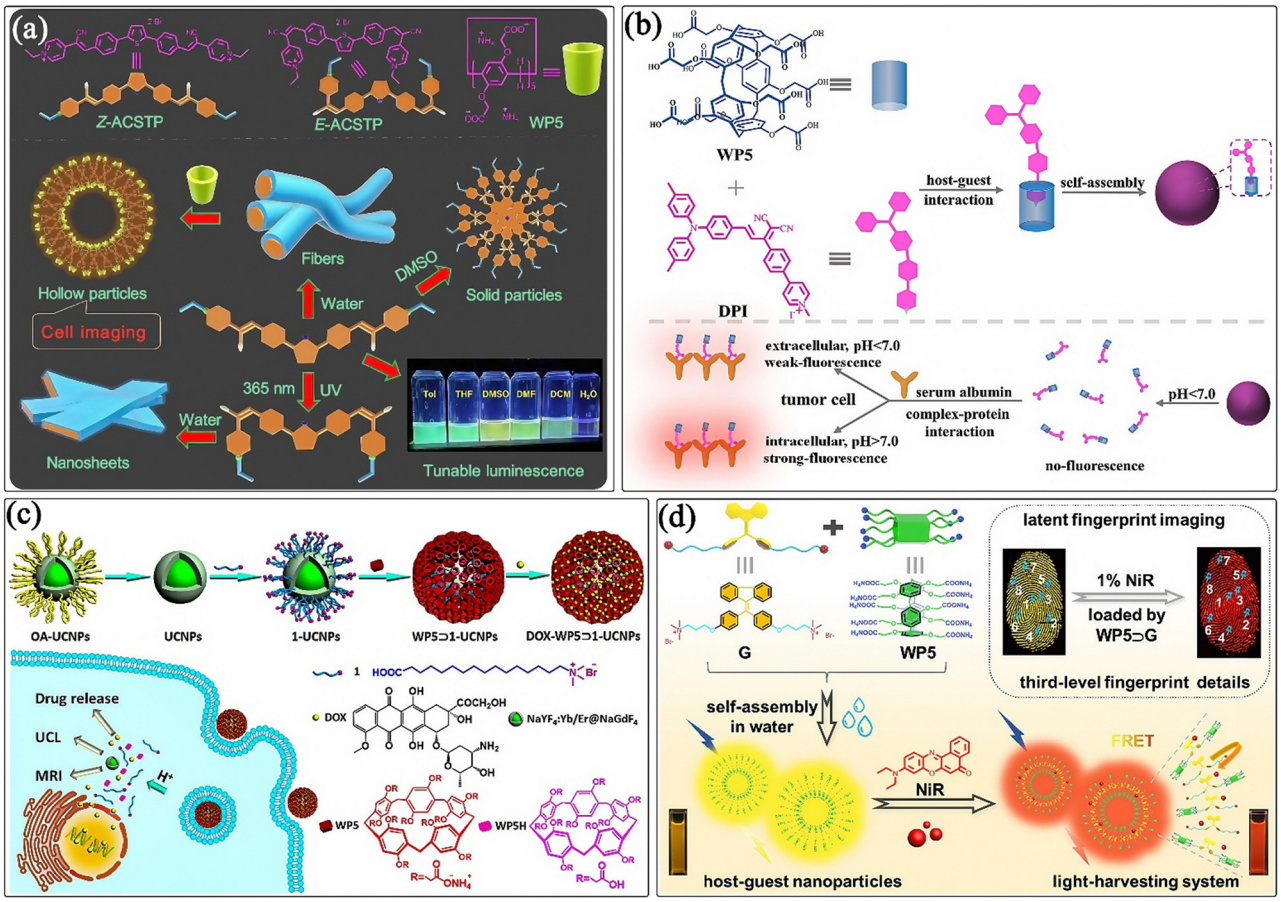

Fig. 8 IPAs are employed for bioimaging. (a) The schematic of a supramolecular assembled material with triple-responsive morphology and luminescence transformation constructed by combining an amphiphilic dicyanostilbene-functionalized thiophene derivative Z-ACSTP with WP5, and its application in cell imaging research (Reproduced with permission from ref. 164. Copyright 2023, Elsevier). (b) The schematic of the strategy for the construction of a pH-sensitive supermolecular fluorescent probe for albumin-mediated cell imaging (Reproduced with permission from ref. 169. Copyright 2023, Elsevier). (c) The schematic of a smart self-assembled nanosystem based on water – soluble pillararenes and rare-earth-doped upconversion nanoparticles for pH-responsive drug delivery, upconversion luminescence (UCL) imaging, and magnetic resonance imaging (MRI) (Reproduced with permission from ref. 171. Copyright 2018, American Chemical Society). (d) The schematic of the construction of a supramolecular light-harvesting system based on WP5 and TPE derivative G, and its application in fingerprint imaging (Reproduced with permission from ref. 174. Copyright 2023, The Royal Society of Chemistry).

functionalized thiophene, Z-ACSTP, exhibits strong fluorescence emission when dissolved in organic solvents, and its fluorescence can be adjusted using solvent polarity. However, in an aqueous solution, due to the hydrophobicity of its organic components, intermolecular aggregation occurs, triggering aggregation-caused quenching (ACQ) and resulting in a significant decrease of fluorescence intensity. Yao and colleagues constructed a complex through the host–guest interaction between the WP5 and the pyridinium group of Z-ACSTP (Fig. 8a).[164] This interaction inhibits the strong π–π stacking between Z-ACSTP molecules, reduces the non-radiative energy loss caused by molecular aggregation, and effectively improves the solubility of Z-ACSTP in water, thereby decreasing the degree of aggregation. At the same time, the pyridinium group inserts into the cavity of WP5, changing the electron cloud distribution of the Z-ACSTP molecule and optimizing the intramolecular charge transfer process. Ultimately, this significantly enhances its fluorescence intensity in water. In addition, they designed a series of 9,10-bis[(*E*)-2-(pyridin-4-yl)vinyl]anthracene derivatives, ENDT$_n$. ENDT$_n$ exhibits good solubility and fluorescence emission properties in organic solvents such as DMSO. However, in water, due to strong π–π stacking and hydrophobic interactions, molecular aggregation occurs, resulting in a significant weakening of the fluorescence intensity. However, by forming supramolecular amphiphiles with WP5 and ENDT$_n$, not only does it induce a nanomorphological transformation (for example, the microfiber structure of ENDT$_9$ is transformed into uniform micelles with an average diameter of approximately 90 nm), but it also changes the arrangement of the photosensitizer groups, promotes the formation of J-aggregates, and thus generates a new fluorescence emission peak at around 625 nm. This new emission region, located in the red fluorescence band, has important imaging advantages: compared with other bands, red fluorescence has a stronger penetration ability for biological tissues, can effectively reduce background fluorescence interference, and

provides higher-quality images for cell imaging.[165] These supramolecular imaging systems constructed based on IPAs all exhibit low cytotoxicity and excellent cancer cell imaging performance.

Aggregation-induced emission (AIE) molecules, which exhibit enhanced luminescence in the aggregated state and overcome the ACQ defect of traditional fluorescent probes, have become a research hotspot in tumor imaging. Their unique property of fluorescence ''turn-on'' through restricted intramolecular rotation provides a new strategy for high-contrast biological detection. On this basis, Huang's group designed and synthesized a cyanostilbene based AIE photosensitizer bearing a trimethylammonium group.[166] In water, this photosensitizer self-assembles into nanoribbons with low fluorescence intensity *via* π–π stacking and hydrophobic interactions. When the trimethylammonium group undergoes host–guest recognition with WP5 to form a 1 : 1 supramolecular amphiphile (WP5 ⊃ 1), the pillararene plays a dual role: firstly, its rigid cavity restricts the intramolecular rotation of the photosensitizer's aromatic rings, inhibiting non-radiative transitions; secondly, synergistic electrostatic and hydrophobic interactions induce the assembly to transform from nanoribbons into tightly packed spherical nanoparticles. This process significantly enhances near-infrared (NIR) fluorescence emission at 665 nm while improving water solubility and biocompatibility. In the mildly acidic TME, protonation of the carboxylate groups on WP5 leads to dissociation of the host–guest complex, causing the nanoparticles to collapse and quench fluorescence, thus achieving pH-responsive signal regulation. By leveraging the host–guest recognition properties and structural rigidity of pillararenes, this system systematically enhances the fluorescence efficiency and biocompatibility of the AIE photosensitizer through restricting molecular motion, regulating aggregation states, and enabling a responsive assembly. Therefore, this method provides a novel supramolecular probe design strategy for live-cell imaging responsive to the TME.

Tetraphenylethylene (TPE) is a typical AIE molecule. Due to its unique photophysical properties, it shows potential application value in fields such as biological imaging. Yu *et al.* made full use of the AIE characteristics of TPE and carried out a series of fruitful research works. First, they designed and synthesized a TPE derivative (G) containing a pyridyl guest group. They formed an inclusion complex with a monofunctionalized pillar[5]arene (H) through host–guest interactions, which restricted the intramolecular motion of the benzene rings in G, thereby enhancing the fluorescence emission. This assembly further self-assembled to form nanoparticles with an average diameter of about 43 nm. These nanoparticles have good cell penetration and low cytotoxicity and have been successfully applied for cell imaging.[167] Meanwhile, they synthesized TPE derivatives (TPE-NP and TPE-PQ) containing four guest groups. They used charge-transfer (CT) interactions to make TPE–NP and TPE–PQ self – assemble into 1D nanorods, significantly enhancing the AIE effect. To reduce the toxicity of TPE–PQ, a water-soluble pillar[6]arene (H) was introduced to form a stable inclusion complex. Based on the pH-responsiveness of H, a ternary system composed of H, TPE–NP, and TPE–PQ was constructed, which achieved specific imaging of cancer cells.[168] This research not only provided new ideas and methods for the development of high-performance biological imaging materials but also further expanded the application scope of TPE and pillararenes in the biomedical field.

As the most abundant plasma protein in the human body, HSA shows abnormal enrichment in tumor tissues due to the high vascular permeability (EPR effect). The unique acidic pH of the TME results in a significant difference from the weak alkalinity of normal tissues, providing a crucial biological basis for the design of targeted imaging. Xu and colleagues constructed a supramolecular fluorescent probe WP5 ⊃ DPI based on WP5 and an intramolecular charge transfer (ICT) probe DPI. This system uses the host–guest recognition ability of WP5 and its pH-responsive properties to encapsulate DPI, which exhibits ''fluorescence turn-on'' towards BSA (a homologous model molecule of HSA). In the weakly alkaline environment of normal tissues, WP5 ⊃ DPI maintains a compact conformation, and the fluorescence signal is suppressed to reduce background interference. However, when the probe enriches in tumor tissues with the blood circulation, the acidic microenvironment triggers the release of DPI from WP5 which specifically binds to the high-concentration of BSA at the tumor site. Then due to the ICT effect, a strong fluorescence signal is activated, achieving ''environment-responsive'' precise imaging. This design not only solves the problem of fluorescence quenching caused by the aggregation of traditional probes through host–guest interactions, but also uses the passive targeting property of HSA in tumors (EPR effect) and the pH difference of the microenvironment to construct a ''double screening'' mechanism. The fluorescence is only turned on under the conditions of HSA enrichment and an acidic environment, significantly improving the specificity and contrast of imaging (Fig. 8b).[169] Wang and colleagues synthesized a novel HSA-sensitive ICT probe MBD by modifying the fluorescent agent MPM and further constructed a WP5–MBD complex for cell imaging and drug delivery. This design retains the strong binding ability between MPM and HSA while incorporating alkyl chain cations to enable a response with albumin. WP5 also, plays a role in constructing smart drug carriers. The WP5–MBD complex is stable and exhibits good interference resistance. Experimental results indicate that the WP5–MBD complex can self-assemble into nanoparticles, has strong doxorubicin (DOX) encapsulation capacity, and exhibits stronger cytotoxicity against cancer cells, providing a new approach for imaging-guided precise chemotherapy.[170]

Upconversion luminescent materials can absorb low-energy light (such as NIR light) and emit high-energy light (such as visible or ultraviolet light). These materials have excellent bioimaging properties, especially exhibiting significant advantages for deep tissue imaging and light penetration within biological organisms. They have shown great potential in the biomedical field, particularly in tumor imaging and drug delivery. IPAs can form effective complexes with upconversion luminescent materials, thus enhancing their imaging

performance and biocompatibility. Li and colleagues successfully modified upconversion nanoparticles (1-UCNPs) with 15-carboxyl-*N*,*N*,*N*-trialkyl-15-octadecyl-1-bromonium to interact with carboxylate pillar[5]arenes (WP5) *via* host–guest complexation, resulting in WP5⊃1-UCNPs nanocomplexes. The study indicated that under acidic conditions, WP5 can be protonated, leading to the collapse of the nanocomplex and drug release, allowing effective entry into human cervical cancer cells (HeLa) and accumulation of drugs inside the cells. This system exhibits excellent pH-responsive drug release performance and cellular uptake ability. Additionally, the nanocomplex provided significant contrast enhancement in T_1-weighted magnetic resonance imaging (MRI) (Fig. 8c).[171] Meanwhile, Xu and colleagues applied a similar ligand exchange method to modify phosphoryl pillar[5]arenes (PP5) on β-$NaYF_4$:Yb/Er nanoparticles (OA-UCNPs), obtaining PP5–UCNPs. They loaded the system with Rhodamine B (RhB) or 5-amino salicylic acid (5-ASA), successfully achieving controlled drug release and cellular imaging under different pH conditions, illustrating promising results in the construction of pH-responsive drug delivery systems and cellular imaging.[172] To address the issue of low thermoelastic expansion efficiency in photoacoustic imaging, Yu *et al.* innovatively designed a supramolecular hybrid material system based on graphene oxide (GO) and a pillar[6]arene host–guest complex (CP6⊃PyN). The design concept was to form a host–guest complex CP6⊃PyN using pillar[6]arene CP6 and amphiphilic molecule PyN, and then modify the surface of GO through π–π stacking and host–guest interactions to construct the hybrid material GO@CP6⊃PyN. In this system, pillararene plays a crucial role: on the one hand, the host–guest complex CP6⊃PyN based on pillar[6]arene increases the absorption of the hybrid material in the NIR region, enhancing the photothermal effect; while on the other hand, the bicarbonate counterions it carries decompose to generate CO_2 nanobubbles under NIR light excitation. These nanobubbles act as ''molecular boosters'' to significantly enhance the ultrasound and photoacoustic signals. The research results indicate that GO@CP6⊃PyN exhibits excellent photothermal performance, enhanced ultrasound and photoacoustic imaging effects, and good biocompatibility. Thus it exhibits great potential in diagnostic and therapeutic applications and provides an effective strategy for the development of new imaging nanomaterials.[173]

4.4. Biometric identification

In the fields of forensic science and biometrics, fingerprint recognition technologies currently rely on physical contact methods (such as capacitive/optical sensors), non-contact methods (such as ultrasonic waves), and traditional chemical development methods. However, these technologies generally face bottlenecks such as signal attenuation caused by ACQ, insufficient resolution in complex scenarios (only able to recognize Level 1–2 ridge features), and poor adaptability to multiple substrates. With the increasing requirement for imaging of Level 3 microscopic structures such as sweat pores in criminal investigation and physical evidence detection, as well as the specific requirements for material compatibility when achieving portable imaging through the screens of smart terminals, it has become crucial to develop a new fingerprint development system that has both anti-quenching performance, an efficient energy transfer mechanism, and the ability to adapt to multiple scenarios.

Xiao and colleagues designed and constructed a red-emitting supramolecular light-harvesting system for latent fingerprint imaging, based on the host–guest self-assembly of WP5 and TPE-derived guest (G). The system utilizes the AIE properties of G to form strong fluorescent nanoaggregates with WP5 and achieves red emission *via* Förster resonance energy transfer (FRET), with 1% Nile Red serving as the energy acceptor to significantly enhance the red wavelength emission. This design not only solves the common ACQ effect, but also provides high-contrast fingerprint imaging with clear 1–3 level details, such as core points, bifurcations, and sweat pores. Experimental results indicate that the optimal molar ratio of WP5 to G is 0.3 : 1. With the introduction of Nile Red, the energy transfer efficiency reaches 60.9%, and the antenna effect is 12.35. The system enables high-resolution imaging on various substrates, offering a powerful tool for biometric identification and opening new directions for the development of related fluorescent materials and latent fingerprint imaging applications (Fig. 8d).[174]

This section summarizes the latest research progress of IPAs in the fields of fluorescence sensing and bioimaging. Leveraging their unique characteristics such as charge modulation, molecular recognition, and supramolecular assembly, IPAs provide new methods for the analysis of environmental pollutants, detection of bioactive substances, and observation of biological systems. However, many issues remain to be explored in depth. For instance, the mechanism of specific adsorption for IPAs in complex biological environments remains to be further elucidated; strategies to enhance the detection sensitivity and anti-interference capability of IPA-based systems for target analytes in complex natural environments or the human body are needed; and biological safety issues of these systems, particularly the evaluation of potential hazards, must be addressed. Looking ahead, IPAs may bring about breakthrough advancements in precise disease diagnosis and rapid detection of environmental pollutants, enabling more accurate and efficient monitoring of the microscopic world within biological organisms and the external environment.

5. IPAs-based supramolecular antidotes

The accumulation of abnormal amounts of toxic metabolites (products of abnormal secretion or metabolism) in the human body or exogenous toxins from the environment can lead to severe organ damage and the development of various pathologies, ultimately threatening human life and health. At the same time, environmental toxins such as pesticide residues easily cause water resource and soil pollution. This not only has a

huge impact on crops and the ecological environment but also directly exerts various adverse effects on human health through various channels, such as developmental toxicity, immune dysfunction, immunotoxicity, and chronic diseases. In addition, in clinical medicine, neuromuscular blockers and heparin play important roles in clinical surgeries. However, their side effects often have an adverse impact on patients' postoperative recovery and overall prognosis. Reducing the side effects of these two types of drugs is of great significance for improving the success rate of surgeries, ensuring patient safety, and promoting patients' postoperative rehabilitation. Currently, many methods have been studied to remove, reduce, or transform these toxic substances, aiming to minimize the impact of the toxic substances on the environment and human life and health. Among the numerous methods, macrocyclic molecules have become an emerging research hotspot by virtue of their specific recognition and assembly with toxic substances to facilitate the removal of toxic substances. Among them, IPAs have the ability to specifically recognize and efficiently remove many toxic molecules. In this section, we will focus on introducing the research progress for the application of IPAs as supramolecular antidotes.

To meet the demands of the ever increasing population for food and agricultural products, a large amount of pesticides and fertilizers are used during agricultural production. Although they can effectively prevent and control pests and diseases and provide nutrients for crop growth, the excessive application of compounds such as PQ and glyphosate has triggered many problems, including pesticide residues in food that endanger human health, damage to the physical and chemical properties of the soil, weakening of soil fertility, and pollution of water resources, which disrupts the aquatic ecosystem. Among them, PQ has a unique molecular structure. Its chemical name is 1,1′-dimethyl-4,4′-bipyridinium dichloride. It consists of two pyridine rings connected by the 4,4′-position, with a methyl group attached to each 1,1′-position, forming a bipyridinium cation structure. This gives it good water solubility, enabling it to be quickly transported within plants with the help of water. In terms of chemical properties, when the pyridine rings are exposed to light and oxygen, the distribution of electron cloud density makes it prone to redox reactions, generating a large number of free radicals. These free radicals are not only the key to its herbicidal effect but also an important cause of its high toxicity to organisms. They will attack various biological molecules within cells, damaging the structure and function of cells. Yu *et al.* found that carboxylate-functionalized pillar[6]arene (WP6) has an extremely strong complexation ability with PQ. It can form a stable 1 : 1 [2]pseudorotaxane with PQ through electrostatic interactions, hydrophobic interactions, and π–π stacking interactions, and its association constant is as high as $(1.02 \pm 0.10) \times 10^8\ M^{-1}$. In terms of removal potential for PQ in biological systems, the stable host–guest complex formed by WP6 and PQ plays a crucial role. It not only reduces the contact opportunities between PQ and intracellular reducing agents, significantly decreases the generation of PQ radical cations, and thus effectively reduces the toxicity of PQ.[175] Nazarova *et al.* synthesized the ester derivative and betaine derivative of pillar[5]arene containing L-tryptophan residues. This derivative has the characteristics of being able to self-assemble and interact with multiple herbicides. Among them, the betaine derivative has lower toxicity to A549 and LEK cell lines, and its binding constant with PQ is $\log K_a = 3.17$. In terms of removing PQ from the environment, this derivative exhibits significant application value.[176] Yang *et al.* designed and synthesized a material based on supramolecular coordination polymers Zn^{2+}@WP5 and Zn^{2+}@WP6 using carboxylated pillar[5]arenes (WP5) and carboxylated pillar[6]arenes (WP6) in combination with zinc ions. This material exhibits an amorphous structure, a high specific surface area, a negatively charged surface, high-efficiency adsorption of PQ, and regenerability based on guest exchange. Among them, Zn^{2+}@WP5 has a stronger adsorption ability for PQ due to its high specific surface area. In terms of removing PQ from water systems, Zn^{2+}@WP5 can adsorb approximately 98% of PQ within 1 minute. Moreover, the adsorption amount of PQ by Zn^{2+}@WP5 from tap water and river water can also reach 90%, exhibiting great potential for real water sample treatment.[177] Li *et al.* engineered a novel supramolecular scavenger by conjugating carboxylate-functionalized pillar[6]arene (WP6) to a Janus dendritic amphiphile (JDA) platform, which was then anchored onto red blood cells (RBCs) *via* a vesicle-cell interaction strategy. The JDA molecule features dual C18 lipid chains for membrane insertion and three pyridinium moieties that thread WP6 through electrostatic interactions, forming a stable WP6@JDA complex. This complex was preassembled into vesicles (763 nm diameter) that efficiently coat RBCs surfaces, leveraging the natural biocompatibility and long-circulating properties of erythrocytes (half-life ∼ 120 days). The WP6 component, with its negatively charged outer rim and hydrophobic cavity, specifically recognizes PQ through electrostatic and π–π stacking interactions (association constant $K_a = 3.25 \times 10^5\ M^{-1}$), forming a nontoxic inclusion complex. The RBC-anchored scavenger demonstrated dual functions: (1) continuous PQ hunting in plasma *via* dynamic host–guest exchange reactions, and (2) targeted delivery to PQ-accumulating organs like lungs and kidneys. *In vivo* studies showed a 75% reduction in blood PQ levels within 4 h post-injection, with significant mitigation of pulmonary fibrosis (W/D ratio reduced by 38%) and renal damage compared to free WP6 treatment. This RBC-based supramolecular system represents a paradigm shift in toxin removal by combining specific molecular recognition with natural cell-based delivery, offering prolonged detoxification and improved therapeutic outcomes for PQ poisoning (Fig. 9a).[178]

With the development of industrialization, fluoride ions and fluorine-containing compounds are widely present in water and soil in the environment. These fluorine-containing substances are persistent and can accumulate in plants and animals, posing a serious threat to ecological stability and human life and health. Chen *et al.* constructed a multi-stage porous nanochannel membrane composed of microscale etched

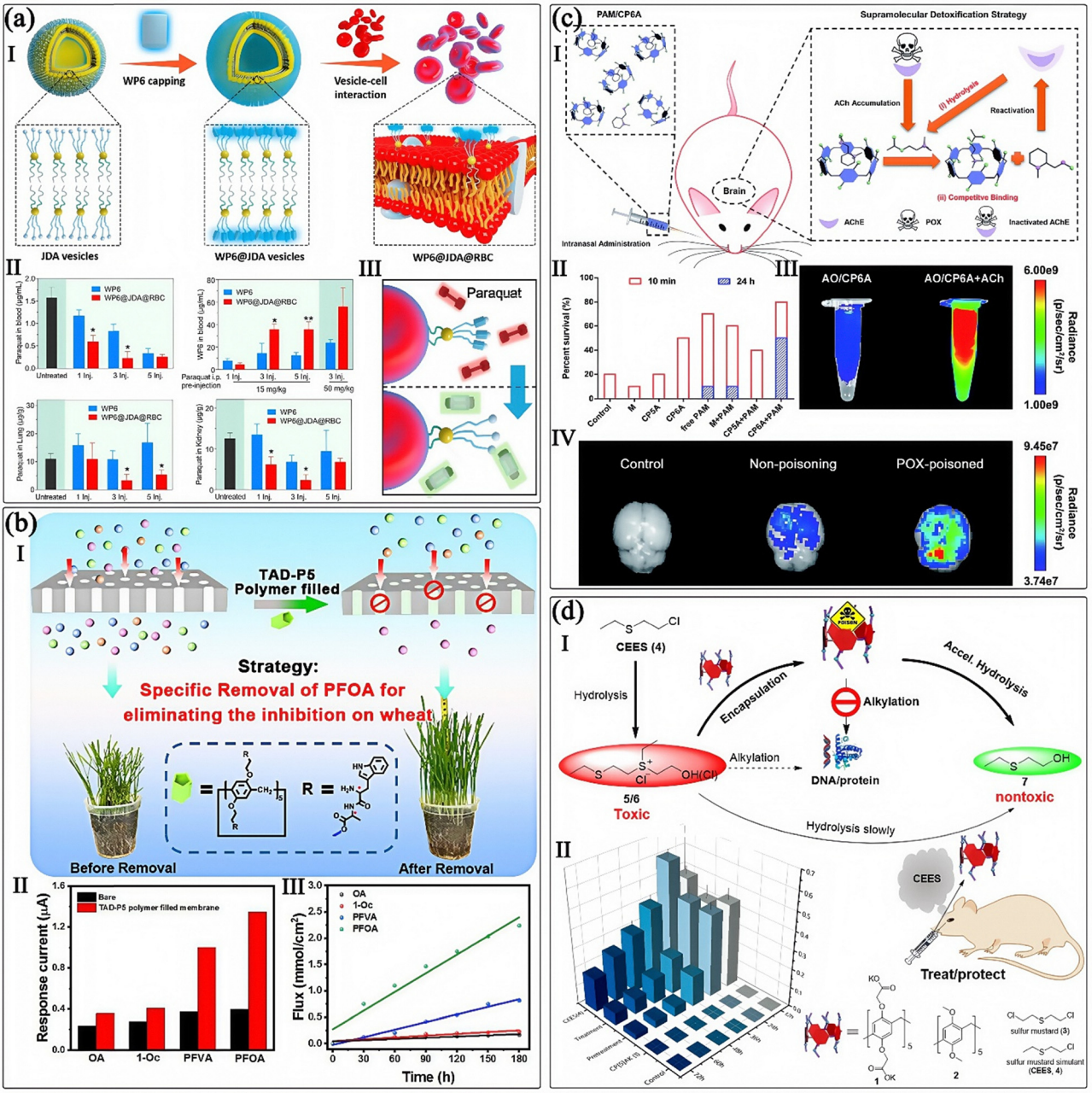

Fig. 9 IPAs are used to remove toxic substances from the body or the environment. (a) Supramolecular "hunters" residing on RBCs based on specific molecular recognition are used to remove PQ from the blood: (I) the schematic of loading WP6 onto RBCs *via* vesicle–cell interaction. (II) and (III) Demonstrated that the constructed supramolecular hunter WP6@JDA@RBC can effectively reduce the PQ concentration in the blood, and also illustrates the working principle (Reproduced with permission from ref. 178. Copyright 2020, American Chemical Society). (b) Specific removal of perfluorooctanoic acid based on pillar[5]arene-polymer-packed nanochannel membrane: (I) the schematic of the specific transport of the perfluorooctanoic acid based on tryptophan–alanine dipeptide pillar[5]arene packed. (II) and (III) Demonstrated that the TAD–P5 polymer-filled membrane has a specific removal effect on PFOA (Reproduced with permission from ref. 180. Copyright 2023, American Chemical Society). (c) IPAs synergistically enhance the emergency treatment effect of organophosphate poisoning: (I) the schematic of the supramolecular detoxification strategy, in which acetylcholine (ACh) triggers the release of pralidoxime (PAM) to reactivate acetylcholinesterase (AChE), while pillar[6]arene (CP6A) can sequester acetylcholine to inhibit its overstimulation of the acetylcholinesterase receptors. (II) Survival rates of rats poisoned with POX after treatment with different groups. (III) and (IV) Showed that by monitoring the dynamic changes in fluorescence signals during the assembly and disassembly of AO and CP6A, it was indirectly proven that CP6A can participate in alleviating the adverse physiological reactions caused by POX poisoning in the brain region (Reproduced with permission from ref. 182. Copyright 2021, The Royal Society of Chemistry). (d) Carboxylatopillar[5]arene potassium salt (CP[5]AK 1) is used to effectively detoxify the sulfur mustard simulant 2-chloroethyl ethyl sulfide (CEES, 4) *in vitro* and *in vivo*. (I) The schematic of the detoxification mechanism. (II) CP[5]AK 1 can effectively reduce the internal corneal damage caused by CEES (Reproduced with permission from ref. 184. Copyright 2021, American Chemical Society).

nanochannels and nanoscale pillar[5]arene cross-linked polymer voids. The electrostatic interactions and hydrogen bonds formed between the branched chain groups of pillar[5]arenes and fluoride ions enable the membrane to effectively adsorb fluoride ions. The removal rate of this membrane for fluoride ions reaches 0.0088 mmol L^{-1} min^{-1}, which is 6–8.8 times faster than that of other control ions. Rice cultivation experiments have demonstrated that the solution treated by this membrane is beneficial to the growth of rice.[179] Xu *et al.* constructed a nanochannel membrane filled with tryptophan–alanine dipeptide pillar[5]arene polymer. The fluorine–hydrogen bonds between this membrane and perfluorooctanoic acid (PFOA) and multiple binding sites within the nanochannels result in a strong interaction. As a result, the supramolecular nanochannel membrane has a removal rate of 0.01 mmol L^{-1} min^{-1} for PFOA, which is 4.5–15 times faster than that of other control chemicals. It has a high recognition ability and selective transport and elimination ability for PFOA, effectively alleviating the growth inhibition of wheat by PFOA (Fig. 9b).[180] Gao *et al.* discovered that there are electrostatic interactions and fluorophilic interactions between deca-ammonium-functionalized pillar[5]arenes (DAFP5s) and polyfluoroalkyl acids, and they combine in a stoichiometric ratio of 1 : 10 with a binding constant as high as 10^6 M^{-1}. The adsorbent prepared by immobilizing DAFP5s on resin can reduce the concentration of PFOS/PFOA in polluted water by 106 times to the level of 15–50 ng L^{-1} within 5 minutes. It has a high adsorption capacity (90 mg g^{-1}) and good regeneration performance (no performance decline after more than 10 regeneration cycles), and is not affected by non-fluorinated organic acids. It can effectively purify a variety of environmental water samples, bringing new directions for the remediation of PFAS-polluted water bodies.[181]

Poisoning by organophosphorus compounds (OPs) is a serious public health problem worldwide. These compounds can irreversibly inhibit acetylcholinesterase (AChE), leading to the accumulation of acetylcholine (ACh) and subsequent overstimulation of acetylcholine receptors. Chen *et al.* designed a supramolecular detoxification system aiming to deliver pyridine-2-aldoxime methochloride (PAM) through host–guest encapsulation to synergistically inhibit the hyperstimulation caused by acetylcholine. The implementation results show that the complexation of CP6A helps to improve the reactivation efficiency of PAM on acetylcholinesterase. *In vivo* experiments indicate that the PAM/CP6A complex significantly enhances the ability of PAM, which can not only relieve seizure symptoms in rats but also increase the survival rate of paraoxon-poisoned model rats (Fig. 9c).[182] The excessive use of glyphosate-based herbicides can cause severe damage to the genetic material of organisms, leading to DNA damage in fish, amphibians, and human lymphocytes. Nazarova *et al.* utilized low-toxicity pillar[5]arenes containing amino acid residues (GlyGly and L-Phe) to develop a new method for DNA protection against the damage caused by glyphosate isopropylamine salt (GIS). The research indicates that GIS can bind tightly to the DNA of salmon sperm. Although the synthesized pillar[5]arene derivatives do not interact with GIS, the betaine derivative of pillar[5]arene containing L-phenylalanine fragments exhibits significant inhibitory effects through its stronger binding ability to DNA, and can effectively prevent the interaction between GIS and DNA. This discovery illustrates the potential application value of betaine derivatives of pillar[5]arenes in protecting nucleic acids through competitive binding with biomacromolecules, providing approaches for solving the problem of DNA damage caused by glyphosate-based herbicides.[183]

Sulfur mustard (HD), a highly toxic chemical compound historically utilized as a chemical warfare agent, continues to pose significant risks to human health and ecological systems due to residual contamination. Given the absence of specific pharmacological treatments or antidotes for HD poisoning, the development of targeted countermeasures remains a critical priority in contemporary toxicology and public health domains. Zhou *et al.* conducted a supramolecular detoxification study on the sulfur mustard simulant CEES (4) both *in vitro* and *in vivo* using carboxylatopillar[5]arene potassium salts (CP[5]AK 1) based on host–guest interactions. The encapsulation of CEES (4) by CP[5]AK 1 was confirmed through ^{1}H NMR titration, density functional theory (DFT) studies, and independent gradient model (IGM) studies. Cell and animal experiments indicated that CP[5]AK 1 can effectively inhibit the bioactivity of sulfonium salts and has a good therapeutic effect on the damage caused by CEES (4). Due to its low cytotoxicity and remarkable therapeutic effect, anionic pillar[5]arenes are expected to be developed into specific antidotes against sulfur mustard (Fig. 9d).[184] Nitrogen mustard (NM), which has a similar structure to sulfur mustard, is often used as a chemotherapeutic drug for treating cutaneous lymphoma. Due to its dose-dependent toxicity, especially cutaneous toxicity, it still poses a threat to public health. NM degrades into reactive aziridinium salts in an aqueous phase. These salts can irreversibly alkylate DNA and proteins, thus causing severe tissue damage. Zhou *et al.* used carboxylatopillar[5]arene potassium salts (CP[5]AK) to encapsulate the toxic aziridinium salts, and the association constant between them is as high as 4.10×10^4 M^{-1}. The experimental results show that the formation of the resulting complex can effectively inhibit the alkylation of DNA and has a good therapeutic effect on the damage caused by NM.[185]

Neuromuscular blocking agents are a class of drugs widely used in clinical anesthesia to relax skeletal muscles, meeting the requirements for muscle relaxation during surgery and playing a crucial role in ensuring the smooth progress of surgery. However, some neuromuscular blocking agents can cause a variety of adverse effects after use. For example, succinylcholine (Sch) can lead to serious side effects such as hyperkalemia, arrhythmia, and even cardiac arrest, posing a great risk to patients. Therefore, it is necessary to take effective measures promptly to reduce the damage caused by these neuromuscular blocking agents. The research by Zhang *et al.* shows that water-soluble carboxylatopillar[6]arene has a high binding affinity with Sch. In mouse and rat models, it can effectively reverse multiple side effects induced by Sch, such as

reducing mortality, alleviating arrhythmia, inhibiting hyperkalemia, and reducing rhabdomyolysis. It can also reverse the depolarization induced by Sch at the cellular level and reduce the efflux of intracellular potassium ions.[186] According to the research of Chai *et al.*, carboxylatopillar[6]arene (CP6A) has a strong binding affinity with the classic depolarizing muscle relaxant decamethonium (C10), with an association constant of $(1.070 \pm 0.14) \times 10^7$ L mol^{-1}. In a mouse model, intravenous injection of CP6A can accelerate the metabolism of C10 from the blood to the urine, effectively shortening the recovery time of muscle relaxation.[187]

In addition, Zhao *et al.* designed seven anionic pillar[5]arenes (AP5As) with different aliphatic chains and anionic groups. The research results indicate that there is a strong interaction between AP5As and the neuromuscular blocking agent decamonium bromide (DMBr). Among them, PC4 and PC5 have the highest reversal efficiency for DMBr, and AP5As exhibit low toxicity and high biocompatibility.[188] Shurpik *et al.* synthesized a water-soluble pillar[5]arene containing thioether and carboxylate fragments. The research results indicate that this pillar[5]arene can form a 1:1 inclusion complex with the muscle relaxant rocuronium bromide, with an association constant of 4500 M^{-1}. For *in vitro* and *in vivo* experiments, it can restore the muscle contraction inhibited by rocuronium bromide as effectively as Sugammadex, demonstrating the potential of water-soluble pillar[5]arenes in reversing neuromuscular blockade (Fig. 10a).[189]

Heparin is an anionic polysaccharide widely used as an anticoagulant in clinical practice. However, when using heparin, effective detection and antidotes are required to ensure safe operations during and after surgeries. Välimäki *et al.* designed and synthesized a series of cationic macrocycles in order to evaluate their binding and sensing properties towards heparin. The research found that multivalency plays a crucial role in the electrostatic binding between macrocyclic hosts and heparin (Fig. 10b). P10+ (trimethylammonium pillar[5]arene) and R16+ (resorcin[4]arene with multiple ammonium groups), which carry more positive charges, exhibit good binding with heparin and can effectively neutralize heparin. Among them, P10+ shows the best performance. Multiple experimental methods have indicated that the host–guest binding between P10+ and methyl orange does not affect its binding with heparin. Moreover, the host–guest system constructed based on this can be used to monitor the heparin concentration, and corresponding calibration curves can be obtained at different plasma concentrations. This study provides a deeper understanding of the application of macrocyclic receptors in signalling systems and is expected to promote the development of supramolecular host–guest-polymer systems in the biomedical field.[190]

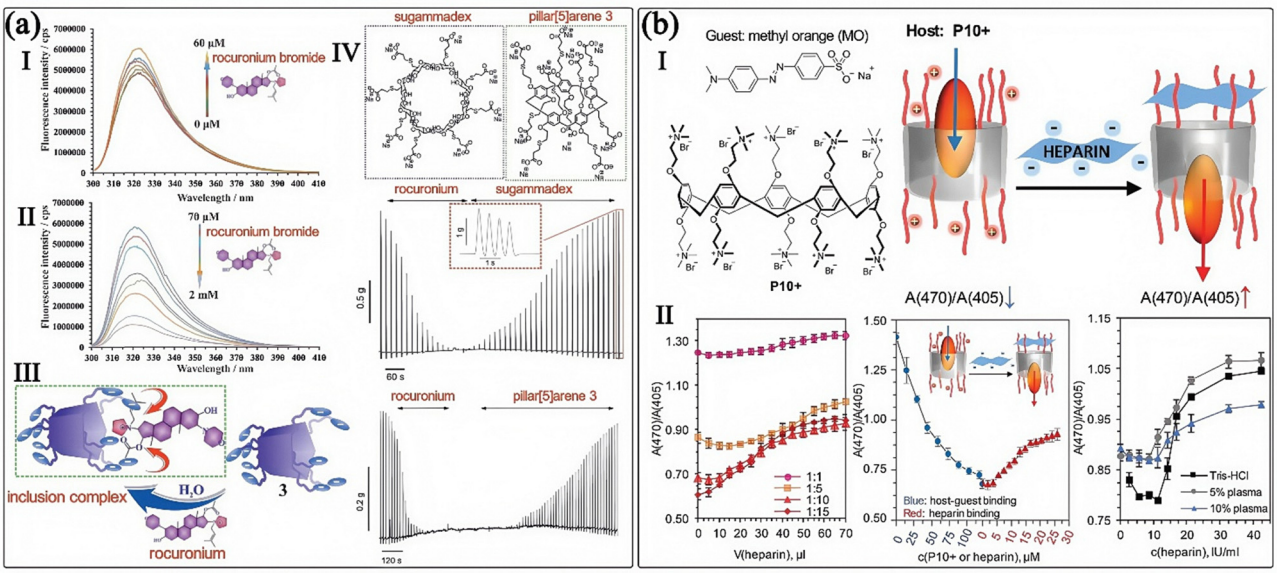

Fig. 10 IPAs are used to reduce the adverse effects of clinical drugs (such as neuromuscular blockers and heparin). (a) Supramolecular neuromuscular blocker inhibition by a pillar[5]arene through aqueous inclusion of rocuronium bromide: (I) and (II) Indicated that with the addition of different concentrations of rocuronium bromide, the fluorescence value of pillararene changes significantly, suggesting that pillararene 3 can interact strongly with rocuronium bromide. (III) The diagram of the host–guest interaction mechanism between pillararene 3 and rocuronium bromide. (IV) Representative record diagram of muscle contraction under the action of rocuronium bromide and subsequent recovery after application of either sugammadex or pillar[5]arene 3. It indicates that pillar[5]arene 3 has a stronger ability to reverse the muscle contraction inhibition induced by rocuronium bromide (Reproduced with permission from ref. 189. Copyright 2019, The Royal Society of Chemistry). (b) A supramolecular host–guest complex for the binding and sensing of heparin constructed based on IPAs: (I) diagram of the mechanism of the host–guest complex for binding heparin. (II) Studied the process of monitoring the binding of methyl orange (MO) to heparin by detecting its release from the host–guest complex. Specifically, it explored the effects of different molar ratios and individual concentrations of methyl orange and P10+, as well as the performance of this monitoring method under different plasma concentrations, and evaluated the feasibility of the system for monitoring the binding of methyl orange to heparin (Reproduced with permission from ref. 190. Copyright 2018, The Royal Society of Chemistry).

In conclusion, in the research field of supramolecular antidotes, IPAs exhibit exceptional advantages due to the precision of their molecular recognition and the diversity of their functional expansion. As a class of rigid macrocyclic hosts, IPAs achieve specific capture and efficient removal of environmental toxins (such as pesticides and fluorides) and clinical drugs (such as neuromuscular blocking agents) through charge complementarity (such as the electrostatic interaction between carboxylate and PQ cations) and cavity adaptation (such as the capture of perfluoroalkyl acids by hydrophobic cavities). This ''molecular sponge'' property not only blocks the harmful interactions between toxins and biological targets (such as inhibiting the oxidative damage induced by PQ and reversing the anticoagulant effect of heparin), but also endows them with biocompatibility for *in vivo* delivery through water-solubility modifications (such as red blood cell membrane anchoring and amphiphilic molecule assembly), providing a new approach to solve the problems associated with low selectivity and strong side effects of traditional antidotes.

However, research in this field still faces many challenges: (i) Interference from competition with biomolecules: high concentrations of natural substrates in the body (such as nucleic acids and proteins) may compete with toxins for binding to IPAs, reducing the antidote efficiency. It is necessary to improve the anti-interference ability by introducing multivalent recognition sites or designs with steric hindrance. (ii) Controllability of the dynamic antidote process: existing IPAs systems mostly rely on static host–guest binding, lacking dynamic regulation of the entire process of toxin ''capture–transport–metabolism'', making it difficult to deal with persistent poisoning or multi-stage drug side effects. (iii) The potential toxicity of long-term *in vivo* use (such as the immunogenicity of nanocarriers) and the excretion mechanism of the complexes after detoxification are still unclear. In the future, if breakthroughs can be made in adapting to the biological complexity and verifying clinical practicality, this class of supramolecular systems is expected to be more widely applied in clinical scenarios such as emergency treatment of poisoning and the regulation of drugs after surgery.

6. Antimicrobial activity of IPAs

In the field of modern biomedical research, the increasing resistance of pathogenic microorganisms to antibiotics is becoming a global issue for humanity. In recent years, more and more research results have shown that bacteria in bacterial biofilms have lower sensitivity to antibiotics (reduced by at least three orders of magnitude) compared to planktonic bacteria (bacteria growing in suspension). The existence of biofilms greatly reduces the therapeutic effect on clinical diseases caused by bacterial infections. Most of the approved antibiotic drugs currently target very limited sites such as DNA synthesis, protein synthesis, membrane integrity, or cell wall biosynthesis of pathogenic microorganisms. However, these therapeutic mechanisms are gradually being counteracted by numerous and increasingly common resistance mechanisms, that prompts scientists to continuously develop new methods in the fight against infectious diseases.

Among numerous novel functional molecules, macrocyclic compounds stand out due to their unique structural features and antibacterial mechanisms. Their core advantage lies in the precise intervention of key bacterial targets through molecular design: (i) Membrane-targeted disruption: the rigid cyclic structure of macrocyclic molecules can form specific interactions with lipid or protein components of the bacterial cell membrane (such as lipopolysaccharides and phospholipid bilayers). By inserting into the membrane structure, they disrupt its integrity, leading to the leakage of intracellular substances. (ii) Inhibition of biofilm formation: the multivalent binding ability of macrocycles (such as the synergistic action of multiple hydrophobic or charged sites) can block the recognition of bacterial quorum sensing signalling molecules and inhibit the synthesis and assembly of biofilm matrices (such as extracellular polysaccharides). (iii) Evasion of antibiotic resistance: unlike the single-target mechanism of traditional antibiotics, macrocyclic molecules can act through physical disruption (membrane damage) or multi-pathway interference (such as simultaneously affecting membrane function and intracellular signal transduction), reducing the probability of resistance development. (iv) Delivery and synergistic enhancement: the cavity of macrocycles can serve as a drug carrier to encapsulate antibiotics, achieving targeted delivery through host–guest interactions. Meanwhile, their own membrane-penetrating ability can enhance the penetration efficiency of antibiotics against drug-resistant bacteria.

As a new class of macrocyclic hosts, IPAs perfectly conform to the above antibacterial design principles and exhibit unique advantages. Their rigid columnar skeletons provide precisely tunable molecular sizes and cavity structures. By modifying cationic groups (such as quaternary ammonium salts) or anionic groups (such as carboxylates), IPAs can form strong electrostatic interactions with negatively charged (such as lipopolysaccharides) or positively charged components on the surface of the bacterial cell membrane, directly inserting into and disrupting the membrane structure (as demonstrated by studies showing the selective permeation of IPAs through the outer membrane of Gram-negative bacteria). Meanwhile, the multi-functional group modification ability of IPAs allows the introduction of hydrophobic side chains or antibacterial peptide fragments, enhancing the efficiency of membrane disruption through synergistic effects. Their cavities can also encapsulate antibiotic molecules (such as vancomycin and tetracycline), enabling sustained drug release and targeted enrichment through host–guest interactions, effectively reversing antibiotic resistance caused by biofilms. In addition, the water solubility and biocompatibility of IPAs make them suitable for *in vivo* antibacterial applications while avoiding the toxicity issues of traditional macrocyclic molecules. These characteristics make IPAs an ideal molecular platform for breaking through the resistance dilemma and developing novel antibacterial strategies.

In this section, we will describe the development of IPA-based antimicrobial agents, as well as the structural design and antimicrobial properties of related supramolecular materials.

6.1. Unimolecular IPAs for antimicrobial activity

Some cationic IPAs can be inserted into bacterial membranes to form ion channels or attach to bacterial membranes by electrostatic interaction with negatively charged groups such as carboxylates, sulphates, and phosphates on the bacterial membranes. Such processes can result in bacterial membrane breakdown or abnormal function, thereby inhibiting bacterial activity. For example, the tubular single-molecule transmembrane channel 1c molecule reported by the Hou group mentioned earlier (Tubular Unimolecular Ion Channels) shows excellent antibacterial activity against *B. subtilis*. The maximum half inhibitory concentration is 10 μM, which is close to alamethicin (2 μM), a natural voltage-gated channel-forming peptide.[106] Furthermore, the tubular single-molecule transmembrane channel GA-based pillararene with D-arginine residue reported by the Xin *et al.* mentioned earlier (Tubular Unimolecular Ion Channels) has a high density of positive charges, which generates a strong electrostatic attraction with the negatively charged membrane of Gram-positive bacteria (*B. subtilis*, *S. aureus*), thus exhibiting extremely strong antibacterial activity.[108]

In addition to the modification of peptide segments, pillararenes directly modified by other cationic groups also exhibit excellent antibacterial activity and anti-biofilm activity. Subakaeva *et al.* designed and synthesized pillar[5]arene derivatives containing sulfanilamide fragments, where those modified with different substituents exhibited significant differences in antibacterial activity. Pillar[5]arenes containing sulfanilamide fragment exhibit a minimum inhibitory concentration (MIC) of 37.5–75 μM for various bacteria (the MIC for *K. pneumoniae* is 150 μM). It can also inhibit the formation of biofilms of *S. aureus* and *P. aeruginosa*, with biofilm prevention concentrations (BPC) of 20 μM and 50 μM respectively. Additionally, pillar[5]arene 2 and 6 are non-mutagenic, and pillar[5]arene containing a sulfanilamide fragment exhibits only slight toxicity to cells at 300 μM.[191] Atacan *et al.* synthesized two water-soluble pillar[5]arene derivatives. They determined their structures by various characterization techniques and evaluated their antibacterial activities against *E. coli*, *S. aureus* and *S. typhimurium*, as well as their catalytic activities for the reduction of 4-nitroaniline.[192] Under physiological conditions, the guanidine group can form multiple stable salt bridges with cell membranes when compared to amino or quaternary ammonium groups. In recent years, the membrane-binding and -penetrating abilities, as well as the antibacterial ability of guanidine derivatives have attracted great attention. Wang *et al.* designed and synthesized a guanidine-functionalized pillararene (GP5), which shows high antibacterial efficacy against *E. coli* and *S. aureus*. More importantly, GP5 effectively disrupts preformed *E. coli* biofilms by effectively penetrating the biofilm barrier and subsequently destroying the biofilm-encapsulated bacteria. In addition, the host–guest complexation between GP5 and cefazolin sodium shows greatly enhanced synergistic disruptive activity against *E. coli* biofilms (Fig. 11a).[193] Aleksandrova *et al.* developed molecular structures combining nine guanidine fragments and a thioalkyl substituent into the pillar[5]arene structure and changed the length of the thioalkyl substituents. Results indicated that pillar[5]arene containing nine guanidine fragments and an octyl substituent exhibited weak antibacterial activity in solution but exhibited a significant inhibitory effect on *S. aureus* biofilms. While the pillar[5]arene with a longer alkyl substituent exhibited a certain inhibitory effect on Gram-negative bacteria. Pillar[5]arene 14 with a fluoroalkyl substituent exhibits enhanced activity against *S. epidermidis*. In terms of cytotoxicity, compounds 4, 12, and 13 have certain toxicity to A549, LEK, and HSF cells at higher concentrations, while compound 14 has lower toxicity. These results indicate that the number of guanidine fragments and the length and type of alkyl substituents in the molecular structure will affect antibacterial activity and cytotoxicity (Fig. 11b).[194]

However, how to inhibit biofilm formation without affecting the viability of some beneficial bacterial cells and human cells still poses a great challenge during clinical treatment. Researchers have designed and efficiently synthesized a series of structurally simple IPAs and have respectively verified their biofilm inhibition activity. The research results show that some cationic IPAs, although not having obvious bacterial toxicity, can significantly inhibit bacterial biofilms. For example, Cohen *et al.* demonstrated that modifying the pillararene scaffold with positively charged quaternary ammonium or imidazole groups can produce effective inhibition of biofilms formed by several clinically important Gram-positive pathogens. Positive charges, the accessibility of the positive charges, and the inner diameter of pillararenes (which determines host–guest properties) all contribute to the inhibition of biofilm formation by these compounds.[195] Phosphate-modified IPAs exhibit a similar ability to their corresponding ammonium analogues.[196] Subsequently, they further evaluated 16 cationic IPAs containing positively charged quaternary ammonium and imidazole groups. The results indicated that 12 derivatives are effective inhibitors of biofilm formation by Gram-positive pathogens. Multiple accessible positive charges are an important determinant of the anti-biofilm activity of these IPAs, rather than the nature of the groups. Increasing the number of positive charges of the IPAs from 10 to 20 does not significantly increase their activity. Conversely, reducing the number of charged moieties resulted in increased lipophilicity of the compounds, which attenuated their anti-membrane activity. Experimental evidence revealed that while the pillararene cavity itself was non-essential for biofilm inhibition, its rigid skeleton significantly facilitated cationic charge accumulation through geometric confinement. Meanwhile, these biofilm-inhibiting compounds demonstrated negligible hemolytic activity and exhibited no inhibitory effects on bacterial cell growth, highlighting their biocompatibility (Fig. 11c).[197] The research of Jonkergouw and colleagues shows that quaternary ammonium-based IPAs without obvious antibacterial activity can bind to key virulence

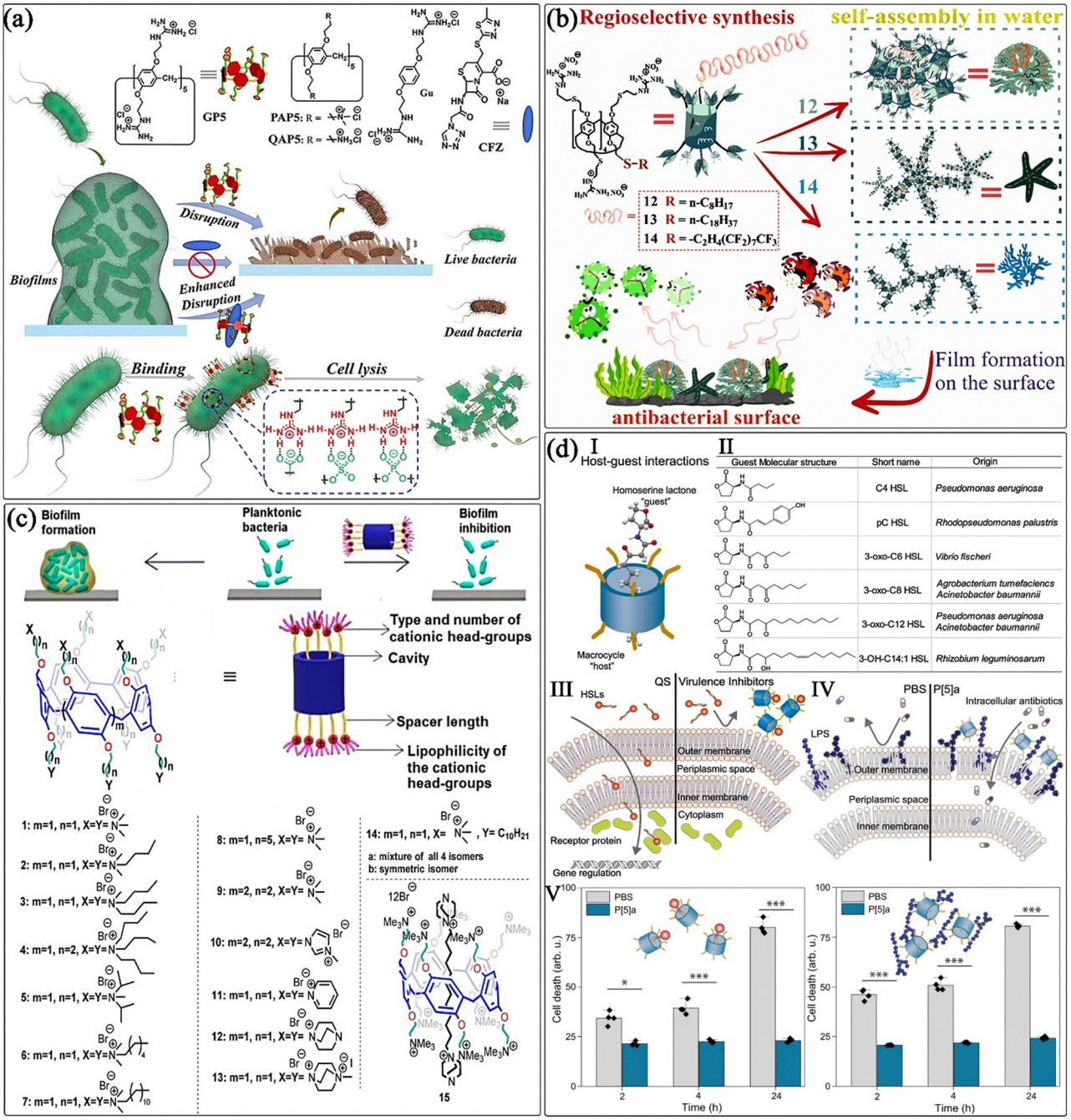

Fig. 11 Unimolecular IPAs for antimicrobial activity. (a) The schematic of the mechanism of the guanidinium-functionalized pillar[5]arene (GP5) penetrating the biofilm barrier, subsequently destroying the bacteria within the biofilm, and significantly enhancing the synergistic antibacterial activity through the formation of host–guest complexes with cefazolin sodium (Reproduced with permission from ref. 193. Copyright 2021, John Wiley & Sons, Inc.). (b) The schematic of the research on the antibacterial activities of different guanidine derivatives of pillar[5]arene against films with different morphologies (Reproduced with permission from ref. 194. Copyright 2024, American Chemical Society). (c) The schematic of the structures of various cationic pillar[n]arenes and their application in studying the ability to prevent biofilm formation by Gram-positive pathogens (Reproduced with permission from ref. 197. Copyright 2021, American Chemical Society). (d) A novel and unconventional supramolecular antibacterial approach: using non-toxic trimethylammonium-functionalized pillararenes (P[5]a) to bind with key virulence factors, homoserine lactones (HSLs) and lipopolysaccharides (LPS), of Gram-negative pathogens, thereby enhancing the inhibitory effect on bacteria. (I)–(IV) Are the main mechanisms for the interactions between pillararenes and HSLs as well as LPS. (V) P[5]a can chelate toxins (3-oxo-C12 HSL and LPS), significantly protecting A549 epithelial cells from toxin-induced apoptosis in *in vitro* experiments, demonstrating the important role of P[5]a in counteracting the damage of bacterial toxins to eukaryotic cells (Reproduced with permission from ref. 198. Copyright 2023, Springer Nature).

factors such as homoserine lactone and the lipopolysaccharide of Gram-negative pathogens, thereby inhibiting the biofilm of drug-resistant bacteria. It can also enhance the penetration and efficacy of antibiotic drugs in combination therapy. This avoids the existing antibiotic resistance mechanisms of drug-resistant bacteria and limits the rapid development of tolerance/drug resistance, providing a new strategy for improving the efficacy against Gram-negative infectious diseases (Fig. 11d).[198]

6.2. IPAs-based materials for antimicrobial activity

Some IPAs can form antibacterial supramolecular complexes or nanomaterials by means of host–guest interaction or covalent polymerization. For example, sanguinarine (SA) is a quaternary benzo[*c*]phenanthridine alkaloid with multiple biological effects, especially antibacterial and anti-inflammatory activities. However, it has drawbacks such as poor water solubility and exists largely in the form of inactive alkanolamine (SAOH) at physiological pH (7.4), which limits its applications in the biomedical field. Li's group used water-soluble carboxylatopillar[6]arene (CP6A) for the host–guest encapsulation of sanguinarine. The research results indicate that at pH 7.4, the complex formed by SA and CP6A has an association constant as high as $2.4 \pm 0.3 \times 10^5\ M^{-1}$, which can effectively increase the water solubility of SA by 4.3 times and double the antibacterial activity of SA against the Gram-positive bacterium *S. aureus* and the Gram-negative bacterium *E. coli*.[199] Gao *et al.* designed a zwitterionic pillar[5]arene (ZW-PA), which can self-assemble into nearly spherical nanoaggregates of about 30–50 nm in aqueous solution through host–guest interaction and electrostatic interaction. The research results indicate that ZW-PA can kill bacteria by causing the deformation of the bacterial membrane through the interaction between nanoaggregates and the bacterial membrane and exhibits good antibacterial activity against both *E. coli* and *S. aureus*. Meanwhile, it can also disrupt *E. coli* biofilms and kill the bacteria inside the biofilms without inducing bacterial resistance (Fig. 12a).[200] Subsequently, inspired by biomimetic microenvironment regulation, they encapsulated nitroaromatic molecules within the precisely engineered cavity of pillar[5]arene *via* host–guest interactions. The electron-rich microenvironment and geometric confinement of this supramolecular system collectively induced a 34.1° increase in ground-state nitro-aromatic torsion angle (from 12.3° to 21.8°), suppressed intersystem crossing relaxation in the S_1 excited state by 42%, and reduced the isomerization reaction barrier by 23% (17 kcal mol^{-1} *vs.* 21 kcal mol^{-1} for free molecules). These structural-functional modulations resulted in a 5.2-fold enhancement in visible-light-driven NO generation efficiency, establishing a novel antibacterial platform with spatiotemporally controlled NO release. This supramolecular NO generation system exhibits the activity of a broad-spectrum antibacterial, biofilm inhibition and dispersion. In addition, it can accelerate the healing of *methicillin-resistant Staphylococcus aureus* (*MRSA*) infected wounds *in vivo*.[201] Amikacin is a semi-synthetic aminoglycoside antibiotic. However, the high-concentration dosage required to achieve the target antibacterial effect often leads to serious side effects such as nephrotoxicity and ototoxicity. Barbera *et al.* used the interaction between amikacin and carboxylate-based IPAs to form a stable supramolecular drug delivery system. This system uses the pH-response of carboxyl-based IPAs to regulate the selective release of the drug in a slightly acidic environment, avoiding the side effects associated with the use of a high-concentration of drugs.[202]

The reactive oxygen species (ROS) generated by photodynamic therapy can not only damage the bacterial cell membrane and cause the leakage of cytoplasmic components, but also damage the DNA in the cell matrix, showing excellent antibacterial and antibiofilm activities without inducing drug resistance. It has received continuous and extensive attention in recent years. Zhang's group used the host–guest interaction between sodium carboxylate-based pillararenes and photosensitizer tetrafluorophenyl porphyrin derivatives[203] or porphyrin (Fig. 12b)[204] respectively to construct two supramolecular nanophotosensitizer systems. In the inflammatory tissues of acidic bacterial infections, the photosensitizer dissociates from the pillararenes. The ROS generated by the photosensitizers after illumination effectively inhibits the activity of bacteria and dissipates the bacterial biofilms. Hu *et al.* used a pillar[5]arene host with AIE activity, a spiropyran derivative (SP-G) guest, and Nile blue (NiB) dye in an aqueous medium to construct a ternary supramolecular photosensitive system based on a two-step FRET process. The reversible isomerization process of SP-G endows this PS with ''on–off'' switch. Under ultraviolet light irradiation, the guest SP-G (non-emissive closed-loop form) can be converted into merocyanine MC-G (emissive open-loop form). The *in situ* formed MC-G can act as a energy acceptor and an efficient ROS-generating photosensitizer. Meanwhile, the introduction of NiB promotes the synergistic ROS-generating activity, resulting in a two-step dynamic FRET process in response to ultraviolet and visible light irradiation. This system exhibits excellent antibacterial activity and anticancer cell activity.[205]

Additionally, Liu *et al.* prepared a positively charged monolayer nanosheet (P5PD) with a perylene diimide derivative (DAPDI) through covalent self-assembly with a laterally brominated pillar[5]arene (LBP5), and fixed a mannose derivative (Man-HQA) on to the P5PD nanosheet through host–guest complexation with LBP5 to improve its biocompatibility and the ability to recognize microorganisms (Fig. 12c).[206] The research indicated that the nanosheet can generate a large number of radical anions in the presence of *E. coli* in a hypoxic environment and exhibits excellent photothermal conversion efficiency under 808 nm laser irradiation, improving the damage of *E. coli*. Similarly, using a covalent polymerization method, Gu *et al.* prepared a quaternary ammonium salt-modified pillar[5]arene polymer QPBP[5]. This polymer can efficiently remove pollutants in water (using Rhodamine B, Sulfadimidine, and Fulvic acid as model pollutants). At the same time, the quaternary ammonium groups in the polymer make it a solid disinfectant with excellent antibacterial properties.[207]

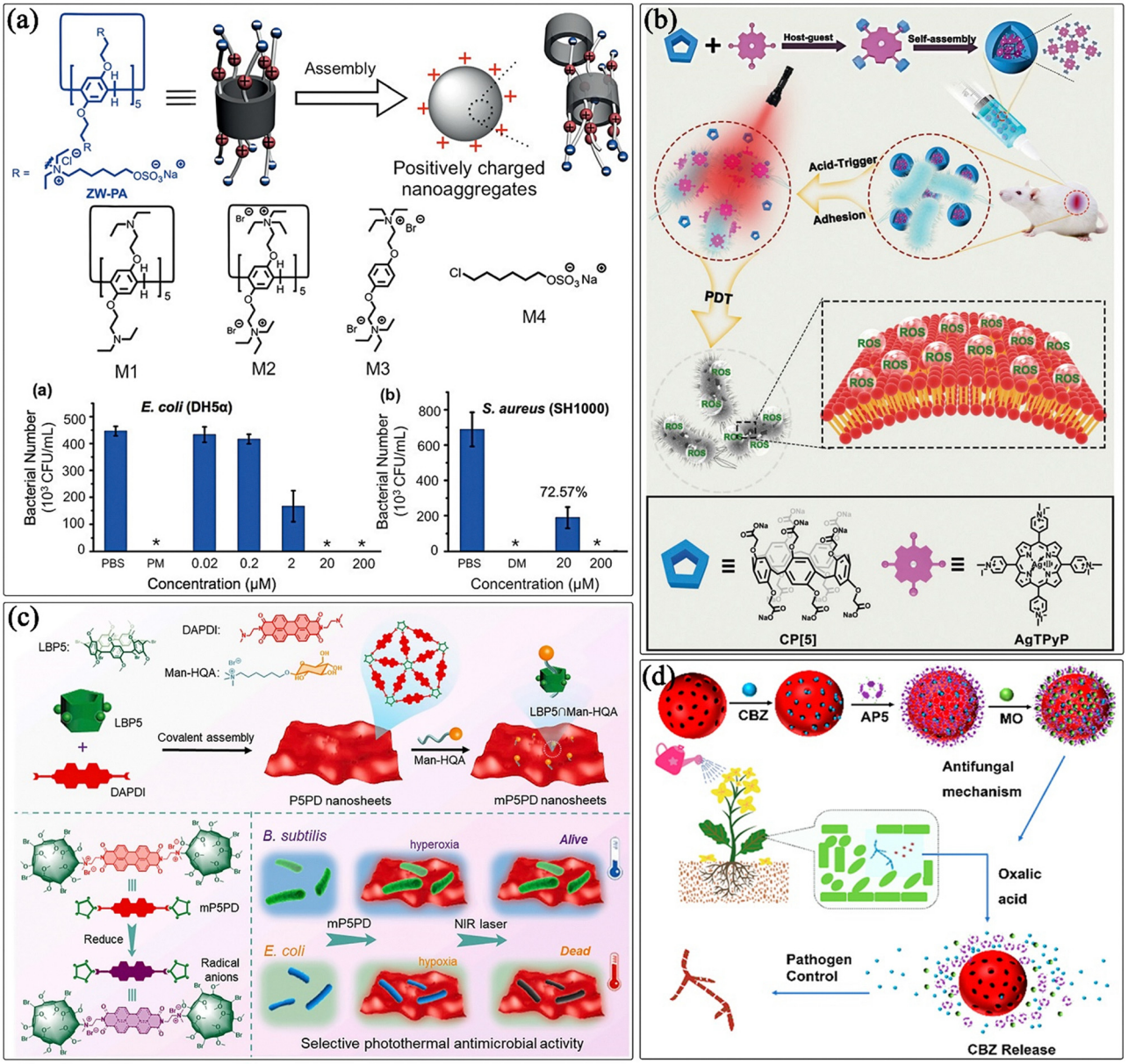

Fig. 12 IPAs-based materials for antimicrobial activity. (a) The schematic of the formation process of positively charged nano-aggregates of zwitterionic pillararenes and the antibacterial ability of ZW-PA against *E. coli* and *S. aureus* (Reproduced with permission from ref. 200. Copyright 2019, John Wiley & Sons, Inc.). (b) The schematic of the construction of supramolecular photosensitizer AgTPyP@P[5] complex and its antibacterial process for healing a MRSA-infected wound (Reproduced with permission from ref. 204. Copyright 2022, The Royal Society of Chemistry). (c) The schematic of the construction of mP5PD nanosheets *via* the covalent assembly strategy, and the schematic of their selective photothermal therapy for *E. coli* rather than *B. subtilis* (Reproduced with permission from ref. 206. Copyright 2022, Elsevier). (d) The schematic of pH-responsive eco-friendly pillar[5]arene-modified selenium nanoparticles for smart delivery of carbendazim to suppress sclerotinia diseases (Reproduced with permission from ref. 208. Copyright 2023 American Chemical Society).

S. sclerotiorum is a destructive fungus. It can change the pH value of the infected site by secreting acidic substances, enhance the activity of cell wall degrading enzymes, thus destroying the plant cell wall and reducing the yield of crops. Huang *et al.* constructed a pH-responsive controlled-release nanopesticide (CBZ@AP5/MSe⊃MO) by loading the fungicide carbendazim (CBZ) onto mesoporous selenium (MSe) and using the host–guest complex of pillar[5]arene (AP5) and methyl orange (MO) as a nanovalve. The host–guest complex of pillararene and MO functions as a nanovalve to control the release of CBZ. In an acidic environment, MO is shed due to protonation, and the AP5-functionalized MSe gradually dissolves, thus enabling the rapid release of CBZ. This research indicates that the pH-responsive CBZ@AP5/MSe⊃MO system exhibits a cumulative release rate of carbendazim (CBZ) at pH 4.5 that is 1.74-fold higher than in neutral conditions. Mechanistically, this nanosystem significantly reduces contact angles on maize and rape leaf surfaces (89.6° *vs.* 106.5° for CBZ

emulsion), enhances leaf retention efficiency by 40% after simulated rainwashing, and exhibits dose-dependent inhibitory effects on *S. sclerotiorum* growth through dual actions: reducing fungal dry biomass by 31.9–55.1% and depleting intracellular reducing sugar content by 5.1–31.9%. It exhibits good safety for plants, animal cells, and the environment, providing a new strategy for the design and development of nanopesticides and the control of *S. sclerotiorum* (Fig. 12d).[208]

Although IPAs have demonstrated great potential and application prospects in antibacterial activity, several issues urgently need to be addressed for their future development. First, reducing the toxicity to beneficial microorganisms and human cells while maintaining high antibacterial activity remains a significant challenge. Current research has shown the effectiveness of certain IPAs in inhibiting bacterial biofilm formation. However, in clinical applications, further in-depth exploration is required to ensure that these compounds have sufficient biocompatibility and safety. Second, despite the initial progress in optimizing the macroscopic structure and function, quantifying the specific impact of molecular modifications on antibacterial activity and biofilm inhibition performance will provide crucial data enabling the design of more targeted antibacterial agents. In addition, in response to the emergence of new drug-resistance mechanisms, the development of IPAs with multi-target functions or the design of molecules that combine other antibacterial strategies (such as combination drug therapy) will be a key direction for future research. Finally, with the increasing severity of the antibacterial resistance problem, exploring the potential of IPAs in controlling drug release, enhancing drug permeability, and reversing drug resistance will surely provide new ideas and strategies for anti-infection treatments. Solving these problems will not only promote the research progress of IPAs but also lay the foundation for the design and development of a new generation of antibacterial materials.

7. IPAs for cancer therapy

The high recurrence rate of cancer and the systemic toxicity caused by traditional chemotherapy drugs remain the major challenges in current clinical cancer treatment. Although significant progress has been made in targeted therapy and immunotherapy in recent years, issues such as low drug delivery efficiency, insufficient response to the TME, and multidrug resistance still severely limit the treatment efficacy. It is worth noting that IPAs with precise host–guest recognition capabilities offer new ideas for innovative anti-cancer strategies, thanks to their adjustable cavity, excellent water solubility, and unique supramolecular interactions. Research shows that IPAs can not only achieve a killing effect by directly interfering with the membrane potential or metabolic pathways of cancer cells, but also serve as intelligent carriers. Through host–guest assembly technology, they can integrate functional molecules such as chemotherapeutic drugs and photosensitizers, and further self-assemble to construct multifunctional nano-delivery systems. In addition, their unique role in the surface functionalization/modification of inorganic nanomaterials has further promoted the development of composite anti-tumor platforms. Moreover, some supramolecular systems constructed based on IPAs can respond to specific stimuli in the TME (such as pH, GSH), enabling controlled drug release and thus improving the precision and effectiveness of treatment. In this section, we will summarize the research progress on the applications of IPAs in cancer therapy.

7.1. Unimolecular IPAs for cancer therapy

In the previous section, we elaborated on the mechanisms by which various IPAs achieve transmembrane ion transport by embedding into the cell membrane. Based on this property, through rational molecular design, IPAs can be developed into therapeutic molecules. By leveraging their ion-transport function, IPAs can specifically damage cancer cells, providing a new strategy for cancer treatment. The group of Hou designed a tubular molecule with terminal positively charged amino groups. Through single-channel conductance measurements and KCl transmembrane transport experiments, it was found that this molecule could efficiently embed into the lipid bilayer composed of phosphatidylcholine (such as DPPC) and form unimolecular transmembrane channels. This embedding process is mainly driven by the electrostatic interaction between the positively charged amino groups at the end of the channel molecules and the negatively charged phosphate groups in the lipid molecules. The EC_{50} value for its embedding into the DPPC bilayer is as low as 0.023%, which is significantly better than other known artificial channels. Further observations using confocal laser scanning microscopy (CLSM) and fluorescence microscopy indicated that this molecule could effectively embed into the cell membranes of rat erythrocytes and human hepatocellular carcinoma cells (HepG2), and exhibited significant cytotoxicity to HepG2 cancer cells, with a IC_{50} of 5.1 μM.[209] Based on the antibacterial-active molecules previously reported by Hou's group,[106] Chang and colleagues introduced pH-responsive charge-reversing groups at the molecular termini through ingenious chemical modifications, endowing the molecules with unique properties in different pH environments. Experimental results have determined that the specific response mechanism of P5NH–DCA in the acidic TME, involves the acid-labile amide groups undergoing hydrolysis, reversing the charge of the molecular headgroups from negative to positive. The resulting hydrolysis product, P5NH3, can efficiently target the cancer cell membrane and induce its disruption. In the neutral microenvironment of normal cells, the molecule remains stable, and its cytotoxicity is significantly reduced. The experimental results indicate that the IC_{50} of P5NH–DCA against HepG2 cancer cells is 0.67 μM, while the IC_{50} value for normal cells is greater than 100 μM, demonstrating excellent selectivity. Further *in vivo* experiments confirmed that P5NH–DCA can significantly inhibit the growth of HepG2 tumors without observing obvious side effects (Fig. 13a).[210] This research provides important theoretical support and experimental evidence for the development of highly effective

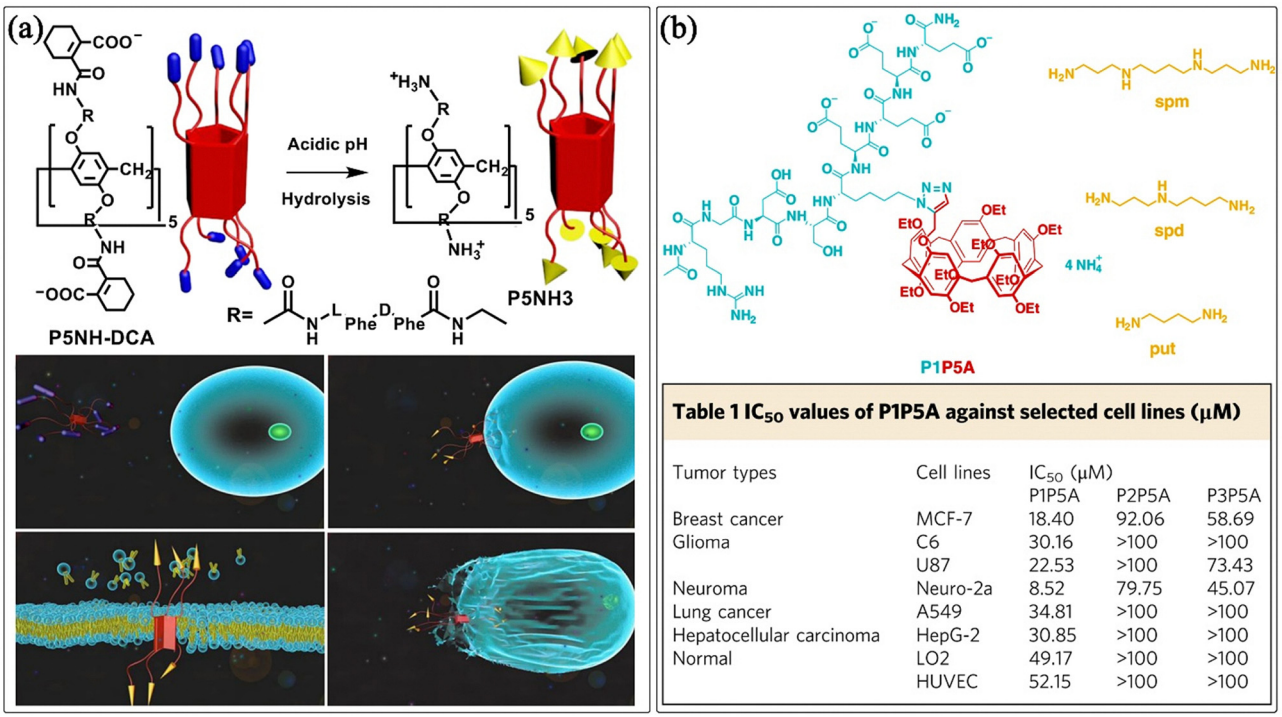

Table 1 IC_{50} values of P1P5A against selected cell lines (μM)

Tumor types	Cell lines	IC_{50} (μM)		
		P1P5A	P2P5A	P3P5A
Breast cancer	MCF-7	18.40	92.06	58.69
Glioma	C6	30.16	>100	>100
	U87	22.53	>100	73.43
Neuroma	Neuro-2a	8.52	79.75	45.07
Lung cancer	A549	34.81	>100	>100
Hepatocellular carcinoma	HepG-2	30.85	>100	>100
Normal	LO2	49.17	>100	>100
	HUVEC	52.15	>100	>100

Fig. 13 Unimolecular IPAs for cancer therapy. (a) The schematic of the mechanism for the selective killing of cancer cells by targeting the cell membrane with charge-reversal amphiphilic pillar[5]arene (Reproduced with permission from ref. 210. Copyright 2019, American Chemical Society). (b) Molecular structure for achieving anti-tumor effects by capturing intracellular polyamines with a supramolecular trap, and the IC_{50} values for different cancer cell lines (Reproduced with permission from ref. 212. Copyright 2019, Springer Nature).

and anti-cancer strategies with low-toxicity based on the membrane-disruption mechanism. In addition, Duran and colleagues tested the anticancer activities of two trimethylamine-functionalized cationic pillar[5]arenes, ws-penta-P[5] and ws-deca-P[5]. Cytotoxicity analysis indicated that the IC_{50} values of ws-penta-P[5] and ws-deca-P[5] for MCF7 cells were 15.62 μM and 250 μM, respectively, and for A549 cells, they were 62.5 μM and 250 μM, respectively. Meanwhile, the research results indicated that in the two cell lines treated with ws-deca-P[5], the expressions of pro-apoptotic genes were upregulated, while the expressions of anti-apoptotic genes and caspase activation genes were downregulated. Compared with the control group, the flow cytometry apoptosis and cell cycle analysis of the treatment group showed that the apoptosis rate increased after treatment with ws-deca-P[5], and ws-deca-P[5] could cause G0/G1 phase arrest in both groups of cells. These results demonstrate that ws-deca-P[5] has the potential to be a promising new candidate for the chemotherapy of breast and lung cancers.[211]

Polyamines (such as spermine, spermidine, and putrescine) play a crucial role in the growth of eukaryotic cells and are involved in and regulate a series of physiological processes such as cell proliferation and differentiation. Since the rapid proliferation of tumor cells depends on the supply of polyamines, polyamines have become key substances for maintaining the survival and development of tumor cells. Based on this characteristic, a team led by Li developed a peptide-pillar[5]arene conjugate P1P5A (P1 = RGDSK(N_3)EEEE) as a supramolecular trap to capture polyamines in tumor cells, providing new ideas for tumor treatment. The molecular design of P1P5A has dual functions. On the one hand, its RGD sequence can specifically recognize and bind to tumor cells overexpressing integrin $\alpha_v\beta_3$, achieving precise targeting. While, on the other hand, the negatively charged glutamic acid residues enhance the inclusion affinity between pillar[5]arene and cationic polyamines through electrostatic interactions and improve the water solubility of the conjugate. The research results indicate that P1P5A can form stable host–guest inclusion complexes with polyamines, and its association constant (K_a) is as high as 10^5–10^6 M^{-1}), indicating excellent polyamine capture ability. Meanwhile, P1P5A exhibits concentration-dependent cytotoxicity against multiple tumor cells. Its IC_{50} ranges from 8 to 53 μM in different tumor cell lines, while it shows low toxicity to normal cells, demonstrating good selectivity. In addition, P1P5A can effectively induce apoptosis of tumor cells, further verifying its anti-tumor activity. It is worth noting that although P1P5A does not change the total concentration of polyamines in cells, it significantly upregulates the expression of ornithine decarboxylase (ODC), a rate-limiting enzyme in the polyamine biosynthesis pathway. This may inhibit tumor growth by interfering with the polyamine metabolic balance. For *in vivo* experiments, P1P5A exhibits significant anti-tumor effects and can effectively inhibit the growth of breast adenocarcinoma xenografts in female nude mice (Fig. 13b).[212]

7.2. IPAs-based supramolecular systems for cancer therapy

In contrast to the unimolecular IPAs for cancer therapy strategy, IPAs-based supramolecular systems place more emphasis on research into the synergistic promotion of cancer treatment between IPAs and other substances. According to the differences in the interactions between IPAs and other substances, IPAs-based supramolecular systems can be classified into three types: supramolecular host–guest complexes, supramolecular self-assembled nanocarriers, and supramolecular organic–inorganic hybrid nanocarriers.

7.2.1. Supramolecular host–guest complexes. In the field of cancer chemotherapy, many chemotherapeutic drugs have inherent drawbacks that severely limit their therapeutic efficacy and clinical applications. However, due to their unique structures and properties, IPAs provide effective solutions to these problems by forming host–guest complexes (Table 1).

Camptothecin (CPT), 10-hydroxycamptothecin (HCPT), topotecan (TPT),[213] and tamoxifen (TAM)[214] all face the problem of poor water solubility. For example, the solubility of CPT in water is only about 5 μM, and it is almost insoluble in common physiological solutions. The solubility of HCPT is slightly higher, but it is still only 29 μM. This characteristic makes it difficult for these drugs to disperse evenly in the body, hinders their absorption, and prevents them from fully reaching their target sites. As a result, their bioavailability is low, which seriously affects the treatment outcome. Some studies have shown that when WP6 forms complexes with CPT and HCPT, their water solubility is significantly enhanced. The solubility of CPT increases to 1.9 mM, showing a 380-fold increase, and the solubility of HCPT reaches 1.2 mM, representing a 40-fold increase.[213] This solubilization effect is achieved through host–guest encapsulation, which greatly improves the drugs' dispersion and transportation capabilities in the body and lays a foundation for enhancing the treatment effect.

Certain chemotherapeutic agents, including oxaliplatin (OXA) and CPT, are plagued by both poor aqueous solubility and instability in the bloodstream. During blood circulation, they are highly susceptible to the catalytic action of enzymes, attack by free radicals, and other physiological factors, which can lead to degradation or rapid inactivation. For instance, when OXA exists alone in plasma, after 24 h of incubation, the remaining percentage of the drug is only 13%. The cavity structure of IPAs plays a crucial protective role in this situation. Research has found that the complex formed by carboxylated pillar[6]arene (CP6A) and OXA has different binding constants under different pH conditions.[215] At pH 7.4, the binding constant K_a = (1.02 ± 0.05) × 10^4 M^{-1}, and the binding is strong, improving the drug's stability. At pH 5.4, K_a = (4.21 ± 0.06) × 10^2 M^{-1}, the binding force weakens, resulting in drug release. This pH-response enables the drug to be targeted and released in the acidic TME. In addition, taking advantage of the high affinity between spermine (SPM) overexpressed in tumor cells and pillararenes, the binding constant of CP6A and SPM is K_a = 2.58 × 10^7 M^{-1}, OXA can be released from the complex by competition with SPM (Fig. 14a).[216,217] This enhances the drug's targeting ability and anti-cancer activity against tumor

Table 1 Supramolecular host–guest complexes for cancer therapy constructed based on IPAs

Pillar[*n*]arene	Ionic property	Ionic group	Type of guest	Guest	Association constant (M^{-1}) or binding affinity (kcal mol^{-1})	Stimulus-responsive factors	Ref.
n = 6	Cationic	Pyridinium	Chemotherapeutic drug	Pemetrexed	(8.32 ± 0.27) × 10^4 M^{-1}	ATP	218
n = 6	Anionic	Carboxylate	Chemotherapeutic drug	Camptothecin	(8.4 ± 1) × 10^6 M^{-1}	—	213
				10-Hydroxycamptothecin	(1.2 ± 0.2) × 10^5 M^{-1}		
				Topotecan	(1.3 ± 0.1) × 10^4 M^{-1}		
n = 6	Anionic	Carboxylate	Chemotherapeutic drug	Tamoxifen	5.1 × 10^4 M^{-1}	—	214
n = 6	Anionic	Carboxylate	Chemotherapeutic drug	Oxaliplatin	(1.02 ± 0.05) × 10^4 M^{-1} (pH 7.4)	pH	215
					(4.21 ± 0.06) × 10^2 M^{-1} (pH 5.4)		
n = 6	Anionic	Carboxylate	Chemotherapeutic drug	Oxaliplatin	1.66 × 10^4 M^{-1}	SPM	216
n = 6	Anionic	Carboxylate	Chemotherapeutic drug	Oxaliplatin	(1.15 ± 0.08) × 10^3 M^{-1} (CLT6)	SPM	217
					(1.29 ± 0.19) × 10^2 M^{-1} (CBpP6)		
n = 6	Anionic	Carboxylate	Chemotherapeutic drug	Nitrogen mustard	(2.28 ± 0.15) × 10^4 M^{-1}	SPM	219
n = 5, 6, 7	Anionic	Carboxylate	Chemotherapeutic drug	Chlorhexidine hydrochloride	−6.6, −7.3, −8.9 kcal mol^{-1}	—	220
				Memantine	−2.9, −4.8, −8.4 kcal mol^{-1}		
				Proflavine	−5.7, −8.2, −8.0 kcal mol^{-1}		
n = 6	Anionic	Carboxylate	Photosensitizer	Methylene blue	(1.15 ± 0.30) × 10^7 M^{-1}	—	221
n = 5	Anionic	Carboxylate	Photosensitizer	Tetraphenylethene derivative	(6.22 ± 2.81) × 10^5 M^{-1}	pH	222

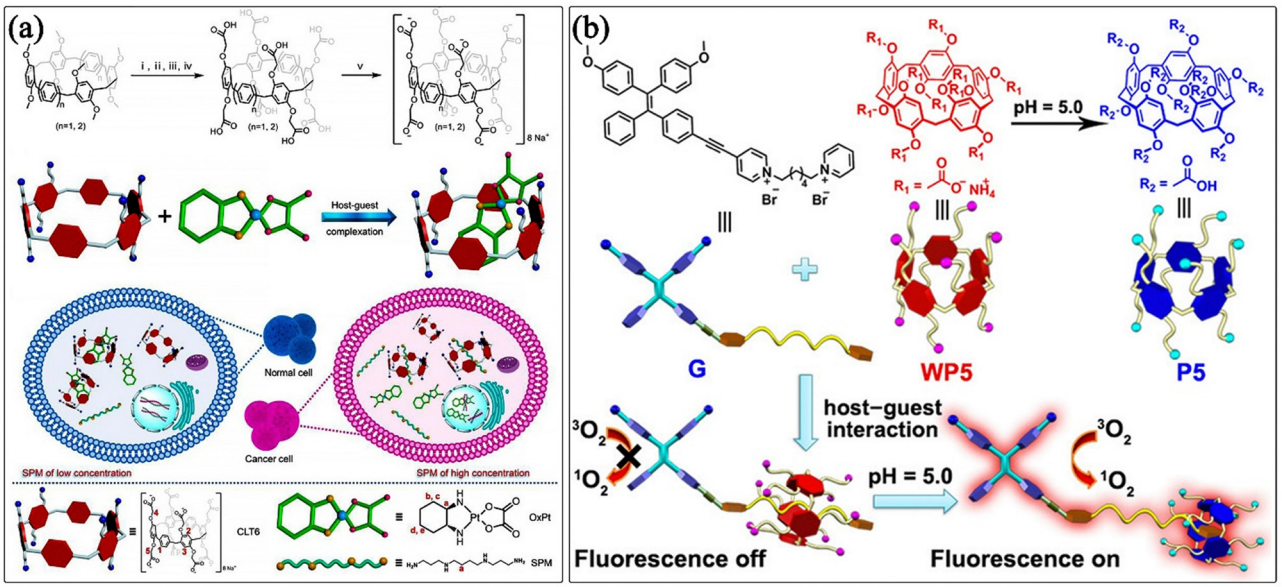

Fig. 14 Supramolecular host–guest complex-based IPAs for cancer therapy. (a) The schematic of the preparation of OXA supramolecular prodrugs and their application for enhancing the efficacy of cancer chemotherapy (Reproduced with permission from ref. 218. Copyright 2020, Elsevier). (b) The schematic of the mechanism for constructing adaptive photosensitizers based on the host–guest complexation between WP5 and an AIE-containing photosensitizer (G). Different pH environments can control the quenching and restoration of the fluorescence of the photosensitizer, enabling the selective killing of cancer cells. (Reproduced with permission from ref. 222. Copyright 2020, John Wiley & Sons, Inc.).

cells, reduces its distribution in normal tissues, and decreases damage to normal cells.

In addition, many anti-cancer drugs, such as pemetrexed, OXA, and NM, while they can kill cancer cells, also exhibit significant toxicity to normal cells or tissues. During the treatment process, these drugs can damage normal tissues and organs, causing a series of severe side effects like nausea, vomiting, hair loss, and bone marrow suppression, which greatly affect the patients' quality of life and treatment compliance. Taking pemetrexed as an example, it has high toxicity to normal pulmonary epithelial cells (BEAS-2B). Research shows that when cationic pillar[6]arene (WP6A) containing pyridinium groups binds to pemetrexed, the high concentration of ATP in tumor cells exhibits a higher affinity for WP6A (K_a = (5.67 ± 0.31) × 10^5 M^{-1}). This can competitively replace pemetrexed, causing it to be released in tumor cells, reducing damage to normal cells and enhancing the anti-cancer activity against lung cancer cells (such as A549 cells).[218]

NM also has high toxicity to normal cells. Studies have found that when carboxylated pillar[6]arene (CP6A) forms a complex with NM, the binding constant of CP6A and NM is K_a = (2.28 ± 0.15) × 10^4 M^{-1}, and the binding constant with SPM is K_a = (3.06 ± 0.48) × 10^7 M^{-1}. In the breast cancer microenvironment with overexpressed SPM, NM can be competitively released from the complex. For *in vitro* experiments, compared with free NM, the NM/CP6A complex shows significantly reduced toxicity to normal mammary epithelial cells (MCF-10A). While for *in vivo* experiments, the inhibition efficiency of the NM/CP6A complex against MCF-7 breast cancer cells increased from 42.75% (free NM) to 87.61%, with reduced toxicity to normal cells and improved treatment effect.[219]

Furthermore, some researchers have explored pillararenes with different sizes (n = 5, 6, 7) and found that their binding abilities to drugs such as chlorhexidine hydrochloride, Memantine, and proflavine gradually increase. This change in binding ability is related to the cavity size and structure of the pillararenes. Larger-sized pillararenes can provide a more suitable space and more interaction sites, thus enhancing the binding with these drugs. This discovery provides an important reference for selecting appropriate pillararene carriers according to the characteristics of the drugs, and further expands the application potential of pillararenes in the field of drug delivery.[220]

In terms of photodynamic therapy, MB as a photosensitizer has issues such as high dark toxicity and photobleaching during treatment. These problems result in a short generation time of reactive oxygen species, affecting the treatment outcome. Research has indicated that the supramolecular photosensitizer system WP6–MB formed by WP6 and MB can significantly reduce the dark toxicity of MB, overcome the photobleaching phenomenon, prolong the generation time of reactive oxygen species, and enhance the photodynamic therapy effect.[221] In addition, the tetraphenylethene-based photosensitizer G exhibits an ''always on'' phenomenon in a neutral environment, leading to poor tumor specificity. Relevant research shows that the supramolecular switch constructed based on WP5 and photosensitizer G can inhibit fluorescence and the generation of reactive oxygen species by G in a neutral environment. In the acidic TME, WP5 is protonated, and G

regains its ability to fluoresce and generate reactive oxygen species, achieving control of the photosensitizer and improving the precision of tumor treatment (Fig. 14b).[222]

IPAs have remarkable effects in improving the water solubility and stability of chemotherapeutic drugs, as well as reducing their toxic side effects. Meanwhile, they also play an important role in enhancing the performance of photosensitizers in photodynamic therapy. They provide new strategies and methods for enhancing the efficacy of cancer chemotherapy and photodynamic therapy, demonstrating broad application prospects.

7.2.2. Supramolecular self-assembled nanocarriers. IPAs possess remarkable advantages in molecular design and synthesis as well as host–guest assembly, which endows them with great potential in the preparation of intelligent supramolecular nano-multifunctional materials. In particular, supramolecular self-assembled nanocarriers constructed based on IPAs have achieved fruitful research results in the efficient targeted delivery, controlled release, and multi-mode synergistic therapy of anti-cancer agents, providing a new direction for cancer treatment research. In this section, we will provide a detailed introduction to the basic design concepts of intelligent supramolecular self-assembled nanocarriers constructed based on IPAs, the inherent relationship between molecular structure and function, as well as applied research progress in improving the effectiveness of cancer treatment.

Supramolecular self-assembled nanocarriers based on IPAs are typically constructed through host–guest complexation between hydrophilic IPAs (host molecules) and guest molecules with diverse structures, forming supramolecular amphiphiles with specific functions. Meanwhile, driven by the delicate balance of non-covalent interactions such as hydrophobic effects, π–π stacking, and electrostatic forces, these amphiphiles spontaneously organize into well-defined nanostructures (such as vesicles and micelles) in aqueous media. Compared with single-molecule diagnostic and therapeutic agents, nanocarriers have many significant advantages. Thanks to their larger space and unique structures, nanocarriers can achieve a higher loading capacity and greater stability. At the same time, they can effectively improve the solubility and bioavailability of drugs. Through the optimized design of the carriers, the targeting ability of the system and the controlled-release performance of drugs can be enhanced, thus significantly improving the effectiveness of cancer treatment.

At present, three basic strategies are used to achieve the specific delivery of various therapeutic agents to tumor tissues and their precise stimulus-responsive release (Table 2): (1) Active targeting through ligand conjugation: by means of chemical synthesis, tumor-targeting ligands (such as galactose, biotin, folic acid, RGD peptide, phenylboronic acid, *etc.*) and organelle-targeting groups (such as triphenylphosphine for mitochondrial targeting) are covalently linked to the host or guest molecules. This molecular design significantly enhances the uptake efficiency and high-efficiency enrichment of therapeutic agents by cells through the receptor-mediated endocytosis mechanism. (2) Passive targeting based on TME response: by introducing functional structural units that can selectively experience cleavage, conformational transitions, or competitive disassembly (such as pH, GSH, ROS, Hypoxia-sensitive groups) under the stimulation of the TME into host or guest molecules, it becomes possible to promote the selective release of therapeutic agents by nanocarriers in tumor tissues. (3) Precise control using external triggers: photo-responsive groups such as azobenzene are introduced into the molecules to achieve

Table 2 Targeting groups and stimulus-responsive factors within IPAs-based supramolecular self-assembled nanocarriers

Host	Guest	Ref.
(I) Targeting groups		
Triphenylphosphine	—	223
—	Triphenylphosphine	224–226
—	RGD	227 and 228
—	Galactose	229–231
—	Biotin	232 and 233
—	Folic acid	234
—	Phenylboronic acid	235
(II) Stimulus-responsive factors		
Acid	—	224, 225, 227, 232 and 236–245
GSH	—	231 and 246
Acid & GSH	—	229 and 247
Acid & H_2O_2	—	235
—	Acid	248–252
—	GSH	228, 233 and 253–257
—	Acid & GSH	258
—	H_2O_2	259
—	Acid & H_2O_2	260
—	UV	261
—	ATP	262
Acid	Acid	263 and 264
Acid	GSH	265–267
Acid	UV	268–271
Acid	ROS	272
Acid	Hypoxia	273 and 274

remote control of the morphological structure of nanocarriers and drug release.

Based on the above-mentioned strategies, a supramolecular self-assembled nanocarrier system with the capabilities of targeted delivery and controlled release can be effectively constructed. However, the different forms of drug molecules existing in the nanocarriers will have an impact on the morphology of the nanoparticles, drug loading capacity, loading stability, release behavior, and biocompatibility. According to the forms of the drug, they can be divided into three types: drug molecules directly covalently linked to host molecules, drug molecules participating in host–guest assembly as modified guests, and drug molecules directly encapsulated by nanocarriers. Among them, the covalent bridging and host–guest assembly modes not only participate in regulating the hydrophilic-lipophilic ratio of the assembly system, but also affect the structural stability of the assembly and the drug-loading microenvironment. The delivery stability of drug molecules in these two modes is significantly higher than that of direct encapsulation. In contrast, the direct encapsulation strategy does not require complex modification of drug molecules, and the operation is relatively simple, with a wider adaptability to various types of drugs. The following will classify and summarize the research progress of supramolecular self-assembled nanocarriers constructed by IPAs based on these three drug-loading methods:

The first type is to connect the drug to the host molecule of IPAs through covalent bonds. Hu *et al.* grafted DOX onto trimethylammonium pillararene *via* acid-cleavable hydrazone bonds and assembled it with the guest molecule RGD-SG with RGD peptide in different ratios to form a supramolecular nanoprodrug, achieving targeted delivery and acid-responsive controlled release of DOX (Fig. 15a).[227]

The second type is to use the derivative of the drug as the guest molecule of IPAs. Numerous studies have successfully linked DOX to specific guest groups *via* hydrazone bonds and further assembled them with IPAs into a supramolecular nanodrug delivery system, enabling the rapid release of DOX in the TME.[243,247,263,264] Notably, results from the group of Wang indicate that the carboxyl groups of carboxylate pillar[6]arenes can be protonated in an acidic environment, and this process can further catalyze the cleavage of hydrazone bonds and accelerate the release rate of DOX.[264] This acid-responsive property enables more efficient drug release in tumor tissues, thereby improving the drug's targeting ability and therapeutic effect. Meanwhile, to further enhance the controllability of drug release, researchers have also utilized ROS-responsive thioether bonds to link DOX and combined with photosensitizers to achieve precise drug release controlled by external light sources.[272] This design makes drug release not only controlled by the acidic conditions and ROS levels in the TME but also allows for more precise drug release through the control of an external light source, thus improving the accuracy of treatment and reducing damage to normal tissues.

CPT is a chemotherapeutic drug with significant anti-tumor activity. The reactive hydroxyl group in its molecular structure provides the possibility for its functionalization. CPT can be connected to specific guest molecules through disulfide bonds, making it a guest molecule of IPAs, and then self-assembling to form supramolecular nano-prodrugs. This design takes advantage of the high concentration of GSH in the TME. Stimulated by high concentrations of GSH, the disulfide bonds break, thus achieving the specific release of CPT.[233,255] SN-38 is an active derivative of camptothecin with stronger anti-tumor activity. By connecting SN-38 through disulfide bonds, a GSH-sensitive CPT supramolecular prodrug system can be constructed. When this prodrug is in a high-GSH environment in the TME, the disulfide bonds break in a responsive manner, releasing SN-38 whose fluorescence was originally quenched. This process not only realizes the precise release of the drug but also utilizes the fluorescence property of SN-38 to track the drug release and tumor tissue distribution in real time (Fig. 15b).[253,257]

The molecular dimensions of chlorambucil (CB), a bifunctional alkylating agent, exhibit precise geometric complementarity with the cavity of pillararenes, enabling the formation of stable host–guest inclusion complexes through noncovalent interactions such as hydrophobic effects and van der Waals forces. Utilizing this feature, Huang *et al.* rationally designed and synthesized a photocleavable prodrug Py–Cbl by covalently conjugating CB to the fluorophore pyrene *via* a photolabile ester linker. This prodrug served as a supramolecular guest that formed a stable host–guest inclusion complex with WP6, significantly enhancing its aqueous solubility. Upon UV irradiation, Py–Cbl underwent photodegradation to release free CB and 1-pyrenemethanol (PyOH), accompanied by distinct fluorescence changes from 500 nm to 400 nm, enabling real-time visualization of drug release kinetics.[261] Ding *et al.* covalently linked CB with TAPP (tetraphenylporphyrin) *via* an azobenzene to form a drug-photosensitizer conjugate as the guest molecule. Using the hypoxia environment-responsive cleavage ability of the azobenzene group, they achieved the selective release of CB in the TME.[273] Bai *et al.* conjugated CB with phenylboronate ester to serve as the H_2O_2-responsive guest prodrug.[259] Moreover, leveraging the dynamic formation of boronate esters between phenylboronic acid (PBA) and curcumin (Cur), Bai *et al.* covalently integrated Cur into the chlorambucil–arylboronic acid (Cb–BA) prodrug through a pH-responsive boronate ester linkage, constructing a novel "drug–drug" dual-drug guest molecule for supramolecular prodrug self-assemblies (SPSAs). This innovative design enabled simultaneous GSH consumption by the PBA moiety and TrxR inhibition by Cur (Fig. 15c).[252] By adopting similar strategies, the CB–Pt drug conjugate was also successfully designed as a guest molecule.[267] In addition, the team of Hu developed a dual-drug conjugate by linking CB and CPT with a disulfide bond.[256] These prodrug molecules based on CB can all self-assemble with IPAs to form supramolecular nanoprodrug systems. Under the stimulation of the TME or external light, they can selectively release the anticancer drug CB and effectively improve the anticancer effect.

Some other chemotherapeutic drugs, such as OX-type Pt(IV) prodrug (PtC_{10}), have been used as guest molecules. The

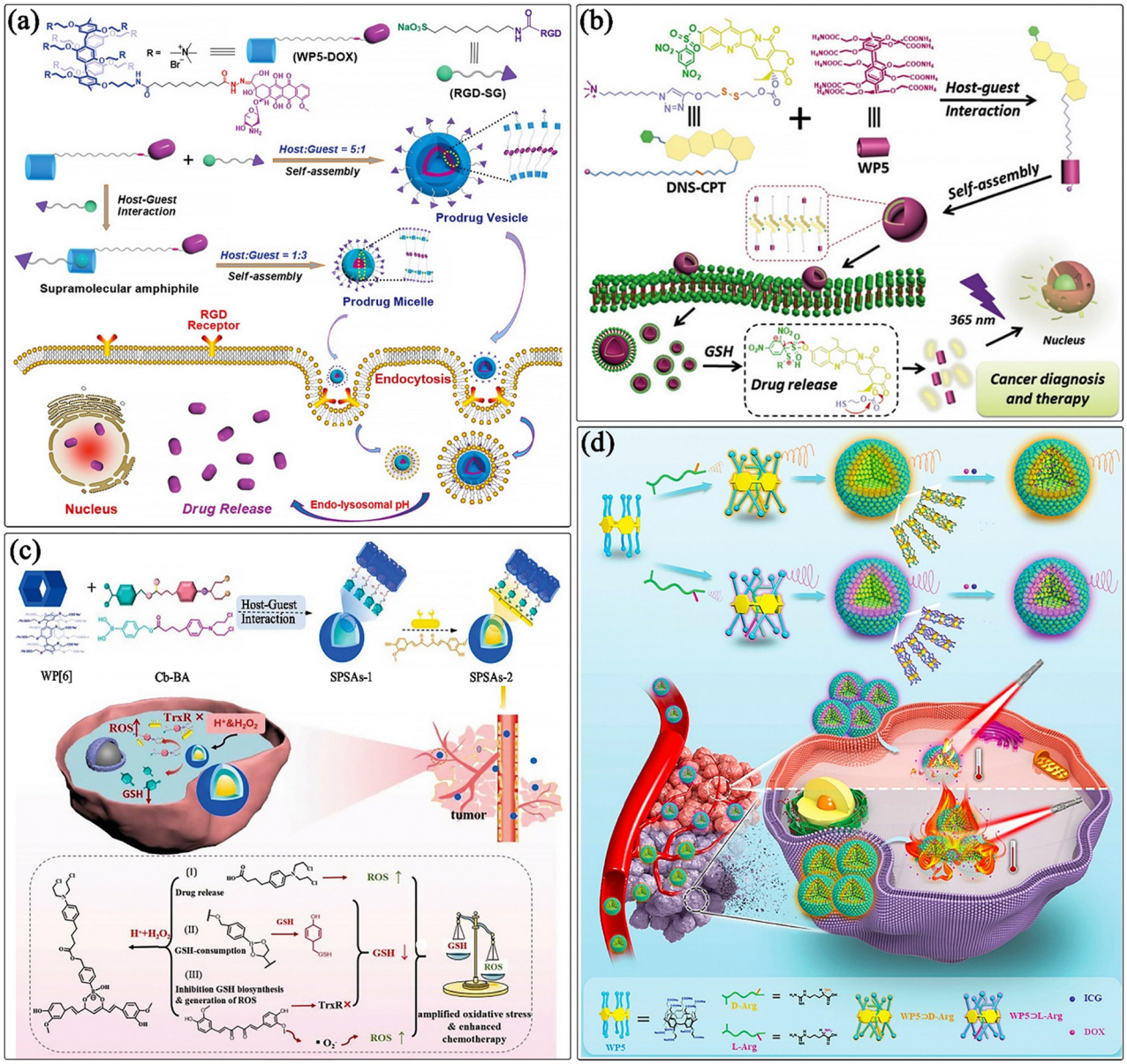

Fig. 15 Supramolecular self-assembled nanocarriers constructed based on IPAs are used for the precise delivery of chemotherapeutic drugs. (a) Schematic diagram of constructing a tumor-targeting nano-drug delivery system based on the host–guest interaction between pillar[5]arene-based prodrug host and RGD–sulfonate-targeted guest molecule (Reproduced with permission from ref. 227. Copyright 2018, John Wiley & Sons, Inc.). (b) Schematic diagram of the preparation of bifunctional supramolecular prodrug vesicles for cancer diagnosis and treatment, constructed from a CPT derivative and water-soluble pillar[5]arene (Reproduced with permission from ref. 257. Copyright 2019, The Royal Society of Chemistry). (c) Schematic diagram of supramolecular prodrug self-assemblies based on the host–guest interaction between water-soluble pillar[6]arene and dual-drug guest molecule Cb–BA for GSH-depletion-augmented chemotherapy (Reproduced with permission from ref. 252. Copyright 2022, The Royal Society of Chemistry). (d) Schematic diagram of targeted co-delivery of DOX and indocyanine green by chiral WP5⊃D/L-arginine self-assembled nanocarriers. (Reproduced with permission from ref. 275. Copyright 2024, John Wiley & Sons, Inc.).

complexation constant between PtC_{10} and carboxyl-functionalized pillar[6]arene (CP6A) is $(1.16 \pm 0.03) \times 10^4\ M^{-1}$ at pH 7.4 and $(1.73 \pm 0.15) \times 10^3\ M^{-1}$ at pH 5.0. This significant difference enables the supramolecular nano-prodrugs formed by their assembly to exhibit acid dissasembly.[244] Betulinic acid (BA) is a pentacyclic triterpenoid compound widely present in green plants. It has good compatibility with normal cells but shows specific cytotoxicity to cancer cells. However, its poor water solubility and pharmacokinetic properties limit its clinical application. Hu *et al.* used its derivative BA–D with superior activity as a guest molecule. By assembling it with carboxyl-functionalized pillararene, a supramolecular nano-prodrug was formed, enabling efficient drug delivery and acid-responsive controlled release.[245] In the treatment of colorectal cancer, drug resistance at the tumor site caused by *Fusobacterium nucleatum* often leads to the failure of chemotherapy. Cationic

polymers have good antibacterial activity. Liu *et al.* designed an intelligent supramolecular quaternary ammonium nanoparticle, and connected azobenzene (AZO) to the cationic dendritic quaternary ammonium polyamidoamine (PAMAM). A supramolecular system was formed through host–guest interactions with carboxylatopillar[5]arene (CP[5]A). Azobenzene can respond to azoreductase in the TME, thus breaking the –N=N– bond, promoting the morphological recovery of supramolecular nanoparticles and achieving the treatment of colorectal cancer. This not only improves the anti-cancer efficacy but also significantly reduces the toxic side effects on normal tissues.[251]

The third type is to directly encapsulate drugs into supramolecular self-assembled nanovesicles or micelles constructed from IPAs by means of various forces such as π–π interaction, hydrogen bond, electrostatic interactions, hydrophobic interactions and van der Waals forces. By virtue of the targeting groups or TME stimulus-responsive groups of pillararene host or guest molecules, the targeted delivery and controlled release of anti-cancer drugs loaded in nanocarriers can be achieved. In addition, this strategy does not require additional chemical modification for the encapsulation of chemotherapeutic drugs, and the operation process is simple and easy to carry out. Moreover, it can easily achieve the co-delivery of multiple drugs, photosensitizers, genes, enzymes and other types of diagnostic and therapeutic agents, providing a strong platform for the construction of a multi-pathway combination therapeutic systems. For example, Chang *et al.* co-delivered DOX and siRNA using cationic ferrocene-based pillararenes responsive to GSH.[246] The siRNA downregulated the expression of drug resistant proteins in drug-resistant cancer cells, synergistically enhancing the chemotherapeutic effect. Liu *et al.* loaded glucose oxidase (GOx) into a supramolecular nano-prodrug system constructed based on gambogic acid (GA). GOx consumed glucose and generated H^+ and H_2O_2 to enhance the chemodynamic therapeutic (CDT) effect, and inhibited GSH regeneration by blocking the ATP supply. Multiple pathways worked synergistically to enhance the chemotherapeutic effect.[228] Zhou *et al.* prepared nanocarriers by specifically binding chiral WP5 to D/L-arginine. Meanwhile, DOX is introduced as a chemotherapeutic drug and indocyanine green is used for photothermal therapy to achieve chiral-specific chemo-photothermal synergistic therapy, precisely targeting tumor cells, improving the therapeutic effect and reducing side effects for normal tissues (Fig. 15d).[275]

Photosensitive molecules have attracted significant attention in the fields of photodynamic therapy (PDT), photothermal therapy (PTT) of cancer, and cancer diagnosis, thanks to their unique optical and chemical properties. Introducing photosensitive molecules into supramolecular nanocarriers based on IPAs can not only effectively regulate the size and morphology of the nanocarriers, but also enable the precise diagnosis and treatment of cancer. Similar to the drug-loading modes described previously, for the supramolecular nanocarriers constructed based on IPAs, photosensitizers mainly present in three forms: first, they directly participate in the main-molecular skeleton or are connected to pillararenes through covalent bonds; second, they act as guest molecules or are covalently bound to guest molecules, and participate in the construction of the supramolecular nano-photosensitizer system by virtue of the specific interactions between the host and guest; third, they are directly encapsulated inside the nanocarriers and achieve safe and efficient transportation relying on the protective effect of the nanocarriers.

Tetraphenylethene (TPE) has the advantage of AIE. It can be introduced into the skeleton of a pillararene, forming m-TPEWP5 with unique optical and host–guest properties. Hu *et al.* used m-TPEWP5 and the CPT prodrug molecule DNS-G. Through host–guest interactions, they assembled AIE nanoparticles and constructed a supramolecular nanodrug delivery system. For this system, the fluorescence of m-TPEWP5 changes from blue-green to pale yellow after binding with DNS-G, and then turns bright yellow after the addition of GSH. Such fluorescence changes can visually display the drug release process. This process not only enables real-time tracking of drug release but also effectively inhibits the proliferation of cancer cells and accurately locates tumor tissues, providing new strategies and potential applications for AIE-based cancer diagnosis and treatment (Fig. 16a).[253] In addition, TPE derivatives can be directly used as guest molecules to participate in the construction of pillar[5]arene-based host–guest supramolecular nanoparticles, enabling efficient loading, controlled release of DOX, and visual tracking of the drug release process.[237]

Aniline tetramer (TANI) molecules have the characteristics of undergoing state transitions under different pH conditions (such as the transition from the emeraldine base (EB) state to the emeraldine salt (ES) state) and exhibiting absorption in the NIR region. The group of Han found that TANI can interact with WP5 through host–guest interactions to form amphiphilic complexes, which can further self-assemble into WP5⊃TANI supramolecular vesicles. In an acidic microenvironment (pH 5.3) or upon irradiation using a NIR laser, the vesicle structure transforms into disordered nanoaggregates, enabling the controlled release of DOX. Meanwhile, the NIR laser irradiation generates photothermal effects.[276] They further modified the TAPE molecule derived from TANI with PEG chains, enhancing water solubility and biocompatibility. The modified TAPEG can self-assemble with WP5 through host–guest interactions to form core–shell structured nanoaggregates. The average diameter of these nanoaggregates is approximately 200 nm under neutral pH conditions, and they can transform into a smaller size of about 60 nm in an acidic microenvironment (such as the TME), which combines the advantages of tumor accumulation and penetration. Meanwhile, the dual-mechanism regulation of its structural transformation and π-conjugation under acidic conditions significantly enhances the absorption in the NIR-II region and the photothermal conversion efficiency (up to 60.2%). After loading DOX onto this nanoplatform, the controlled release of DOX can be achieved in an acidic environment or upon NIR laser irradiation. Verified by *in vitro* and *in vivo* experiments, it shows remarkable effects in

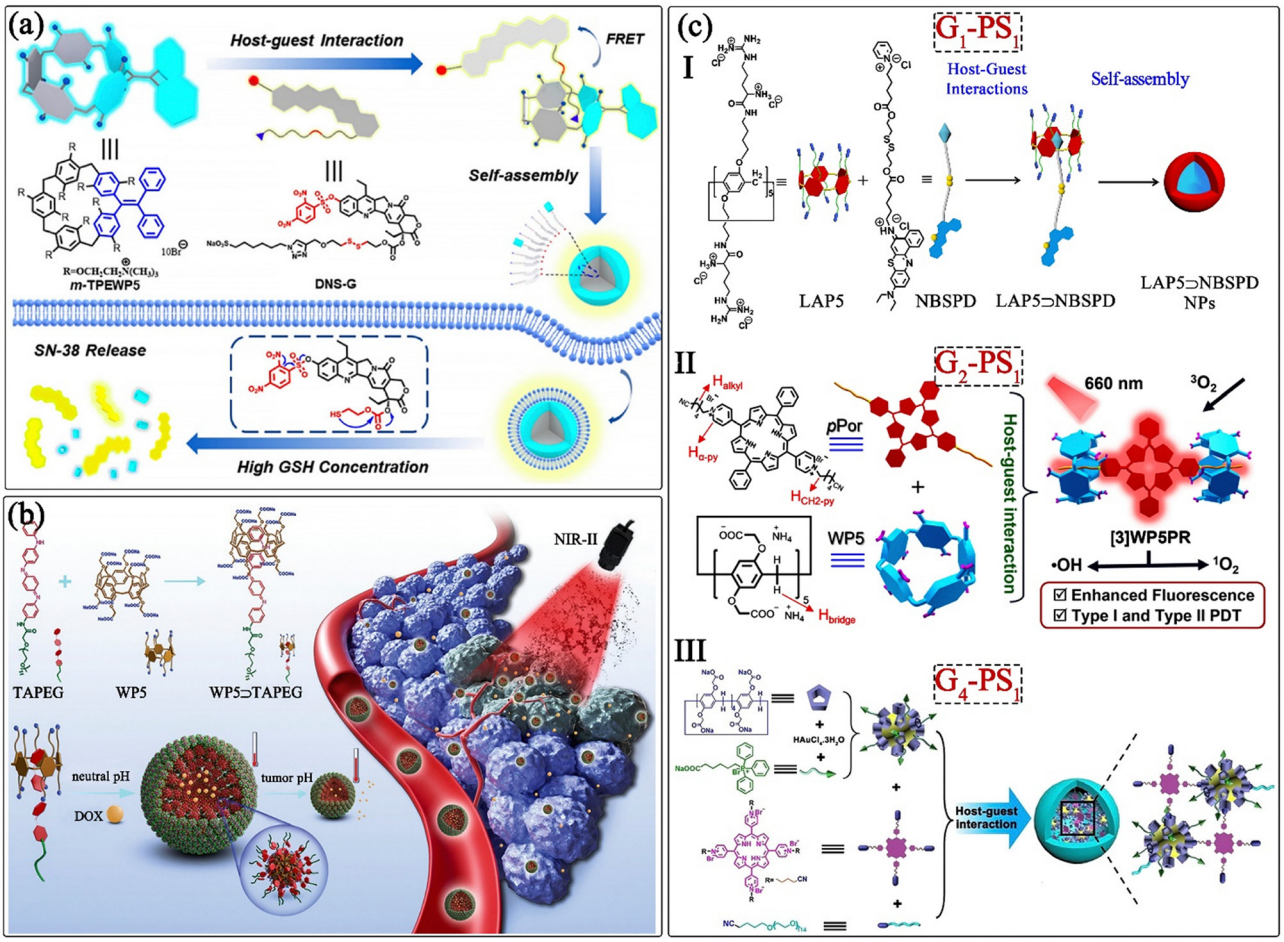

Fig. 16 Supramolecular nano-photosensitizers constructed based on IPAs. (a) The schematic of the orthogonal design of water-soluble *meso*-tetraphenylethene-functionalized pillar[5]arene with AIE property and its therapeutic application (Reproduced with permission from ref. 253. Copyright 2021, American Chemical Society). (b) The schematic of supramolecular core–shell nanoassemblies with TME-triggered size and structure switching for enhanced photothermal therapy (Reproduced with permission from ref. 242. Copyright 2022, John Wiley & Sons, Inc.). (c) Different types of supramolecular nano-photosensitizers: (I) the schematic of constructing G_1–PS_1 type supramolecular nano-photosensitizer based on the interaction between nile blue derivatives and L-arginine-functionalized pillar[5]arene (Reproduced with permission from ref. 254. Copyright 2023, The Royal Society of Chemistry). (II) The schematic of constructing G_2–PS_1 type supramolecular nano-photosensitizer based on the interaction between *para*-modified porphyrin photosensitizer and carboxylated pillar[5]arene (Reproduced with permission from ref. 223. Copyright 2023, The Royal Society of Chemistry). (III) The schematic for constructing a multifunctional supramolecular photosensitizer based on the host–guest interaction between tetrapyridylporphyrin and a pillararene–Au nanoparticle complex with mitochondria-targeting (Reproduced with permission from ref. 273. Copyright 2020, American Chemical Society).

photothermal therapy and chemo-photothermal synergistic therapy for cancer, providing a new approach to improve the efficacy of photothermal therapy (Fig. 16b).[242]

In the field of constructing supramolecular photosensitizers, apart from the relatively straightforward approach of directly using photosensitizers as guest molecules and assembling them into the cavities of pillararenes, the preparation strategy for most supramolecular photosensitizers involves modifying the photosensitizer molecules with one or more specific guest groups (common modifying groups include carbon chains,[224] pyridyl groups,[236,254,277] trimethylamine groups,[239–241,250] cyano groups,[226,278,279] *etc.*). This modification enables photosensitizer molecules with relatively large sizes to act as guest molecules and participate in the construction of supramolecular photosensitizer systems. In addition, depending on the number of guest-assembling groups modified on the photosensitizer, it can be classified into three types: G_1–PS_1,[224,239,240,254,277,280] G_2–PS_1,[223,241,250,278,279] and G_n–PS_1 ($n > 3$)[226,273] (Fig. 16c). These different types of photosensitizers can self-assemble with varying amounts of IPAs, forming a diverse range of supramolecular photosensitizer systems. This not only provides a more precise means of regulating the design of photosensitizers, but also expands the structural richness and functional diversity of the supramolecular photosensitizer systems constructed based on IPAs.

In addition, in the above-mentioned supramolecular nanocarrier systems constructed based on IPAs, some pillararenes exhibit some unique properties. For example, Yang *et al.* designed tryptophan-modified pillar[5]arene (TP5) and used a galactose derivative as the guest molecule. They encapsulated

DOX through host–guest interactions to construct a supramolecular nano-delivery system with HepG2-targeting ability. The tryptophan-rich structure of TP5 acts as a multivalent ligand to produce an amplification effect or cluster effect, enhancing the supramolecular interactions between tryptophan residues and DNA, and generating a synergistically enhanced cytotoxic effect on cancer cells.[230] Yu *et al.* used the strong binding affinity between quaternary ammonium salt pillararenes and ATP to encapsulate ATP in cancer cells. This method reduces the energy supply for the overexpressed drug-resistant proteins on the surface of drug-resistant cancer cell membranes, thereby decreasing the efflux of DOX. As a result, it significantly increases the drug concentration within cancer cells and synergistically enhances the chemotherapeutic effect.[234] Chao *et al.* designed and synthesized a cyclic cell-penetrating peptide based on pillararenes, mimicking the cell-penetrating function of oligoarginine, and constructed a supramolecular photosensitizer system with strong penetration ability through host–guest interactions with type-I photosensitizer derivatives. Under the stimulation of high-concentrations of GSH in the TME, the photosensitizer and L-arginine-based pillararene are released. Where, the L-arginine-based pillararene can damage the cancer cell membrane and various organelles, synergistically enhancing the efficacy of PDT.[254]

7.2.3. Supramolecular organic–inorganic hybrid nanocarriers. In recent years, inorganic nanomaterials represented by hollow manganese dioxide and metal–organic frameworks (MOFs), due to their unique physical and chemical properties such as high specific surface area, tunable pore structures, and stimulus-responsive nature, have shown great application potential in areas such as drug delivery, disease diagnosis, and treatment. At the same time, IPAs, with their excellent multifunctional integration capabilities, can combine with inorganic nanomaterials. Acting as nanovalves or surface-modifying molecules, they can construct hybrid nanotherapeutic platforms with excellent performance. In cancer treatment, this hybrid system can not only accurately deliver anti-cancer drugs to the tumor site but also use the photothermal, magnetothermal, and other properties of inorganic nanomaterials to achieve multimodal synergistic killing of tumor cells. This significantly improves the treatment effect and reduces damage to normal tissues. In this section, we will focus on introducing the latest advances in the research of supramolecular organic–inorganic hybrid materials constructed based on IPAs for cancer treatment.

Hollow manganese dioxide (H-MnO_2), with its unique hollow multi-cavity structure, high specific surface area, and degradable properties, has emerged as an ideal carrier for tumor-targeted drug delivery systems. Its cavities enable ultra-high loading rates of chemotherapeutic drugs, macromolecular proteins, or gene therapy agents, while the abundant Mn–O bonds and hydroxyl functional groups on its surface confer multi-stimuli response to the TME (*e.g.*, pH 5.0–6.5, GSH overexpression, metal ion concentration gradients), triggering precise drug release through skeleton dissociation or ligand exchange mechanisms. However, the clinical translation of H-MnO_2 is still hindered by two major challenges: (1) the mismatch between drug release kinetics and TME heterogeneity, leading to off-target toxicity; and (2) the low efficiency of passive targeting relying on the enhanced permeability and retention (EPR) effect, which may cause toxicity to normal tissues.

To address these limitations, the dynamic host–guest recognition capability and charge-reversal properties of IPAs provide a novel strategy. Currently, two main approaches are employed to construct IPAs-H-MnO_2 supramolecular hybrid systems: (1) electrostatic self-assembly strategy: utilizing the pH-dependent charge-reversal properties of IPAs (*e.g.*, protonation of carboxyl groups in the TME), reversible nanovalves are formed through electrostatic interactions with the negatively charged surface of H-MnO_2, whose open and closed states can be precisely regulated by TME acidity or chelated metal ions;[281–284] (2) covalent-host–guest synergistic strategy: by covalently anchoring guest molecules to the surface of H-MnO_2, molecular switches are formed through supramolecular interactions between IPAs and the guests. By precisely designing the chemical structure of the guest molecules, the response of the pillar[*n*]arene host–guest complexes to stimuli such as acid,[285–291] alkaline,[287,289] metal ions,[285–287,289] redox,[282,289,290] competitive binding agents (*e.g.*, methyl viologen (MV),[285,286] ethylenediamine[291,292]), and temperature[291,292] can be enhanced, further coordinating drug release with TME heterogeneity. Such nanovalves effectively prevent premature drug leakage during delivery. To further improve the targeting specificity of the nanosystem, targeting ligands (*e.g.*, folic acid,[291] galactose,[281] lactose,[283] glucosamine[293]) are embedded into the host–guest complexes as guest molecules, or targeting groups are directly modified onto the nanocarrier surface through covalent conjugation or electrostatic adsorption, enabling precise tumor cell recognition *via* receptor–ligand interactions.

Notably, the introduction of IPAs not only optimizes the controlled release performance of H-MnO_2 but also promotes the construction of multimodal synergistic therapeutic platforms. For example, chemotherapeutic drugs (*e.g.*, DOX,[282,284,286–291] isoniazid,[283] F16[290]) are loaded into the cavities of H-MnO_2, while photosensitizers (*e.g.*, Ce6,[283] BODIPY[293]), photothermal agents (*e.g.*, Au NPs,[281,285,290] copper sulfide nanoparticles[291,292]), or NO donors (*e.g.*, *S*-nitrosothiols[281]) are encapsulated to achieve combined therapies such as chemotherapy with photodynamic therapy, photothermal therapy, or gas therapy. The luminescence of fluorophores specifically activated by the TME enables the fluorescence imaging and tracking capabilities of the nanosystem.[282] Additionally, studies have explored the regulation of the TME by MnO_2 under TME conditions, where the generated Mn^{3+} mediates immunogenic cell death, extending combined therapies to emerging fields such as chemodynamic therapy and immunotherapy (Fig. 17a).[283] These studies provide important references for developing antitumor nanomedicines with high targeting specificity, controlled drug release, and multi-mechanism synergy.

MOFs are a class of porous materials constructed from metal ions or clusters and organic ligands. They possess many

excellent properties such as high specific surface area, large porosity, good biocompatibility, adjustable structure, and functional diversity, showing great application potential in biomedical fields such as drug delivery, bioimaging, and disease treatment. Similar to the method of constructing IPAs-H-MnO_2 hybrid nanomaterials, researchers can modify IPAs on the surface of MOF materials such as ZIF-8,[294,295] UMCM,[296] and UiO-66[297,298] as nanogates through electrostatic interactions or host–guest interactions between IPAs and the surfaces of these MOF materials, and have successfully constructed a variety of multifunctional nanodelivery systems with targeting and TME-responsive properties (Fig. 17b). Among them, the research group led by Yang coated UiO-66 layers on the surfaces of materials such as PPy nanoparticles[299] and Fe_3O_4[300] respectively. By virtue of the good photothermal conversion ability of PPy, the synergistic effect of nanomaterials in drug delivery and photothermal therapy was achieved. When combined with Fe_3O_4, the magnetic property of Fe_3O_4 was used to endow the nanomaterials with MRI imaging functionality. The coordinated combination of these multiple functions significantly enhanced the treatment effect for cancer, providing innovative strategies and effective means for cancer treatment.

In addition to the previously introduced H-MnO_2 and MOF, many other inorganic nanomaterials with excellent properties are also widely used in the construction of IPAs-based supramolecular hybrid systems. For example, gold nanorods (Fig. 17c)[301] and gold nanospheres[302] exhibit excellent performance in the fields of photothermal and photocatalysis due to their surface plasmon resonance effect; copper sulfide (Fig. 17d)[303] and copper selenide[304] have good optoelectronic properties and biocompatibility; upconversion materials[171] can convert low-energy NIR light into high-energy visible light and

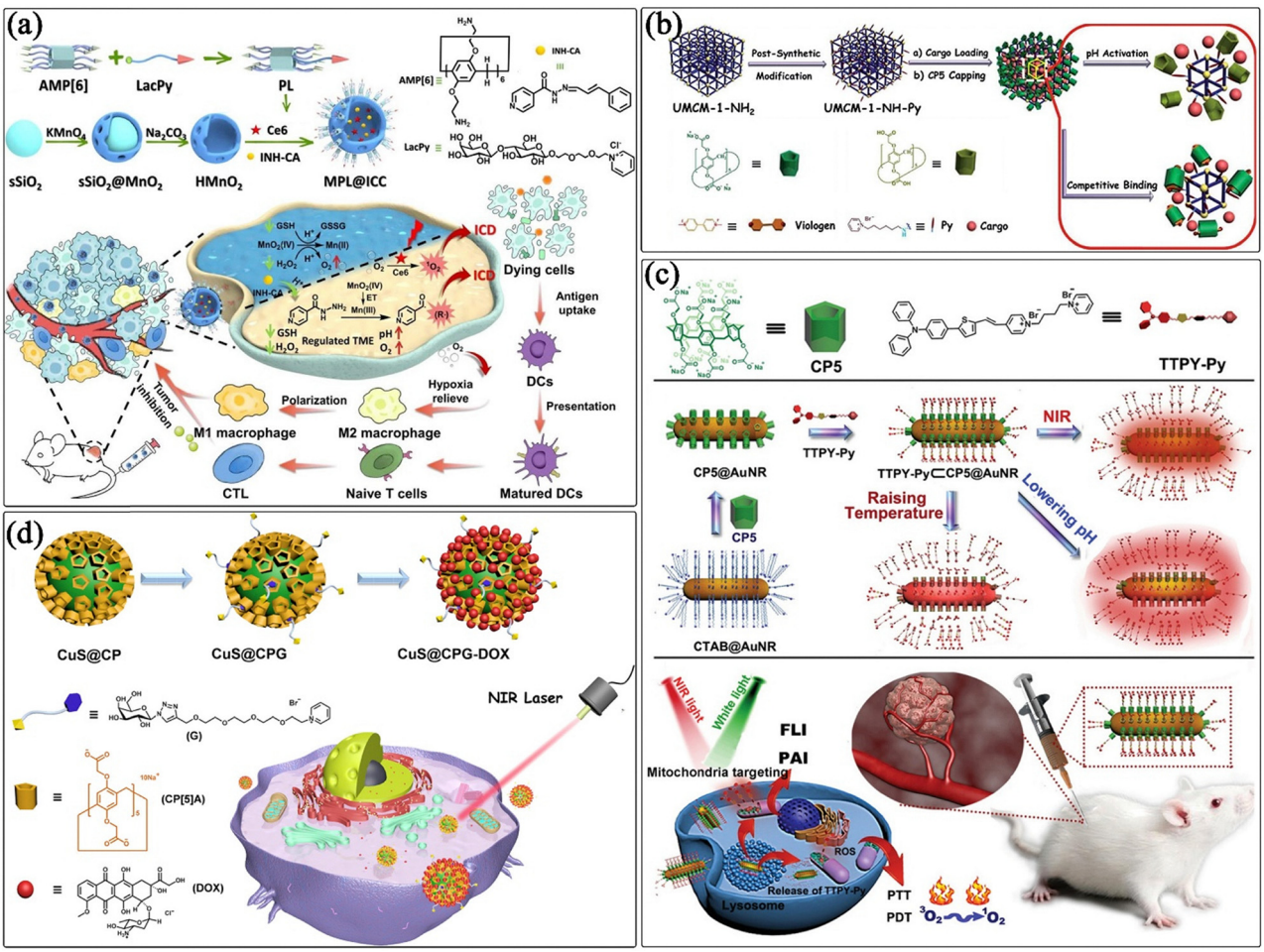

Fig. 17 IPAs-based supramolecular organic–inorganic hybrid nanocarriers for cancer therapy. (a) The schematic of the MPL@ICC nanovaccine prepared from IPAs and H-MnO_2 for inducing immunogenic cell death to trigger an anti-tumor immune response (Reproduced with permission from ref. 283. Copyright 2024, The Royal Society of Chemistry). (b) The schematic of stimuli-responsive nanocarriers based on mechanized nanoMOFs (UMCM-1-NH_2) with positively-charged pyridinium units (Py) as stalks encircled by pillarenes on the surfaces. The mechanized (UMCM-1-NH_2) nanovalves can be operated either by pH changes or by competitive binding to regulate the release of cargo molecules, *i.e.*, Rh6G and DOX (Reproduced with permission from ref. 296. Copyright 2015, The Royal Society of Chemistry). (c) The schematic of the construction of pillar[5]arene-modified gold nanorods as nanocarriers for multi-modal imaging-guided synergistic photodynamic-photothermal therapy (Reproduced with permission from ref. 301. Copyright 2025, John Wiley & Sons, Inc.). (d) The schematic of the supramolecular nanosystem based on pillararene-capped CuS nanoparticles for targeted chemo-photothermal therapy (Reproduced with permission from ref. 303. Copyright 2018, American Chemical Society).

have potential application value in fields such as bioimaging and photodynamic therapy; black phosphorus nanosheets[305] show great application potential in fields such as electronics and biomedicine due to their unique layered structure and tunable bandgap; superparamagnetic nanoparticles[306] play an important role in magnetic resonance imaging, magnetothermal therapy, and drug targeted delivery. Modifying IPAs on the surface of these nanomaterials can form a variety of multifunctional therapeutic systems. In addition, IPAs can also act as linkers to connect multiple Ag_2S quantum dots[307] to form a novel supramolecular nano-assembly, achieving efficient drug delivery and TME-responsive release, and enhancing the antitumor effect through the combination of chemotherapy and photodynamic therapy. These multifunctional supramolecular hybrid materials show great potential in improving drug delivery efficiency, enhancing therapeutic effects, and reducing side effects, providing new ideas and methods for cancer treatment.

Although IPAs show remarkable potential in cancer treatment, there are still two major challenges in their future development. In terms of the drug release mechanism, although IPAs can achieve drug delivery by responding to the TME (such as acidic pH, enzymes, *etc.*), their release kinetics still need to be improved. How to precisely control the drug release rate under complex physiological conditions (such as avoiding premature leakage or delayed release) and balance the stability of drug encapsulation with the release efficiency at the target site remains a key problem. In terms of safety, although the biocompatibility of IPAs has been preliminarily verified, the potential toxicity of long-term use (such as the accumulation of metabolites and immune risks) and the synergistic safety when combined with other therapies still require in-depth toxicological evaluation and preclinical research. Solving these problems will lay the foundation for the safe application of IPAs in precise cancer treatment.

8. Others

IPAs, with their distinctive cavity structures, numerous sites for modification, and adjustable charge characteristics, show immense potential for applications in the biomedical field and have emerged as a focal point of research. Beyond the applications previously described, IPAs perform well in various areas. This includes the efficient transportation of nucleic acids and proteins, the adsorption and separation of proteins, the creation of supramolecular artificial enzymes that replicate the functions of natural enzymes, novel treatment strategies for diseases such as Alzheimer's and diabetes, and the regulatory research of cell fusion and communication. These capabilities offer novel perspectives and approaches to tackle intricate challenges in life sciences and medicine, driving the continuous advancement of related disciplines.

8.1. Efficient transport of nucleic acids/proteins

In recent years, the rapid development of gene therapy and nucleic acid delivery technologies has made efficient and precise gene delivery and nucleic acid detection methods a research hotspot. In the fields of life science and medicine, gene therapy exhibits great potential in conquering many stubborn diseases that are difficult to cure with traditional medicines, especially some genetic diseases, cancers, viral infections, and so on. Meanwhile, the efficiency and precision of nucleic acid delivery are directly related to the therapeutic effect and the safety of patients. In the physiological environment, nucleic acids (such as DNA and RNA) carry a negative charge, while cationic pillararenes possess a positive charge, enabling them to bind tightly through electrostatic interactions. Such a strong electrostatic attraction not only enhances the specific binding between pillararenes and nucleic acids but also significantly improves the stability of the complexes. As a result, nucleic acids can be more effectively protected from degradation during *in vivo* transportation. Meanwhile, through ingenious molecular design, pillararenes can be combined with various targeting molecules, which provides new possibilities for the directed delivery of nucleic acids. This design allows nucleic acids to accurately reach the target cells or tissues, improving the precision of treatment. At the same time, when pillararenes are complexed with stimuli-responsive molecules, the delivery system can intelligently release nucleic acids under specific physiological or pathological conditions, further enhancing the safety and effectiveness of the treatment. Next, we will provide a detailed review of the research progress of IPAs in the fields of gene therapy and nucleic acid delivery over recent years and explore their important role in promoting novel therapeutic strategies.

In the basic research of gene therapy and nucleic acid delivery, it is crucial to understand the interaction between vectors and nucleic acids. Skvortsova *et al.* designed and synthesized quaternary ammonium salt-functionalized cationic pillar[5]arene. They employed multiple techniques including NMR, CD spectroscopy, and molecular docking to explore the interaction mechanism with nucleic acids. The study revealed that this pillar[5]arene can form complexes with oligonucleotides in a 1 : 1 or 1 : 2 ratio. Moreover, through its interaction with plasmid DNA, it can condense the plasmid DNA into aggregates with a diameter of approximately 100 nm. This condensation effectively promotes the transformation of plasmid DNA into bacterial cells, significantly enhancing the transformation efficiency.[308] Meanwhile, Yakimova *et al.* designed and synthesized a cationic pillar[5]arene (AP[5]A) bearing ten ammonium groups and mixed it with water-soluble thiacalix[4]arene (STC[4]A) featuring four alkyl sulfonate fragments at the lower rim in a cone conformation to construct a nanostructured polyelectrolyte complex. Experimental results demonstrated that this complex can effectively package calf thymus DNA, forming stable nanoparticles and presenting two distinct structural forms: micelleplexes and polyplexes. During this process, the secondary structure of DNA remains in its native B-form without significant alteration (Fig. 18a).[309]

To study the transfection efficiency of pillar[5]arenes modified with different peptide structures on DNA, Hu and colleagues designed and synthesized a pillar[5]arene-modified

peptide containing guanidiniumcarbonylpyrrole (GCP). This was achieved by amide coupling of mono-alkylamine-modified nona-cationic water-soluble pillar[5]arene (WP5–NH_2) and GCP–Ala–Ala–Ala–Ala–OH (GCP–alanine–alanine–alanine–alanine–hydroxyl). In an aqueous solution, this modified peptide can spontaneously assemble into a twisted β-sheet tape structure. This unique structure endows it with excellent gene transfection performance. Experiments have verified that it can effectively bind and condense DNA and then successfully deliver DNA into cells, thus achieving gene transfection (Fig. 18b).[310] Meanwhile, they also designed and synthesized peptide 1 (a short peptide with one GCP linked to pillar[5]arene), peptide 2, and peptide 3 (short peptides with two GCPs linked to pillar[5]arene. In peptide 2, the methylene lengths connecting the two GCPs are different, while in peptide 3, the two GCPs can form a parallel conformation). The study found that these peptides have different abilities to form condensed complexes with DNA. Among them, peptide 3 can bind to the cell membrane synergistically due to the parallel conformation of its two GCP groups, showing high transfection efficiency, while the structural difference of the two GCP groups in peptide 2 leads to its lower transfection activity. This research provides an important basis for understanding the relationship between the structure of pillar[5]arene-modified peptides and their transfection activity, which is helpful for more precisely designing efficient gene transfection vectors (Fig. 18c).[311]

Li *et al.* designed and synthesized imidazolium-modified decacationic pillar[5]arene (P5A) and used it to construct ionic supramolecular polymers for short DNA delivery. By precisely controlling the molar ratio of P5A and hyaluronic acid (HA) with an average molecular weight of 3000 Da, three ionic

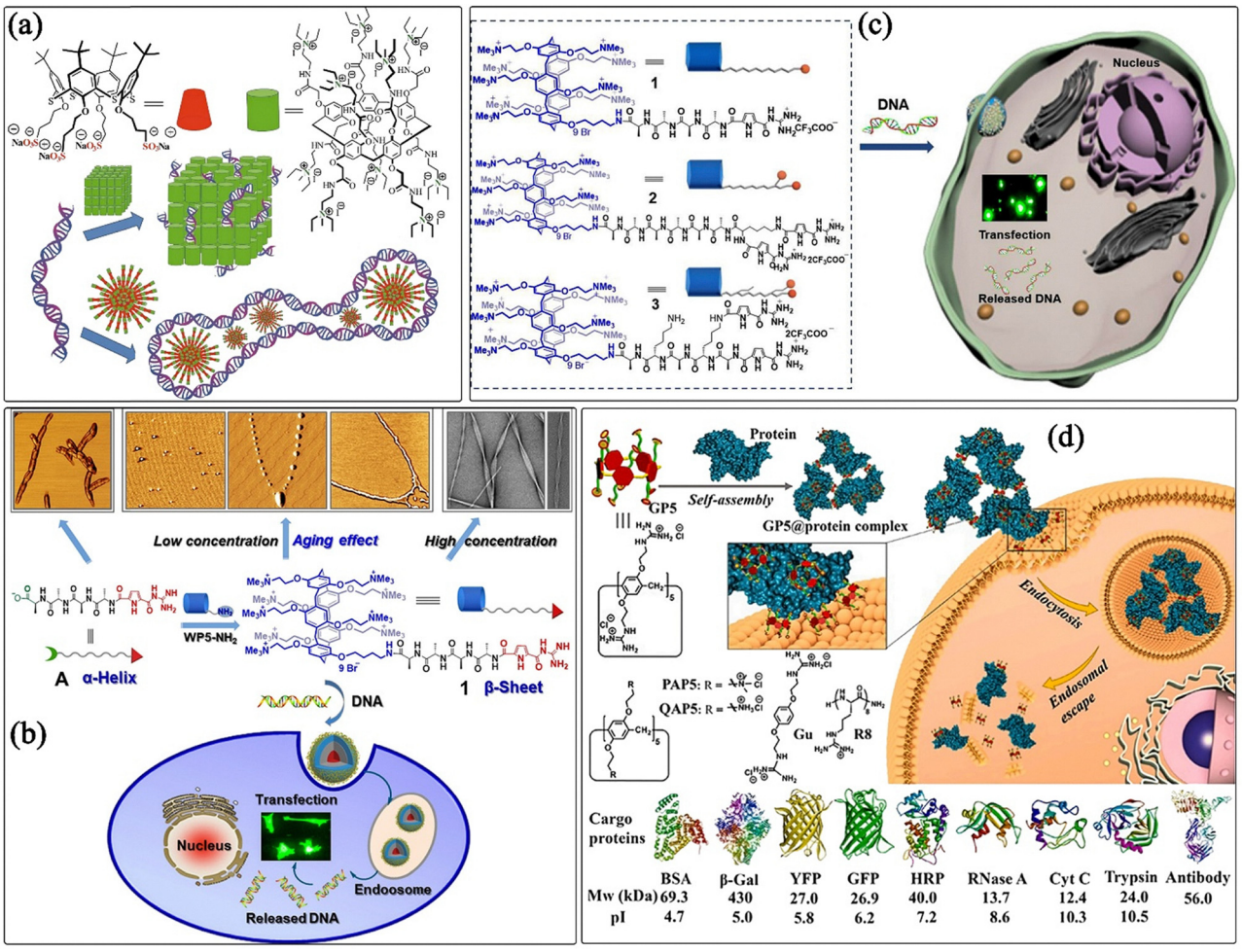

Fig. 18 IPAs are used for the efficient transportation of nucleic acids/proteins. (a) The schematic of the co-assembly of water-soluble thiacalix[4]arene and pillar[5]arene with DNA to form micelle-type or aggregate-type complexes. In both cases, DNA maintains its native B-form secondary structure (Reproduced with permission from ref. 309. Copyright 2020, MDPI). (b) The schematic of the formation of twisted β-sheet tapes from a self-complementary peptide based on the novel pillararene–GCP host–guest interaction and its process of being used for gene transfection (Reproduced with permission from ref. 310. Copyright 2018, John Wiley & Sons, Inc.). (c) The schematic of the self-assembly of peptide-guanidinocarbonylpyrrole-modified pillararene amphiphiles with plasmid DNA (pDNA) into nanoparticles, enabling the process of cellular uptake and release of DNA (Reproduced with permission from ref. 311. Copyright 2023, Elsevier). (d) The schematic of efficient intracellular delivery of native proteins facilitated by preorganized guanidiniums on the pillar[5]arene skeleton (Reproduced with permission from ref. 314. Copyright 2022, Elsevier).

supramolecular polymers (ISP–$P5A_{1.0}HA_{0.2}$, ISP–$P5A_{1.0}HA_{0.4}$, ISP–$P5A_{1.0}HA_{0.6}$) were prepared. These polymers can form nano-sized aggregates, effectively encapsulate short DNA strands, and efficiently deliver them into normal and cancer cells. The second polymer exhibits the highest biocompatibility, and mixing it with hyaluronic acid can further improve the biocompatibility of P5A.[312]

Barraán-Berdón *et al.* designed and used a water-soluble polycationic pillararene to construct a novel lipid-based complex system for gene delivery based on pillar[5]arene. In this system, the pillar[5]arene, as a polycation, effectively bridges the anionic lipid 1,2-dioleoyl-*sn-glycero*-3-phospho-(10-*rac*-glycerol) (DOPG) and plasmid DNA, achieving charge reversal of the lipid complex. Through various biophysical and biochemical experimental methods, it was found that this complex exhibits a nano-sized dimension and a specific liquid crystal phase structure. In cell transfection experiments, this complex system exhibits moderate to high transfection efficiency and good cell viability. This achievement provides a promising non-viral vector system for gene delivery and promotes the further development of P5A in the field of gene therapy.[313]

Proteins play a crucial role in various biological processes, especially in the regulation of cell functions, signal transduction, immune responses, and the treatment of diseases. They are not only fundamental components of the cell structure but also participate in key biological processes such as enzymatic catalysis, cell metabolism, and gene expression. However, due to the high selectivity and impermeability of the cell membrane, effectively delivering proteins into cells has always been a major challenge in the field of biomedicine. Previous studies have shown that many protein carriers often perform poorly when delivering proteins with different isoelectric points, resulting in low delivery efficiency or insufficient targeting ability. This makes the treatment for specific diseases or cell types more complicated and difficult. In addition, current research on small-molecule non-covalent protein carriers is relatively scarce, which limits innovation and development in protein delivery systems. Therefore, the development of new and efficient carriers, especially those that can overcome the cell membrane barrier and achieve precise targeted delivery, has become the focus of current research.

Guo and colleagues designed and synthesized a guanidinium-functionalized pillar[5]arene (GP5). The study found that GP5 can bind to proteins of varying isoelectric points and sizes through salt bridges, forming nanoaggregates with an average diameter of 60 nm. The GP5@FITC–BSA complex can efficiently enter HeLa cells within 3 h, with a molar ratio of [GP5]/[BSA] = 5/1 being optimal. Cellular uptake experiments indicated that GP5@FITC–BSA primarily enters cells *via* macropinocytosis, escaping from endosomes/lysosomes after 4 h, with some proteins released from the aggregates. Compared to other control carriers, GP5 is unique due to its guanidinium groups, oligoguanidinium, and the pre-organization of guanidinium groups on both sides of the pillar[5]arene backbone, which enhances its protein delivery capability. To assess the bioactivity of the delivered proteins, the researchers used GP5 to deliver model bioactive proteins such as horseradish peroxidase (HRP) and β-galactosidase (β-Gal). The results indicated that approximately 90% of HRP activity and about 80% of β-Gal activity were retained after delivery. Additionally, therapeutic proteins such as RNase A, trypsin, cytochrome *C* (Cyt *C*), and anti-phosphorylated Akt (Ser473) antibodies delivered using GP5 maintained high catalytic activity within cells and were able to perform their respective biological functions. This study provides new insights for the design and development of cell-penetrating peptide mimetics (Fig. 18d).[314]

Sultanaev and colleagues designed a ternary biosupramolecular system based on pillar[5]arene, BSA, and methyl orange. By synthesizing carboxybetaine derivatives of pillar[5]arene with different amino acid fragments such as L-phenylalanine, glycine, and L-alanine, and using techniques such as NMR, UV-vis, fluorescence spectroscopy, circular dichroism (CD), dynamic light scattering (DLS), and molecular docking, an experimental system was constructed to study the interactions between proteins and ligands. The experimental results indicate that pillar[5]arenes modified with different amino acid fragments have different effects on the native conformation of BSA in the system. Pillar[5]arene with L-phenylalanine fragments can retain the native form of BSA to the greatest extent and form more stable complexes. There are multiple interactions in the system, enabling pillar[5]arene to form stable host–guest complexes with methyl orange. Moreover, pillar[5]arene with L-phenylalanine fragments is cytotoxic to tumor cells and can enhance the transfection of intercalating agents in MCF-7 cells at certain concentrations.[315]

In conclusion, IPAs with positively charged groups (ammonium ions, guanidinium ions, *etc.*) can bind tightly to negatively charged nucleic acids and proteins through electrostatic interactions, thus forming stable complexes. Such strong electrostatic attraction not only improves the delivery efficiency but also effectively protects nucleic acids and proteins from degradation enzymes in the physiological environment, ensuring their stability during *in vivo* transportation. Secondly, the flexible and diverse molecular design of IPAs enables them to bind to different targeting molecules, thus achieving precise targeted delivery. This characteristic allows nucleic acids and proteins to accurately reach the target cells or tissues. When combined with stimuli-responsive molecules under specific pathological conditions, it further enhances the intelligence and safety of the delivery system. By adjusting the structure of pillararenes and their binding ability with small molecules or peptides, their transfection efficiency and biocompatibility can be significantly improved. In addition, IPAs exhibit good adaptability when delivering proteins with different isoelectric points, overcoming the limitations of traditional carriers in this regard. In summary, the advantages of IPAs lie in their excellent drug-loading capacity, targeted delivery ability, and adaptability to different biomolecules, making them a promising choice of carriers in the field of gene and protein delivery. These characteristics not only provide a basis for the

development of novel biological treatment strategies but also open up new possibilities for future clinical applications.

8.2. Adsorption and separation of proteins

Proteins are involved in nearly all physiological processes within cells, including material metabolism, energy conversion, and signal transduction. The adsorption behavior of proteins at biological interfaces plays a crucial regulatory role in the normal functioning of these processes. In-depth research on protein adsorption behavior at biological interfaces helps to accurately elucidate the molecular mechanisms of these life processes, revealing the essence of life at a microscopic level. Li and colleagues used the guest-induced planar chirality of pillar[5]arene to prepare a chiral NH_2-pillar[5]arene modified silicon surface (pR-/pS-NP5 surface) for the highly enantioselective adsorption of BSA. The results indicated that NP5 forms stable host–guest complexes with D-/L-His. After introducing chiral His, NP5 exhibits chiral induction and amplification effects, resulting in the formation of planar chiral pR-/pS-NP5. Meanwhile, the pR-NP5 surface demonstrates high adsorption capacity and chiral selectivity for BSA, primarily due to the planar chiral amplification induced by chiral His and the stronger binding interactions between pR-NP5 and BSA. This study provides deeper insights into the chiral effects of protein adsorption at biological interfaces and offers new perspectives for chiral sensing applications (Fig. 19a).[316] Yan and colleagues constructed a chiral biological interface for the adsorption of lysozyme using WP5 and phenethylamine (PEA) through host–guest interactions on a gold surface. Experimental results indicated that the PEA@WP5 surface exhibited high adsorption capacity and strong chiral selectivity for lysozymes. This is primarily attributed to hydrogen bond interactions and charge interactions between WP5 and lysozymes, as well as the increased specific surface area due to the self-assembly of WP5. Additionally, the surface chirality amplification achieved through the self-assembly of WP5 with R/S-PEA also enhances chiral recognition capabilities. This research offers new approaches for constructing biointerfacial materials with high adsorption capacity and selectivity.[317]

Efficient separation of cell membrane proteins is of great significance for elucidating the physiological mechanisms of cells, revealing the development mechanisms of diseases, precisely screening drug targets, and early disease diagnosis. However, the existing protein separation and analysis methods have disadvantages such as low efficiency, poor purity, and susceptibility to interference. Zhu and colleagues reported an innovative strategy based on pillararene host–guest recognition and magnetic solid-phase extraction for the separation and enrichment of cell membrane proteins. They first synthesized water-soluble per-phosphate pillar[5]arene (WP5-P) and modified it on the surface of Fe_3O_4 nanoparticles (MNP) to prepare MNP-P5 with magnetic response and host–guest recognition ability. There is an extremely strong host–guest interaction between WP5-P and the imidazolium guest G1, and the complexation constant is as high as 1.10×10^6 M^{-1}. Evaluation using the coumarin derivative G2 and the imidazolium-labeled hemoglobin Hb-G as models, it was found that MNP-P5 can effectively capture guest molecules and proteins. Further using this strategy to enrich cell membrane proteins, it was confirmed by SDS–PAGE and western blotting analysis that MNP–P5 can efficiently separate and enrich cell membrane proteins with almost no capture of intracellular proteins. This strategy has the advantages of simple synthesis, rapid separation, and excellent performance, providing new ideas for the design of magnetic field-responsive materials (Fig. 19b).[318]

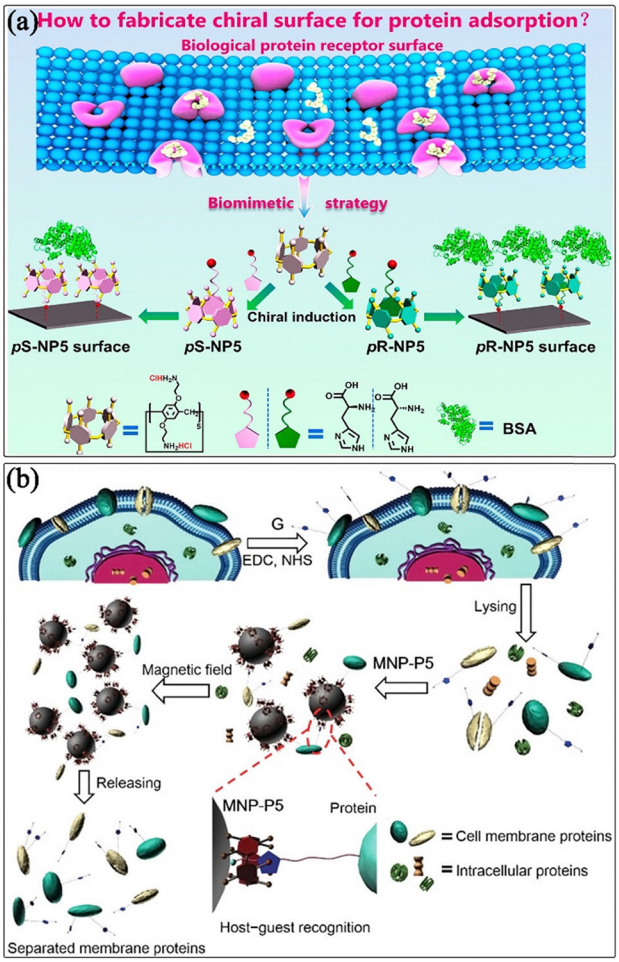

Fig. 19 IPAs are used for the adsorption and separation of proteins. (a) The schematic of the design of a biomimetic chiral surface for the enantioselective adsorption of BSA protein based on the host–guest interaction (Reproduced with permission from ref. 316. Copyright 2021, American Chemical Society). (b) The schematic of the host–guest recognition-involving MSPE strategy for membrane protein separation. The membrane proteins are labelled with imidazolium guests by EDC coupling, and the labelled proteins are selectively recognized by MNP-P5 *via* host–guest interactions in the cell lysate. Upon exposure to a magnetic field, the captured proteins can be separated from the cell lysate and released by heating (Reproduced with permission from ref. 318. Copyright 2018, The Royal Society of Chemistry and the Chinese Chemical Society).

IPAs exhibit remarkable advantages in protein adsorption and separation, primarily in the following aspects: first, their unique molecular structure enables stable complex formation with target proteins through multiple mechanisms

(electrostatic interactions, hydrogen bonds, and hydrophobic effects) significantly enhancing adsorption selectivity and efficiency. Second, water-soluble IPA derivatives self-assemble on metal surfaces to form high-specific-surface-area biointerfaces, strengthening protein interactions and improving overall separation performance. Additionally, innovative designs incorporating magnetic materials endow IPAs with excellent capabilities for rapid separation and enrichment of cell membrane proteins, featuring simple synthesis and operation. In summary, IPAs not only offer new tools for protein research but also open up novel avenues for applications in biomedicine, drug screening, and beyond.

8.3. Supramolecular artificial enzymes

Supramolecular catalysis, as a cutting-edge research direction in the field of chemistry, is dedicated to precisely regulating chemical reactions at the molecular level. It is of great significance for promoting the development of multiple fields such as green chemistry, drug research/development, and materials science. In the research of supramolecular catalysis, mimicking the hydrolysis of phosphodiesters by phospholipase D is an important objective. Liz *et al.* studied the formation and structure of supramolecular complexes between phosphate esters and quaternary ammonium-based pillararene P5A through NMR spectroscopy and molecular dynamics calculations. It was found that under neutral pH conditions, P5A can increase the hydrolysis rate constant of 2,4-dinitrophenyl phosphate monoester (DNPP) by nearly 10 times. Its catalytic effect originates from a dual mechanism: on the one hand, the quaternary ammonium groups (NMe_3^+) of P5A reduce the negative electron density on the PO_3^{2-} oxygen atoms through electrostatic stabilization to optimize the transition state energy; on the other hand, the steric hindrance of NMe_3^+ groups around the cavity prevents DNPP from forming hydrogen bonds with water molecules, weakening the solvation stability of the monoester dianion, and the two effects synergistically accelerate the hydrolysis reaction.[319] The active site of phospholipase D is positively charged, and the nucleophilic attack of histidine imidazole on the phosphorus center promotes the reaction. Based on this, Wanderlind and colleagues synthesized imidazole-functionalized pillar[5]arene (P5IMD) for the study of phosphodiester hydrolysis reactions. It was found that P5IMD has was pH-dependent and can form complexes with various phosphodiester substrates, such as bis(2,4-dinitrophenyl)phosphate (BDNPP), phenyl 2,4-dinitrophenyl phosphate (PDNPP), and ethyl 2,4-dinitrophenyl phosphate (EtDNPP). Through NMR spectroscopic experiments, it was found that when P5IMD complexes with BDNPP, a small induced downfield shift occurs in the imidazole NCHN signal, and the NMR signal of BDNPP itself also shows a complexation-induced downfield shift, indicating that one aromatic ring of BDNPP enters the cavity of P5IMD and the other aryl group is outside the cavity. When PDNPP complexes with P5IMD, the hydrogen atoms at the NCHN position of the imidazole show a complexation-induced downfield shift, while the aromatic hydrogen atoms of the pillararene show a complexation-induced upfield shift. At neutral pH, P5IMD has an outstanding catalytic effect on the hydrolysis of BDNPP. Compared with pure water, the reaction rate is increased by 10^4 times, and the rate constant of its reaction with BDNPP is 270 times that of free imidazole. Moreover, P5IMD shows significant differences in catalytic rates for different substrates. For example, the catalytic rates for BDNPP and EtDNPP differ by 520 times, and the selectivity is increased by 10^2 times compared with that in pure water. With this research, the ionic properties of P5IMD are crucial in its catalytic hydrolysis of phosphodiesters: under different pH conditions, the charge state of P5IMD changes accordingly. At lower pH, the charge increases, enhancing the electrostatic attraction to negatively charged phosphodiester substrates, increasing the binding constant, and more effectively enriching the substrates, creating favorable conditions for catalysis. The nucleophilicity of the imidazole group itself is affected by the ionic properties. The positively charged state stabilizes the negatively charged intermediates in the reaction, optimizes the microenvironment of the active site, reduces the activation energy of the phosphodiester hydrolysis reaction, and accelerates the reaction rate. When forming complexes with asymmetric phosphodiester substrates, factors such as the electrostatic interaction and steric hindrance generated by the ionic properties jointly affect the binding mode and orientation of the substrates. Only complexes with specific binding modes are reactive, greatly improving the selectivity of P5IMD in catalyzing the hydrolysis of substrates (Fig. 20a).[320]

The process of catalyzing the decomposition of hydrogen peroxide to generate reactive oxygen species by catalase in living organisms is crucial for the active metabolism. Mimicking its efficient catalytic mechanism to construct artificial catalytic systems is of great significance in the fields of environmental governance and biosensing. Cheng *et al.* constructed 2D organic–inorganic hybrid nanosheets *via* electrostatic self-assembly of imidazolium-functionalized pillar[6]arene (P6) and polyoxometalate (POM).[321] The research indicates that the macrocyclic cavity of P6 forms a porous single-molecule layer structure by restricting the lamellar arrangement of POM, significantly enhancing the activation efficiency of H_2O_2. In the presence of H_2O_2, the nanosheets promote the diffusion of H_2O_2 to the catalytic sites of POM, generating tungsten peroxide intermediates W^V–O–O$^\bullet$ and releasing $^\bullet$OH radicals, which can completely degrade methyl orange within 60 minutes, with a reaction rate constant of 0.039 min^{-1}. In contrast, the monomer P_1/POM system without a macrocyclic structure only achieves a 19% degradation rate, confirming the key role of the pillararene cavity in enhancing catalytic efficiency. Similarly, mimicking the property of catalase that uses cofactors to enhance catalytic activity, Park *et al.* prepared carboxylated pillar[5]arene (CP)–coated Au NPs (CP–AuNPs) *via* a one-pot hydrothermal method.[322] The multi-carboxyl groups of CP endow CP–AuNPs with excellent chemical stability under high-salt, strong acid/alkali conditions through electrostatic stabilization and steric hindrance effects, maintaining a dispersed state (particle size ~16.7 nm). When silver ions are introduced

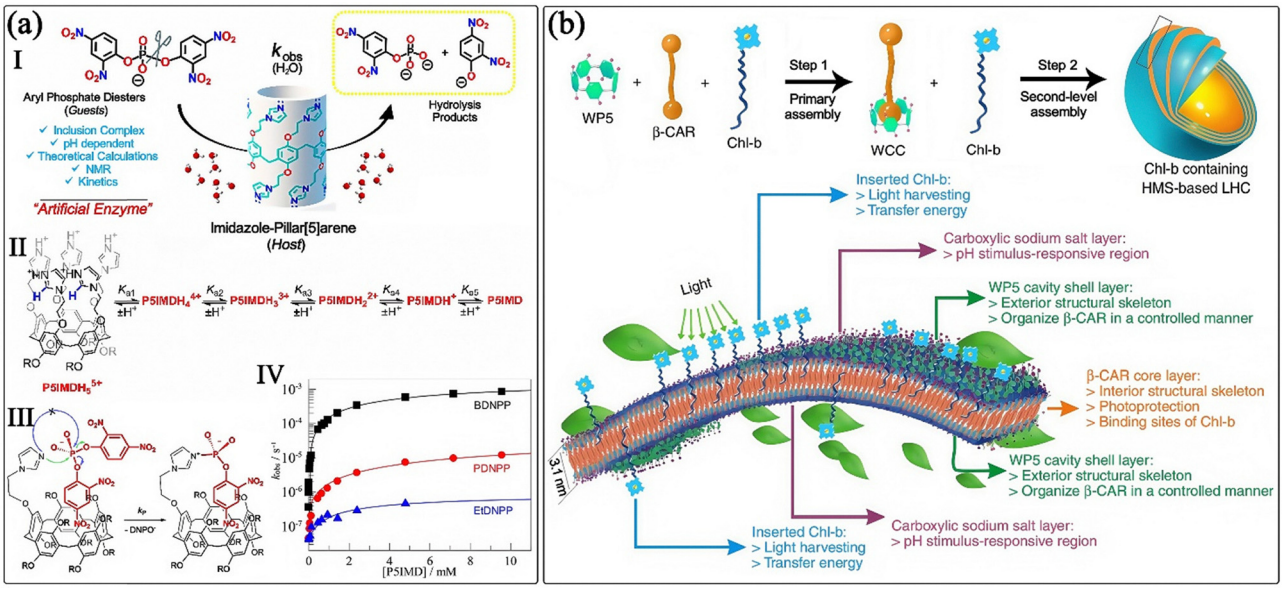

Fig. 20 IPAs and their functionalized nanomaterials, serving as supramolecular artificial enzymes, achieve substrate-selective biomimetic catalysis through host–guest recognition and charge synergism. (a) (I) P5IMD: highly reactive and selective supramolecular artificial enzymes. (II) Acid dissociation equilibria of P5IMD, exemplified with one of the rims of the host. (III) The schematic of the nucleophilic attack pathway for the hydrolysis of phosphate diesters catalyzed by P5IMD. (IV) The influence of the P5IMD concentration on the first-order rate constants for the hydrolysis of different phosphate diester substrates (BDNPP, PDNPP, and EtDNPP). (Reproduced with permission from ref. 320. Copyright 2018, American Chemical Society). (b) The schematic for the preparation of stimulus-responsive light-harvesting assemblies induced by pillararene-mediated co-assembly of β-carotene and chlorophyll. (Reproduced with permission from ref. 324. Copyright 2016, Springer Nature).

as cofactors, CP–AuNPs exhibit remarkable peroxidase-like activity, efficiently catalyzing the oxidation of ABTS by H_2O_2, with a reaction rate significantly higher than that of traditional citrate-stabilized AuNPs. This provides a new strategy for the development of enzyme-like nanocatalysts resistant to harsh environments.

The oxidation of aldehydes to carboxylic acids is a key reaction in nature and the chemical industry, which can be easily achieved in liver cells. However, in industrial production, autoxidation reactions are inert, and the reaction is difficult to carry out under enzymatic conditions (aqueous phase, pH 7, room temperature). Zeng *et al.* prepared supramolecular catalyst nanospheres *via* the self-assembly in water using chromium-centered Anderson-type polyoxometalates ($CrMo_6$) and cationic pillar[5]arenes (P5A) with 10 positive charges.[323] When using air as the oxidant, the nanospheres exhibit a synergistic effect between the oxidation activity of $CrMo_6$ and the phase transfer catalysis of P5A for aldehyde oxidation. Taking benzaldehyde as an example, the conversion rate exceeds 96% within 3 h, significantly superior to using $CrMo_6$ alone (90% in 4 h) or P5A alone (90% in 6 h). Substrate expansion experiments show that the nanospheres are highly efficient for both aromatic aldehydes (such as methyl-substituted and 4-bromobenzaldehyde, with conversion rates >99%) and aliphatic aldehydes (such as lauric aldehyde, 91% conversion), which is attributed to the enhancement of substrate enrichment through hydrogen bonding and CH/π interactions between P5A and the substrates. The catalyst maintains over 80% activity after 6 cycles of use, and FT-IR confirms that its structure remains stable, with only the morphology changing into loose nanoclusters. This study provides a new supramolecular catalytic strategy for aldehyde oxidation under mild conditions.

Carotenoids play a key role for light harvesting and energy transfer in nature. In plants and microorganisms, they are embedded in supramolecular structures through specific molecular geometries and interactions with other molecules, performing functions such as stabilizing light-harvesting complexes, photoprotection, and energy transfer. However, their hydrophobicity leads to numerous challenges in nutritional utilization and supramolecular structure construction. For example, they cannot directly serve as building blocks to form ordered assemblies with physiological functions in aqueous environments, which limits the mimicry of natural photosynthesis mechanisms and the development of artificial photofunctional systems. Sun *et al.* used the rigid cavity of water-soluble carboxyl-modified pillar[5]arene (WP5) to induce the formation of a 1:1 host–guest complex (WCC) with β-carotene (β-CAR) through hydrophobic interactions, which further self-assembled into hollow microspheres (HMS).[324] This "tadpole-like" assembly features the insertion of β-CAR's terpene chain into the WP5 cavity and the exposure of hydrophilic carboxyl groups to the aqueous phase, driving the formation of multi-layered hollow spheres with a diameter of approximately 1855 nm and an interlayer spacing of 3.1 nm. The structure exhibits pH responsiveness, undergoing disruption under acidic conditions. Meanwhile, the introduction of chlorophyll b (Chl-b) for co-assembly results in a natural-like

light-harvesting complex (LHCs-b). In this system, Chl-b is anchored to the hydrophobic layer of HMS *via* its long alkyl chain, while its porphyrin head group is exposed, endowing the system with photocatalytic activity. Under visible light, LHCs-b can reduce 4-nitrophenol to 4-aminophenol within 20 minutes, and also photoreduce metal salts such as K_2PtCl_4, Ag^+, and Pd^{2+} to form corresponding nanoparticles. Circular dichroism spectroscopy confirms the existence of excitonic interactions between Chl-b and β-CAR, verifying the ordered structure of the assembly (Fig. 20b). This study for the first time integrates carotenoids and chlorophyll into a multifunctional supramolecular system, providing new strategies for artificial photosynthetic systems and environmental governance.

The above studies indicate that IPAs exhibit significant advantages in the field of supramolecular biomimetic catalysis due to their unique molecular recognition ability, tunable charge properties, and structural plasticity. By introducing functional ionic groups such as quaternary ammonium groups, carboxyl groups, and imidazole groups, pillararenes can not only precisely regulate substrate binding modes and catalytic microenvironments through electrostatic interactions, hydrophobic effects, and host–guest recognition but also synergistically construct multifunctional nanocatalytic systems with components such as metal nanoparticles and polyoxometalates, achieving efficient mimicry of natural enzyme catalytic mechanisms. In the future, through the precise regulation of the ionic chemical structure of pillararenes and the development of hierarchical assembly strategies, it is expected that it will become possible to further enhance the efficiency and controllability of catalytic systems, opening up broader application prospects in fields such as green chemistry, biosensing, and energy conversion.

8.4. The treatment of Alzheimer's disease and diabetes

Alzheimer's disease, as a complex neurodegenerative disorder, causes abnormal aggregation of β-amyloid protein (Aβ) in the brains of patients, leading to damage of nerve cells and neuroinflammation. Ultimately, it results in cognitive and memory impairments, significantly reducing the quality of life of patients. Developing an efficient therapeutic system capable of effectively alleviating clinical symptoms and slowing disease progression holds critical importance in the management of Alzheimer's disease.

IPAs, due to their unique structures and properties, exhibit significant advantages in the treatment of Alzheimer's disease. For example, they can precisely target diseased sites and have good biocompatibility. They can be used to interfere with the aggregation process of Aβ and regulate the cellular microenvironment. Ye and colleagues designed and synthesized charged tubular supramolecules (CTS, including CTS-A, CTS-A/C, and CTS-C) with pillar[5]arene as the backbone and amino and carboxyl groups modified at the tubular terminals. These supramolecules can interact with Aβ peptides through their special structures, not only inhibiting Aβ fibrillation but also disaggregating mature fibrils and effectively reducing the cytotoxicity induced by Aβ.[325]

In addition, Jia and colleagues utilized the host–guest recognition between carboxylated pillar[5]arene (WP5) and dodecylpyridinium chloride (LPC) to self-assemble into supramolecular vesicles loaded with resveratrol. By virtue of the chelation between WP5 and Zn^{2+}, these vesicles can achieve drug release at the lesion site and regulate the phenotype of microglia, promoting their transformation from the pro-inflammatory M1 type to the anti-inflammatory M2 type. This alleviates neuroinflammation, effectively relieves neuronal damage, and significantly improves the cognitive and memory abilities of mice.[326]

At the same time, Yuan and colleagues constructed a supramolecular organic–inorganic hybrid system. They used palladium nanoclusters (Pd NCs) as carriers to load nerve growth factor (NGF), and capped them with supramolecular nanovalves constructed from carboxyl-containing pillar[5]arene (WP5) to form a Zn^{2+}-responsive nanodrug delivery platform, NWP. This platform enables precise targeting and controlled release of drugs at the lesion site. With this platform, Pd NCs have antioxidant and anti-inflammatory functions and can effectively scavenge ROS to protect neuronal cells from oxidative damage. NGF plays a positive role in promoting the growth and survival of damaged neurons. The two work synergistically to improve the learning and memory abilities of Alzheimer's disease mice, opening up a new strategic direction for the treatment of Alzheimer's disease (Fig. 21a).[327] These research results provide multiple innovative strategies for the treatment of Alzheimer's disease and also offer crucial references for subsequent research in related fields.

Due to the inability of pancreatic β-cells to release sufficient insulin or the occurrence of insulin resistance in islet cells, patients with diabetes have varying degrees of dysregulation in blood glucose regulation. Patients need to continuously monitor their blood glucose levels and frequently inject insulin. However, the current open-loop insulin delivery system has many drawbacks, such as being prone to causing hypoglycemia and serious side effects. Developing a closed-loop insulin delivery system has become an important strategy to reduce the risk of hypoglycemia. Zuo *et al.* constructed a multi-stimuli-responsive supramolecular theranostic nanoplatform for insulin delivery based on pillar[5]arene for the treatment of diabetes. They synthesized a diphenylboronic acid derivative G containing a pyrene fluorophore and a long alkyl-chain quaternary ammonium salt. G and WP5 self-assembled into a supramolecular nanocarrier through host–guest interactions. After loading insulin and glucose oxidase (GOx) into this carrier, in a hyperglycemic environment, G can specifically recognize glucose, trigger intramolecular nitrogen–boron interactions, change its own hydrophilicity, and disrupt the vesicle structure to release insulin. At the same time, GOx catalyzes the oxidation of glucose to generate gluconic acid and H_2O_2, which reduces the local pH, protonates WP5 and causes it to precipitate from the solution. H_2O_2 can also break the C–B bond of G, further promoting the disassembly of the vesicles and the efficient release of insulin. *In vitro* experiments confirmed that it has a good response to glucose, excellent insulin release, the

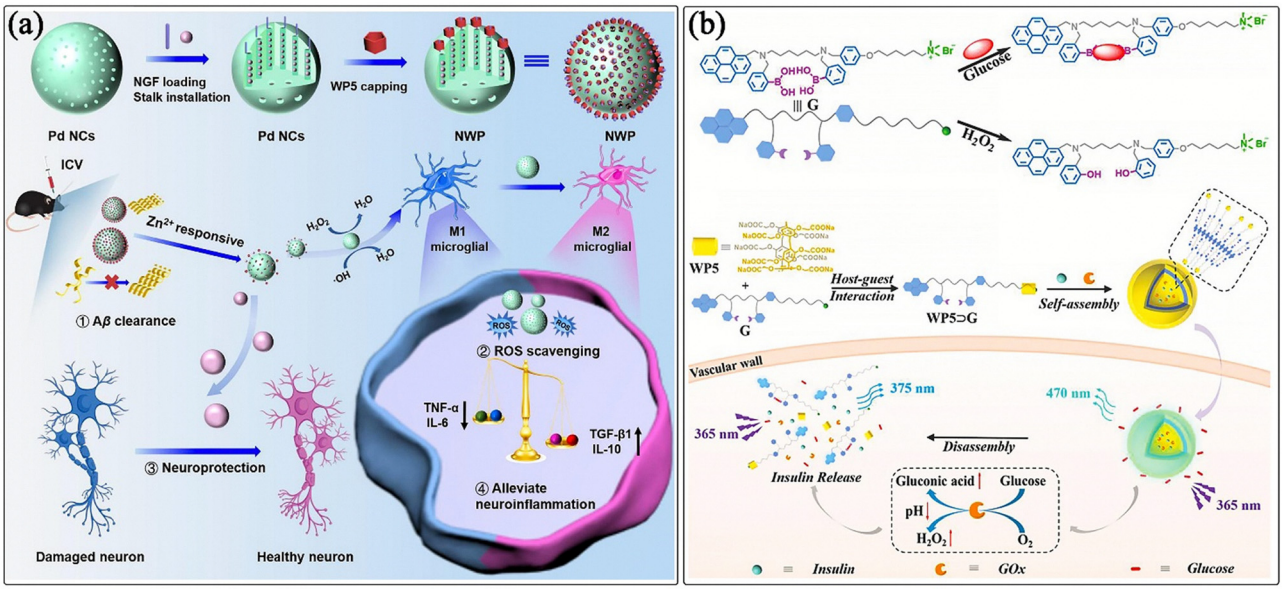

Fig. 21 (a) The schematic of the mechanism by which zinc ion-responsive palladium nanoclusters synergistically address Alzheimer's disease through neuroprotection and inhibition of oxidative stress (Reproduced with permission from ref. 327. Copyright 2023, Elsevier). (b) The schematic of the mechanism of the multi-responsive supramolecular theranostic nanoplatform based on pillar[5]arene and diphenylboronic acid derivatives for performing *in vivo* glucose sensing and insulin delivery (Reproduced with permission from ref. 328. Copyright 2018, John Wiley & Sons, Inc.).

insulin remains unchanged, and it also has good cytocompatibility. *In vivo* experiments indicated that this platform can effectively regulate the blood glucose levels of type I diabetic mice, perform well in a glucose tolerance test, and can also avoid hypoglycemia, providing a new direction for the treatment of diabetes (Fig. 21b).[328]

8.5. Cell bridges: cell fusion and communication

Cell fusion and cell communication, as key forms of intercellular interactions, have a profound impact on processes such as growth, development, immune regulation, and the occurrence and progression of diseases. A deep understanding of the mechanisms behind intercellular interactions and the ability to precisely regulate them are of great significance for the rapid advancement of biology and medicine. In recent years, using supramolecular chemistry techniques to study and regulate intercellular interactions has become one of the hot topics in the field of life science research.

Currently, traditional methods for inducing cell fusion, such as chemical reagent induction and physical methods, have achieved some success but still face issues like significant cell damage and unstable fusion efficiency. The key to inducing cell fusion lies in exploring efficient and precise methods. The group of Hou using clever design, synthesized amphoteric ion tubular molecules 1–3. These molecules have hydrophilic positive and negative charged groups at both ends, while their outer surfaces are rich in hydrophobic tryptophan (Trp) residues. This special structure grants them amphiphilicity, enabling interaction with lipid vesicles. FRET experiments clearly indicate that after adding 1–3, vesicle fusion occurred, with compound 2 showing the strongest fusion ability. Inter-vesicle salt transport experiments further confirmed the fusion, and the degree of fusion was closely correlated with the dosage of compound 2, indicating that the fusion level could be precisely controlled by adjusting the compound's dosage. Finally, using giant unilamellar vesicles (GUVs) for direct observation, it was found that after adding compound 2, vesicles efficiently completed the fusion process in about 2 minutes, providing intuitive and significant evidence for studying vesicle fusion kinetics. These results suggest that amphoteric ion tubular molecules 1–3, especially compound 2, can effectively induce vesicle fusion, and their fusion effects can be precisely regulated, providing a solid foundation for future biomedical applications like drug delivery, disease diagnosis, and treatment.[329]

In living organisms, cells communicate with their surrounding environment and adjacent cells to maintain the stability of the tissue and the consistency of functions. However, the cell membrane and the intercellular gap hinder the direct transfer of substances and signals between adjacent cells. Therefore, living organisms have evolved gap junction channel proteins to achieve such transfer. Nevertheless, *in vitro*, the preparation and integration of these proteins pose challenges, restricting their application in artificial synthetic cells. Previously, we have summarized numerous supramolecular artificial bionic channels constructed based on IPAs, which have achieved the transfer of substances and signals between the inside and outside of cells. However, how to construct tubular molecules long enough to span the intercellular gap and form stable channel structures for the transfer of substances and signals between cells remains a significant challenge.

Hou's group used pillar[5]arenes with positive and negative charges respectively as basic building blocks to synthesize pillar[5]arene pentamers and trimers with alternating positive

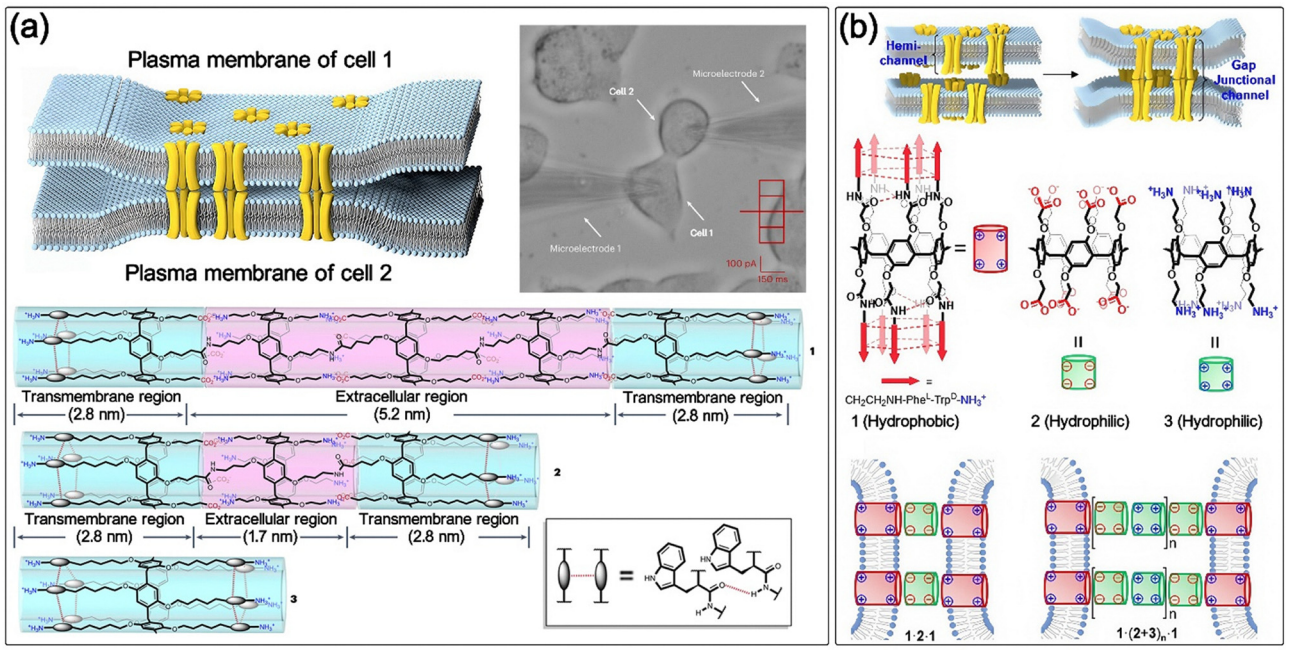

Fig. 22 Applications of IPAs in constructing artificial intercellular communication channels: (a) the schematics of biomimetic cell channel structure based on covalent bonding of multiple pillararenes (Reproduced with permission from ref. 330. Copyright 2024, Springer Nature). (b) The schematics of biomimetic cell channel constructed *via* electrostatic interactions (non-covalent interactions) between cationic and anionic pillararenes (Reproduced with permission from ref. 331. Copyright 2025, American Chemical Society).

and negative charges. Their structures are hydrophobic at both ends and hydrophilic in the middle, which can well match the hydrophobic and hydrophilic environments of adjacent cell membranes, thus spontaneously embedding into adjacent cell membranes. In this channel, the hydrophobic parts at both ends are embedded in the cell membrane to form the transmembrane part, while the hydrophilic part in the middle is located in the intercellular gap and serves as the extracellular part. The research results indicate that both of these two oligomers can mediate the KCl transport between vesicles and form electrical couplings between cells. At the same time, the pillar[5]arene pentamer can significantly enhance the transport of ROS between cells and affect cell viability (Fig. 22a).[330]

At the same time, they also explored a supramolecular non-covalent self-assembly strategy driven by electrostatic interactions.[331] This strategy dynamically couples hydrophobic transmembrane modules with hydrophilic inter-cellular-gap modules to form artificial inter-cellular channels with both structural adaptability and functional tunability. This strategy can control the channel length (such as the 1·2·1 short channel and the $1\cdot(2+3)_n\cdot1$ long channel) by adjusting the module concentration (such as the ratio of 2/3), and flexibly adapt to different inter-cellular-gap widths (Fig. 22b). Compared with the fixed oligomers synthesized by covalent methods, non-covalent assembly avoids complex synthetic steps, significantly reduces the difficulty of molecular design, and allows for real-time regulation of channel functions. Experimental results indicate that in the lipid vesicle model, the non-covalently assembled 1·2·1 channel mediates KCl transport with an efficiency of 58%, which is slightly higher than that of the previous covalent pentamer channels. Whole-cell patch-clamp experiments indicate that non-covalent channels can establish electrical coupling between HEK293 cells that lack natural connexins. The coupling coefficient of the 1·2·1 channel is $53 \pm 3\%$. Although this is lower than that of natural channels ($>90\%$), the system for the first time demonstrates that non-covalent assembly can mimic the ion-permeation function of gap junctions. Moreover, the signals can be transmitted across 1–2 cells, illustrating the potential for constructing multicellular networks. The dynamic channels inhibit the transmembrane movement of tumor cells by enhancing inter-cellular adhesion and interfering with migration-related signalling pathways, reducing the migration ability of HepG2 cells by more than 40%. These studies provide new ideas for artificial cell communication and disease treatment, marking significant progress in the field of supramolecular chemistry for the mimicking of natural inter-cellular interactions.

As core bridging molecules, IPAs play a crucial role in constructing intercellular communication networks. Their unique structural advantages not only make them effective tools for inducing cell fusion but also enable them to spontaneously embed into adjacent cell membranes, forming stable channel structures and facilitating the efficient transmission of substances and signals between cells. These studies are of great significance in elucidating the core mechanisms of natural intercellular interactions, which helps to gain a deeper understanding of the essence of cell communication. They also lay a molecular foundation for the construction of artificial cell networks in synthetic biology, making artificial regulation of

intercellular communication possible. Meanwhile, they provide new insights into the study of the mechanisms for abnormal intercellular communication in disease models and show enormous potential in the field of disease treatment.

9. Summary and outlook

IPAs, as an important molecular tool, play an indispensable role in solving numerous biological problems. In the field of biological applications, IPAs have demonstrated good potential and achieved satisfactory results. However, researchers still face many formidable challenges in the process of promoting their transformation from basic research to practical applications. The resolution of these challenges requires the close collaboration of professionals from multiple fields, including chemists, biologists, materials scientists, engineers, and doctors. Specifically, the following key issues need to be addressed in the future:

(i) Expanding research on large-sized pillararenes: currently, research on the biological applications of IPAs mainly focuses on pillar[5]arene and pillar[6]arene, while exploration of pillar[7–10]arenes is relatively scarce. Large-sized IPAs, due to their larger cavity and more abundant charges, theoretically have stronger specific recognition abilities for some larger bioactive molecules and can significantly enhance the capacity to accommodate multiple guest molecules. This characteristic will greatly expand the applicability of IPAs in constructing multi-dimensional supramolecular nanomaterials and bring more possibilities for biological applications. However, the preparation of large-sized IPAs with various functional groups is quite difficult, which seriously hinders in-depth research on their applications.

(ii) Expanding research on IPA-based polymers: currently, research on the biological applications of IPAs mainly focuses on single-molecule systems, and the research on IPA-based polymers is still in its infancy. Compared with single-molecule IPAs, IPA-based polymers have the following advantages: firstly, the synergistic recognition of the multiple cavity array enhances the adaptability to biological molecules of different sizes, and is especially suitable for the precise capture and specific binding of target molecules in complex physiological environments. Secondly, by utilizing the tunable charge density and spatial conformation, it optimizes the loading efficiency and delivery stability of nucleic acids, providing a new path for the intelligent design of gene therapy vectors. Thirdly, through the multi-site signal amplification mechanism, it enables highly sensitive detection of trace biological markers for the construction of biosensors. However, the covalent bonding method has insufficient control precision over the spatial orientation of IPA units, which is likely to lead to structural heterogeneity of the assemblies. Moreover, the *in vivo* metabolic behavior and biocompatibility of high-order aggregates have not been clearly defined, and it is necessary to combine molecular simulation and *in vivo* imaging techniques to fully analyze their structure–activity relationships.

(iii) Strengthening biological safety and clinical research: in biological application scenarios, the biological safety of IPAs is of utmost importance. However, existing research has not thoroughly understood their absorption, distribution, metabolism, and excretion processes in living organisms, and there is a lack of a complete and systematic evaluation. This situation makes it difficult to accurately assess the long-term effects of IPAs on organisms when developing practical applications such as biosensors and drug carriers, representing a huge obstacle on the path to clinical translation.

(iv) Deepening the exploration of molecular interaction mechanisms: although IPAs exhibit unique properties in supramolecular self-assembly and other aspects, their molecular interaction mechanisms with biomolecules, cells, *etc.* remain incompletely understood. Currently, there is a lack of in-depth research at the systems biology level, and it is impossible to effectively integrate the effects of IPAs on proteins, nucleic acids, signalling pathways, and metabolism to construct a comprehensive molecular regulation network model. Research at the single-cell level is also relatively insufficient, making it difficult for researchers to understand the mechanism of action in complex biological systems. In addition, the discovery and verification of drug targets are progressing slowly, which severely restricts the development of new therapeutic drugs based on IPAs.

(v) Enhancing stability: IPAs face a complex and variable physiological environment in living organisms. The presence of multiple enzymes, different pH values, and changes in ionic strength all pose severe challenges to the structural stability of IPAs and the stability of supramolecular assemblies. In such an environment, IPAs may decompose or dissociate, affecting the continuous exertion of their biological functions. Therefore, in-depth research on the stability of IPAs and the optimization of their molecular structures are of great significance.

(vi) Optimizing the preparation process: currently, the preparation of IPAs relies on complex and multi-step reaction processes. This process not only consumes a large amount of energy and excessive chemical reagents but also has a low yield and causes serious environmental pollution, which is contrary to the sustainable development concept advocated by green chemistry. For biological applications, this preparation situation makes large-scale production and supply a major problem. Taking the development of drug carriers as an example, if stable and large-scale preparation cannot be achieved, the industrialization of drug carriers will be difficult to promote, severely restricting the transformation of related drugs from the laboratory to clinical applications.

With the rapid development of science and technology, the trend of cross-integration among various disciplines is becoming more and more significant, creating many new development directions and opportunities for the common progress of multiple disciplines:

(i) Innovative breakthroughs in biomedical applications: currently, numerous related studies on IPAs have been carried out in fields such as drug delivery, multimodal disease treatment, bioimaging, and biosensors. In the future, the tissue

engineering field is expected to become a new application direction for IPAs. IPAs can specifically interact with extracellular matrix components to precisely regulate cell adhesion, proliferation, and differentiation. Based on this, IPAs are expected to be used to construct bionic scaffold materials in the future, playing a key role in bone tissue engineering, skin regeneration, *etc.*, and providing new solutions for tissue repair and regeneration.

(ii) Deepening cross-disciplinary research integration: making full use of the emerging new technologies and methods in various disciplines to explore the molecular interaction mechanisms of IPAs. By comprehensively applying advanced experimental techniques and accurate theoretical calculation methods, it will become possible to conduct all-around and in-depth research on the interaction mechanisms between IPAs and biomolecules and cells, reveal their action laws in living organisms, and thus lay a solid theoretical foundation for the development of new biological application technologies.

(iii) Expanding application boundaries with the aid of cutting-edge technologies: use cutting-edge methods such as molecular dynamics simulation and quantum chemical calculation to study the interactions between IPAs and biomolecules, accurately predict their behavior and functions in living organisms, and provide a strong theoretical basis for designing safer and more efficient biological materials. In addition, leverage artificial intelligence to conduct deep learning, analyze a large amounts of biological application data of IPAs, to construct accurate structure–property relationship models, and achieve the rapid screening and design of molecular structures suitable for specific biological applications. At the same time, it is important to develop professional software specifically for application in the biological research of IPAs, integrating functions such as molecular design, biological safety prediction, and bioactivity simulation, providing a convenient and efficient platform for researchers.

In conclusion, although IPAs face many challenges in the field of biological applications, as long as researchers focus on overcoming preparation problems, improve biological safety evaluation, strengthen the depth of basic research, and actively combine cutting-edge technologies to expand application boundaries, IPAs are expected to make significant breakthroughs in the biomedical field and bring new opportunities for the improvement of human health.

Conflicts of interest

There are no conflicts to declare.

Data availability

No primary research results, software or code have been included and no new data were generated or analysed as part of this review.

Acknowledgements

This work was financially supported by the National Natural Science Foundation of China (22171230 and 22301246), the Foreign Experts Program of China (G2022172026L), the Project of Science and Technology of Social Development in Shaanxi Province (2023-YBSF-151 and 2024SF-YBXM-294), and the Shaanxi Province Postdoctoral Science Foundation (2023BSHEDZZ101). We would also like to thank the Royal Society for an International Joint Project (IEC\NSFC\211304) that facilitated exchanges between the groups. T. D. J. wishes to thank the University of Bath and the Open Research Fund of the School of Chemistry and Chemical Engineering, Henan Normal University (2020ZD01) for support.

References

1 P. Libby, P. M. Ridker and G. K. Hansson, *Nature*, 2011, **473**, 317–325.
2 L.-L. Chen, N. T. Ingolia, M. L. Insco, J. B. Li, S. Oberdoerffer and K. M. Weeks, *Cell Chem. Biol.*, 2024, **31**, 10–13.
3 J. N. Fullerton and D. W. Gilroy, *Nat. Rev. Drug Discovery*, 2016, **15**, 551–567.
4 Y. Huang, P. Zhang, H. Wang, Y. Chen, T. Liu and X. Luo, *Chem. Rev.*, 2025, **125**, 523–598.
5 O. S. Fenton, K. N. Olafson, P. S. Pillai, M. J. Mitchell and R. Langer, *Adv. Mater.*, 2018, **30**, 1705328.
6 Y. Li, C. Guo, J. Yuan, X. Yang, H. Ji, M. Wu, L. Wu and Y. Qin, *Chem. Eng. J.*, 2024, **487**, 150424.
7 M. Ismail, J. Liu, N. Wang, D. Zhang, C. Qin, B. Shi and M. Zheng, *Biomaterials*, 2025, **318**, 123138.
8 L. Yuan, Z.-Y. Xu, S.-M. Ruan, S. Mo, J.-J. Qin and X.-D. Cheng, *Mol. Cancer*, 2020, **19**, 96.
9 X. Di, Z. Pei, Y. Pei and T. D. James, *Coord. Chem. Rev.*, 2023, **484**, 215098.
10 I. V. Kolesnichenko and E. V. Anslyn, *Chem. Soc. Rev.*, 2017, **46**, 2385–2390.
11 J. Li, J. Wang, H. Li, N. Song, D. Wang and B. Z. Tang, *Chem. Soc. Rev.*, 2020, **49**, 1144–1172.
12 Y. Liu, L. Wang, L. Zhao, Y. Zhang, Z.-T. Li and F. Huang, *Chem. Soc. Rev.*, 2024, **53**, 1592–1623.
13 R. R. Groleau, T. D. James and S. D. Bull, *Coord. Chem. Rev.*, 2021, **428**, 213599.
14 J.-M. Lehn, *Rep. Prog. Phys.*, 2004, **67**, 249.
15 J.-M. Lehn, *J. Inclusion Phenom.*, 1988, **6**, 351–396.
16 J.-M. Lehn, *Chem. Soc. Rev.*, 2017, **46**, 2378–2379.
17 J.-M. Lehn, *Angew. Chem., Int. Ed. Engl.*, 1990, **29**, 1304–1319.
18 O. Ramström and J.-M. Lehn, *Nat. Rev. Drug Discovery*, 2002, **1**, 26–36.
19 P. A. Gale, J. T. Davis and R. Quesada, *Chem. Soc. Rev.*, 2017, **46**, 2497–2519.
20 M. J. Webber and R. Langer, *Chem. Soc. Rev.*, 2017, **46**, 6600–6620.
21 X. Sun and T. D. James, *Chem. Rev.*, 2015, **115**, 8001–8037.

22 C. J. Pedersen, *Angew. Chem., Int. Ed. Engl.*, 1988, **27**, 1021–1027.
23 B. Zheng, F. Wang, S. Dong and F. Huang, *Chem. Soc. Rev.*, 2012, **41**, 1621–1636.
24 S. Di Stefano, G. Capocasa and L. Mandolini, *Eur. J. Org. Chem.*, 2020, 3340–3350.
25 G. Crini, *Chem. Rev.*, 2014, **114**, 10940–10975.
26 V. T. D'Souza and K. B. Lipkowitz, *Chem. Rev.*, 1998, **98**, 1741–1742.
27 Z. Liu and Y. Liu, *Chem. Soc. Rev.*, 2022, **51**, 4786–4827.
28 Y. Chen and Y. Liu, *Chem. Soc. Rev.*, 2010, **39**, 495–505.
29 V. Böhmer, *Angew. Chem., Int. Ed. Engl.*, 1995, **34**, 713–745.
30 D.-S. Guo and Y. Liu, *Chem. Soc. Rev.*, 2012, **41**, 5907–5921.
31 S. B. Nimse and T. Kim, *Chem. Soc. Rev.*, 2013, **42**, 366–386.
32 K. M. Al-Ahmary, A. Shafie, A. Adnan Ashour, K. S. Alrashdi, A. O. Babalghith, S. S. Alharthi and F. Y. Sabei, *Crit. Rev. Anal. Chem.*, 2024, 1–26.
33 Q. Li, Z. Yu, C. Redshaw, X. Xiao and Z. Tao, *Chem. Soc. Rev.*, 2024, **53**, 3536–3560.
34 Y. Zhang, G. Zhang, X. Xiao, Q. Li and Z. Tao, *Coord. Chem. Rev.*, 2024, **514**, 215889.
35 M. Tang, Z. Yang, X. Tang, H. Ma, B. Xie, J.-F. Xu, C. Gao, D. Bardelang and R. Wang, *J. Am. Chem. Soc.*, 2025, **147**, 3488–3499.
36 H. C. Zhang, Z. N. Liu and Y. L. Zhao, *Chem. Soc. Rev.*, 2018, **47**, 5491–5528.
37 T. Ogoshi, S. Kanai, S. Fujinami, T.-A. Yamagishi and Y. Nakamoto, *J. Am. Chem. Soc*, 2008, **130**, 5022–5023.
38 T. Ogoshi, T.-a Yamagishi and Y. Nakamoto, *Chem. Rev.*, 2016, **116**, 7937–8002.
39 W.-C. Geng, J. L. Sessler and D.-S. Guo, *Chem. Soc. Rev.*, 2020, **49**, 2303–2315.
40 Y.-Y. Liu, X.-Y. Yu, Y.-C. Pan, H. Yin, S. Chao, Y. Li, H. Ma, M. Zuo, K.-X. Teng and J.-L. Hou, *Sci. China Chem.*, 2024, **67**, 1397–1441.
41 Y.-H. Song, Q. Bian, F. Wang, J. Liu, Y.-H. Yang, Y.-M. Zhang and Y. Liu, *Coord. Chem. Rev.*, 2025, **524**, 216299.
42 F. A. Mohammed, T. Xiao, L. Wang and R. B. Elmes, *Chem. Commun.*, 2024, **60**, 11812–11836.
43 J. Xie and N. Bogliotti, *Chem. Rev.*, 2014, **114**, 7678–7739.
44 Y.-C. Liu, H. Sun and D.-S. Guo, *Curr. Org. Chem.*, 2018, **22**, 2127–2149.
45 X. Yang, D. Yuan, J. Hou, A. C. Sedgwick, S. Xu, T. D. James and L. Wang, *Coord. Chem. Rev.*, 2021, **428**, 213609.
46 M. Xue, Y. Yang, X. Chi, Z. Zhang and F. Huang, *Acc. Chem. Res.*, 2012, **45**, 1294–1308.
47 N. Song and Y.-W. Yang, *Sci. China Chem.*, 2014, **57**, 1185–1198.
48 K. Kato, T. Kaneda, S. Ohtani and T. Ogoshi, *J. Am. Chem. Soc.*, 2023, **145**, 6905–6913.
49 Z. Li, Z. Shen, Y. Pei, S. Chao and Z. Pei, *Chem. Commun.*, 2023, **59**, 989–1005.
50 X. Y. Lou and Y. W. Yang, *Adv. Mater.*, 2020, **32**, 2003263.
51 H. Zhu, J. Liu, Y. Wu, L. Wang, H. Zhang, Q. Li, H. Wang, H. Xing, J. L. Sessler and F. Huang, *J. Am. Chem. Soc.*, 2023, **145**, 11130–11139.
52 E. Paul, S. R. Dhara, N. N. Lathiotakis and K. Ghosh, *J. Mol. Struct.*, 2025, **1344**, 142910.
53 S. Chao, Z. Shen, Y. Pei and Z. Pei, *Chem. Commun.*, 2021, **57**, 10983–10997.
54 K. Yang, S. Chao, F. Zhang, Y. Pei and Z. Pei, *Chem. Commun.*, 2019, **55**, 13198–13210.
55 X. Chi, G. Yu, L. Shao, J. Chen and F. Huang, *J. Am. Chem. Soc.*, 2016, **138**, 3168–3174.
56 Z. Li, Z. Yang, Y. Zhang, B. Yang and Y.-W. Yang, *Angew. Chem., Int. Ed.*, 2022, **61**, e202206144.
57 G. Kalandia, C.-L. Liu, D. E. Salazar Marcano, M. A. Moussawi, S. Bleus, B. Van Meerbeek, W. Dehaen and T. N. Parac-Vogt, *Angew. Chem., Int. Ed.*, 2025, **64**, e202420773.
58 S. Wei, X. Cui, T. Li, X. Ma and L. Liu, *ChemMedChem*, 2025, e202400822.
59 S. Chao, P. Huang, Z. Shen, Y. Pei, Y. Lv, Y. Lu and Z. Pei, *Org. Chem. Front.*, 2023, **10**, 3491–3497.
60 L. Jiang, X. Huang, D. Chen, H. Yan, X. Li and X. Du, *Angew. Chem., Int. Ed.*, 2017, **56**, 2655–2659.
61 S. Fa, M. Mizobata, S. Nagano, K. Suetsugu, T. Kakuta, T.-A. Yamagishi and T. Ogoshi, *ACS Nano*, 2021, **15**, 16794–16801.
62 C. Sathiyajith, R. R. Shaikh, Q. Han, Y. Zhang, K. Meguellati and Y.-W. Yang, *Chem. Commun.*, 2017, **53**, 677–696.
63 Y. Zhu, Y. Gao, J. Rebek Jr and Y. Yu, *Chem. – Eur. J.*, 2025, e202404424.
64 X. Shu, K. Xu, D. Hou and C. Li, *Isr. J. Chem.*, 2018, **58**, 1230–1240.
65 Y. Chen, F. Huang, Z.-T. Li and Y. Liu, *Sci. China Chem.*, 2018, **61**, 979–992.
66 Q. Yang, W. Xu, M. Cheng, S. Zhang, E. G. Kovaleva, F. Liang, D. Tian, J.-A. Liu, R. M. Abdelhameed and J. Cheng, *Chem. Commun.*, 2022, **58**, 3255–3269.
67 Y. Cai, Z. C. Zhang, Y. Ding, L. P. Hu, J. Wang, T. T. Chen and Y. Yao, *Chin. Chem. Lett.*, 2021, **32**, 1267–1279.
68 H. Zhang and Y. Zhao, *Chem. – Eur. J.*, 2013, **19**, 16862–16879.
69 Y. Yao, X. Wei, J. Chen, H. Dai and Y. Shi, *Supramol. Chem.*, 2018, **30**, 610–618.
70 T.-H. Shi, S. Ohtani, K. Kato, S. Fa and T. Ogoshi, *Trends Chem.*, 2023, **5**, 537–550.
71 H. Zhang, Z. Liu and Y. Zhao, *Chem. Soc. Rev.*, 2018, **47**, 5491–5528.
72 T. Ogoshi, T. Kakuta and T. Yamagishi, *Angew. Chem., Int. Ed.*, 2019, **58**, 2197–2206.
73 S. Fa, T. Kakuta, T.-A. Yamagishi and T. Ogoshi, *CCS Chem.*, 2019, **1**, 50–63.
74 R. Joseph, *Chemistryselect*, 2021, **6**, 3519–3533.
75 Y. T. Li, J. Wen, J. S. Li, Z. J. Wu, W. Li and K. Yang, *ACS Sens.*, 2021, **6**, 3882–3897.
76 S. Yu, Y. Q. Wang, S. Chatterjee, F. Liang, F. Zhu and H. B. Li, *Chin. Chem. Lett.*, 2021, **32**, 179–183.
77 Z. Q. Wang, X. Wang and Y. W. Yang, *Adv. Mater.*, 2024, **36**, 2301721.

78 K. Yang, Y. Pei, J. Wen and Z. Pei, *Chem. Commun.*, 2016, **52**, 9316–9326.
79 F. Guo, Y. Sun, B. Xi and G. Diao, *Supramol. Chem.*, 2018, **30**, 81–92.
80 K. Wada and T. Ogoshi, *Mater. Chem. Front.*, 2024, **8**, 1212–1229.
81 X. Li, M. L. Shen, J. Yang, L. L. Liu and Y. W. Yang, *Adv. Mater.*, 2024, **36**, 2313317.
82 T. X. Xiao, L. J. Qi, W. W. Zhong, C. Lin, R. B. Wang and L. Y. Wang, *Mater. Chem. Front.*, 2019, **3**, 1973–1993.
83 S. A. Fahmy, A. Ramzy, B. M. Saleh and H. Azzazy, *ACS Omega*, 2021, **6**, 25876–25883.
84 C. Wang, H. Li, J. Dong, Y. Chen, X. Luan, X. Li and X. Du, *Chem. – Eur. J.*, 2022, **28**, e202202050.
85 Y. Wang, Z. Pei, W. Feng and Y. Pei, *J. Mater. Chem. B*, 2019, **7**, 7656–7675.
86 D. H. Tuo, T. H. Shi, S. Ohtani and T. Ogoshi, *Responsive Mater.*, 2024, **2**, e20230024.
87 Y. Acikbas, M. Aksoy, M. Aksoy, D. Karaagac, E. Bastug, A. N. Kursunlu, M. Erdogan, R. Capan, M. Ozmen and M. Ersoz, *J. Inclusion Phenom. Macrocyclic Chem.*, 2021, **100**, 39–54.
88 G. A. Evtyugin, D. N. Shurpik and I. I. Stoikov, *Russ. Chem. Bull.*, 2020, **69**, 859–874.
89 S. Cao, L. Zhou, C. Liu, H. Zhang, Y. Zhao and Y. Zhao, *Biosens. Bioelectron.*, 2021, **181**, 113164.
90 Y. Dai, W. Q. Yu, Y. S. Cheng, Y. Zhou, J. Y. Zou, Y. J. Meng, F. Y. Chen, Y. H. Qian and Y. Yao, *Chem. Commun.*, 2025, **61**, 2484–2495.
91 S. Jothi Nayaki, A. Roja, R. Ravindhiran, K. Sivarajan, M. Arunachalam and K. Dhandapani, *ACS Infect. Dis.*, 2024, **10**, 1080–1096.
92 L. E. Khalil-Cruz, P. R. Liu, F. H. Huang and N. M. Khashab, *ACS Appl. Mater. Interfaces*, 2021, **13**, 31337–31354.
93 L. Zhou, S. Cao, C. Liu, H. C. Zhang and Y. L. Zhao, *Coord. Chem. Rev.*, 2023, **491**, 215260.
94 Q. Li, H. Zhu and F. Huang, *Trends Chem.*, 2020, **2**, 850–864.
95 H. Zhang, R. Zou and Y. Zhao, *Coord. Chem. Rev.*, 2015, **292**, 74–90.
96 N. L. Strutt, H. Zhang, S. T. Schneebeli and J. F. Stoddart, *Acc. Chem. Res.*, 2014, **47**, 2631–2642.
97 B. Lu, J. Xia, Y. Huang and Y. Yao, *Chem. Commun.*, 2023, **59**, 12091–12099.
98 W. Feng, M. Jin, K. Yang, Y. Pei and Z. Pei, *Chem. Commun.*, 2018, **54**, 13626–13640.
99 G. V. Zyryanov, D. S. Kopchuk, I. S. Kovalev, S. Santra, A. Majee and B. C. Ranu, *Int. J. Mol. Sci.*, 2023, **24**, 5167.
100 H. Zhu, Q. Li, L. E. Khalil-Cruz, N. M. Khashab, G. Yu and F. Huang, *Sci. China Chem.*, 2021, **64**, 688–700.
101 W. X. Feng, Z. Sun and M. Barboiu, *Isr. J. Chem.*, 2018, **58**, 1209–1218.
102 R. Tang, Y. Ye, S. Zhu, Y. Wang, B. Lu and Y. Yao, *Chin. Chem. Lett.*, 2023, **34**, 107734.
103 Y. Jin, Y. Liu, J. Zhu and H. Liu, *Org. Biomol. Chem.*, 2024, **22**, 4202–4211.
104 S. Daakour, N. D. Hădade and M. Barboiu, *Tetrahedron Lett.*, 2024, **145**, 155178.
105 J. Y. Chen, Q. Xiao, H. Behera and J. L. Hou, *Chin. Chem. Lett.*, 2020, **31**, 77–80.
106 W. Si, Z. T. Li and J. L. Hou, *Angew. Chem., Int. Ed.*, 2014, **53**, 4578–4581.
107 Z. J. Yan, Y. W. Li, M. Yang, Y. H. Fu, R. Wen, W. Wang, Z. T. Li, Y. Zhang and J. L. Hou, *J. Am. Chem. Soc.*, 2021, **143**, 11332–11336.
108 P. Xin, L. Zhao, L. Mao, L. Xu, S. Hou, H. Kong, H. Fang, H. Zhu, T. Jiang and C.-P. Chen, *Chem. Commun.*, 2020, **56**, 13796–13799.
109 Z. J. Yan, D. Wang, Z. Ye, T. Fan, G. Wu, L. Deng, L. Yang, B. Li, J. Liu, T. Ma, C. Dong, Z. T. Li, L. Xiao, Y. Wang, W. Wang and J. L. Hou, *J. Am. Chem. Soc.*, 2020, **142**, 15638–15643.
110 I.-M. Andrei, D. Strilets, S. Fa, M. Baaden, T. Ogoshi and M. Barboiu, *Angew. Chem., Int. Ed.*, 2023, **62**, e202310812.
111 Y. Wang, J.-L. Hou and W. Wang, *Angew. Chem., Int. Ed.*, 2025, **64**, e202502267.
112 Y. Sun, J. Ma, F. Zhang, F. Zhu, Y. Mei, L. Liu, D. Tian and H. Li, *Nat. Commun.*, 2017, **8**, 260.
113 R. Zhang, J. Huang, K. Chen, I. Boussouar, X. Chen, Y. Fan, Y. Sun and H. Li, *Anal. Chem.*, 2021, **93**, 3280–3286.
114 R. Wang, Y. Sun, F. Zhang, M. Song, D. Tian and H. Li, *Angew. Chem., Int. Ed.*, 2017, **56**, 5294–5298.
115 S. Q. Cheng, X. Q. Liu, Z. L. Han, Y. Rong, S. Y. Qin, Y. Sun and H. Li, *ACS Appl. Mater. Interfaces*, 2021, **13**, 27255–27261.
116 F. Zhang, J. Ma, Y. Sun, I. Boussouar, D. Tian, H. Li and L. Jiang, *Chem. Sci.*, 2016, **7**, 3227–3233.
117 G. Li, Y. Wang, H. Luan, Y. Sun, Y. Qu, Z. Lu and H. Li, *ACS Appl. Mater. Interfaces*, 2023, **15**, 32753–32761.
118 H. Qu, S. Dai, Y. Qu, S. Zhang, M. Lu, Z. Lu, J. Zhou and H. Li, *ACS Appl. Nano Mater.*, 2022, **5**, 14970–14977.
119 T. Guan, M. Cheng, L. Zeng, X. Chen, Y. Xie, Z. Lei, Q. Ruan, J. Wang, S. Cui, Y. Sun and H. Li, *ACS Appl. Mater. Interfaces*, 2021, **13**, 49137–49145.
120 Y. Fang, W. Xu, L. Yang, H. Qu, W. Wang, S. Zhang and H. Li, *Small*, 2023, **19**, e2205488.
121 J. Quan, H. Yan, G. Periyasami and H. Li, *Chem. – Eur. J.*, 2024, **30**, e202401045.
122 F. Zhang, J. Ma, Y. Sun, Y. Mei, X. Chen, W. Wang and H. Li, *Anal. Chem.*, 2018, **90**, 8270–8275.
123 L. Tu, S. Qiu, Y. Li, X. Chen, Y. Han, J. Li, X. Xiong, Y. Sun and H. Li, *ACS Appl. Mater. Interfaces*, 2022, **14**, 27421–27426.
124 L. Yang, F. Zhang, C. Chen, Z. Liu, L. Liu and H. Li, *Chem. - Asian J.*, 2022, **17**, e202200455.
125 L. Yang, M. Cheng, J. Quan, S. Zhang, L. Liu, R. P. Johnson, F. Zhang and H. Li, *Angew. Chem., Int. Ed.*, 2021, **60**, 24443–24449.
126 X. Qian, S. Tan, Z. Li, Q. Qu, L. Li and L. Yang, *Biosens. Bioelectron.*, 2020, **153**, 112051.
127 J. Wang, L. Zhou, J. Bei, Q. Zhao, X. Li, J. He, Y. Cai, T. Chen, Y. Du and Y. Yao, *Talanta*, 2022, **243**, 123322.

128 J. Wang, X. Guo, Q. Zhou, Y. Cai, B. Lu, Y. Wang and Y. Yao, *Colloids Surf., A*, 2024, **688**, 133511.
129 J. Ma, F. Shi, D. Tian and H. Li, *Chem. – Eur. J.*, 2016, **22**, 13805–13809.
130 X. Tan, T. Mu, S. Wang, J. Li, J. Huang, H. Huang, Y. Pu and G. Zhao, *Analyst*, 2021, **146**, 262–269.
131 Q. Duan, L. Wang, F. Wang, H. Zhang and K. Lu, *RSC Adv.*, 2020, **10**, 21954–21962.
132 H. Liang, Y. Zhao, H. Ye and C.-P. Li, *J. Electroanal. Chem.*, 2019, **855**, 113487.
133 G. Zhao, X. Zhou, X. Ran, X. Tan, T. Li, M. Cao, L. Yang and G. Du, *Electrochim. Acta*, 2018, **277**, 1–8.
134 D. Luo, Z. Liu, A. Su, Y. Zhang, H. Wang, L. Yang, W. Yang and P. Pang, *Talanta*, 2024, **266**, 124956.
135 X. Zhou, L. Yang, X. Tan, G. Zhao, X. Xie and G. Du, *Biosens. Bioelectron.*, 2018, **112**, 31–39.
136 X. Qian, X. Zhou, Q. Qu, L. Li and L. Yang, *Electrochim. Acta*, 2019, **313**, 235–244.
137 Z. Ran, H. Yang, Z. Li, K. Wang, J. Zhao, X. Ran, G. Du and L. Yang, *ACS Sustainable Chem. Eng.*, 2020, **8**, 10161–10172.
138 Q. Xingean, Z. Xu, R. Xin, N. Hangcheng, L. Zhi, Q. Qing, L. Jun and D. Guanben, *Biosens. Bioelectron.*, 2019, **130**, 214–224.
139 X. Zhou, X. Qian, X. Tan, X. Ran, Z. Li, Z. Huang, L. Yang and X. Xie, *Anal. Chim. Acta*, 2019, **1068**, 18–27.
140 X. Tan, Z. Zhang, T. Cao, W. Zeng, T. Huang and G. Zhao, *ACS Sustainable Chem. Eng.*, 2019, **7**, 20051–20059.
141 Y. Xiong, T. Ma, H. Zhang, L. Qiu, S. Chang, Y. Yang and F. Liang, *Microchim. Acta*, 2022, **189**, 251.
142 G. Zhao, Z. Gao, H. Li, S. Liu, L. Chen, R. Zhang and H. Guo, *Electrochim. Acta*, 2019, **318**, 711–719.
143 Y. Luo, W. Zhang, J. Zhao, M.-X. Yang, Q. Ren, C. Redshaw, Z. Tao and X. Xiao, *Chin. Chem. Lett.*, 2023, **34**, 107780.
144 X. Tan, Y. Liu, T. Zhang, S. Luo, X. Liu, H. Tian, Y. Yang and C. Chen, *RSC Adv.*, 2018, **9**, 345–353.
145 X. Hou, X. Liu, Z. Li, J. Zhang, G. Du, X. Ran and L. Yang, *New J. Chem.*, 2019, **43**, 13048–13057.
146 X. Ran, Q. Qu, X. Qian, W. Xie, S. Li, L. Li and L. Yang, *Sens. Actuators, B*, 2018, **257**, 362–371.
147 X. Tan, X. Liu, W. Zeng, G. Zhao, Z. Zhang, T. Huang and L. Yang, *Anal. Chim. Acta*, 2019, **1078**, 60–69.
148 T. Borjigin, G. Zhao, Y. Zhang, M. Liang, B. Liu, H. Liu, X. Yang and H. Guo, *Sustainable Energy Fuels*, 2019, **3**, 2312–2320.
149 X. Tan, Y. Fan, S. Wang, Y. Wu, W. Shi, T. Huang and G. Zhao, *Electrochim. Acta*, 2020, **335**, 135706.
150 X. Ran, Y. Yu, H. Yang, X. Tan, Z. Ran, R. Zhang, G. Du and L. Yang, *Spectrochim. Acta, Part A*, 2024, **305**, 123499.
151 Q. Lin, P.-P. Mao, F. Zheng, L. Liu, J. Liu, Y.-M. Zhang, H. Yao and T.-B. Wei, *New J. Chem.*, 2017, **41**, 12172–12177.
152 Q. Lin, F. Zheng, L. Liu, P.-P. Mao, Y.-M. Zhang, H. Yao and T.-B. Wei, *RSC Adv.*, 2016, **6**, 111928–111933.
153 Q. Lin, L. Liu, F. Zheng, P.-P. Mao, J. Liu, Y.-M. Zhang, H. Yao and T.-B. Wei, *Tetrahedron*, 2017, **73**, 5307–5310.
154 Q. Yao, B. Lü, C. Ji, Y. Cai and M. Yin, *ACS Appl. Mater. Interfaces*, 2017, **9**, 36320–36326.
155 B. Hua, L. Shao, G. Yu and F. Huang, *Chem. Commun.*, 2016, **52**, 10016–10019.
156 L. Ling, Z. Zhao, L. Mao, S. Wang and D. Ma, *Chem. Commun.*, 2023, **59**, 14161–14164.
157 Y. Zhou, H. Tang, H. Wu, X. Jiang, L. Wang and D. Cao, *Chin. Chem. Lett.*, 2024, **35**, 108626.
158 B. Hua, L. Shao, Z. Zhang, J. Sun and J. Yang, *Sens. Actuators, B*, 2018, **255**, 1430–1435.
159 M. Bojtár, J. Kozma, Z. Szakács, D. Hessz, M. Kubinyi and I. Bitter, *Sens. Actuators, B*, 2017, **248**, 305–310.
160 M. Bojtár, A. Paudics, D. Hessz, M. Kubinyi and I. Bitter, *RSC Adv.*, 2016, **6**, 86269–86275.
161 T.-B. Wei, J.-F. Chen, X.-B. Cheng, H. Li, B.-B. Han, Y.-M. Zhang, H. Yao and Q. Lin, *Org. Chem. Front.*, 2017, **4**, 210–213.
162 Q. Lin, L. Liu, F. Zheng, P.-P. Mao, J. Liu, Y.-M. Zhang, H. Yao and T.-B. Wei, *RSC Adv.*, 2017, **7**, 34411–34414.
163 X. Yang, H. Xiao, J. He, L. Yang, Z. Tao, X. Xiao, Q. Li and H. P. Yang, *Sens. Actuators, B*, 2023, **392**, 134065.
164 Y. Wang, H. Zhong, J. Yang, Y. Yao and L. Li, *Chin. Chem. Lett.*, 2023, **34**, 108452.
165 L. Fang, Y. Dai, Y. Bai, Y. Meng, W. Yu, Y. Gao, R. Tang, Y. Zhang, L. Li, J. Wang, Y. Ding, Y. Wang, T. Chen, Y. Cai and Y. Yao, *Chem. Commun.*, 2024, **60**, 7646–7649.
166 B. Shi, K. Jie, Y. Zhou, J. Zhou, D. Xia and F. Huang, *J. Am. Chem. Soc.*, 2016, **138**, 80–83.
167 J. Zhou, B. Hua, L. Shao, H. Feng and G. Yu, *Chem. Commun.*, 2016, **52**, 5749–5752.
168 G. Yu, G. Tang and F. Huang, *J. Mater. Chem. C*, 2014, **2**, 6609–6617.
169 S.-H. Xu, K.-L. Chang, X.-T. Yan, C.-G. Yan and Q. Wang, *Tetrahedron*, 2024, **150**, 133770.
170 Q. Wang, X.-T. Yan, J.-W. Fan, S.-H. Xu, H. Yao and C.-G. Yan, *J. Mol. Struct.*, 2024, **1297**, 136973.
171 H. Li, R. Wei, G. H. Yan, J. Sun, C. Li, H. Wang, L. Shi, J. A. Capobianco and L. Sun, *ACS Appl. Mater. Interfaces*, 2018, **10**, 4910–4920.
172 X. Wang, J. Yang, X. Sun, H. Yu, F. Yan, K. Meguellati, Z. Cheng, H. Zhang and Y. W. Yang, *Chem. Commun.*, 2018, **54**, 12990–12993.
173 G. Yu, J. Yang, X. Fu, Z. Wang, L. Shao, Z. Mao, Y. Liu, Z. Yang, F. Zhang, W. Fan, J. Song, Z. Zhou, C. Gao, F. Huang and X. Chen, *Mater. Horiz.*, 2018, **5**, 429–435.
174 T. Xiao, L. Zhang, D. Chen, Q. Zhang, Q. Wang, Z.-Y. Li and X.-Q. Sun, *Org. Chem. Front.*, 2023, **10**, 3245.
175 G. Yu, X. Zhou, Z. Zhang, C. Han, Z. Mao, C. Gao and F. Huang, *J. Am. Chem. Soc.*, 2012, **134**, 19489–19497.
176 A. Nazarova, O. Mostovaya, M. Bukharov, A. Nagaeva, G. Yusupov, P. Zelenikhin, B. Hua, F. Huang, P. Padnya and I. Stoikov, *Colloids Surf., A*, 2024, **693**, 134050.
177 Y. Li, J. Wen, J. Li, Z. Wu, W. Li and K. Yang, *Appl. Surf. Sci.*, 2023, **613**, 156071.
178 C. Li, Z. Xie, Q. Chen, Y. Zhang, Y. Chu, Q. Guo, W. Zhou, Y. Zhang, P. Liu, H. Chen, C. Jiang, K. Sun and T. Sun, *ACS Nano*, 2020, **14**, 4950–4962.

179 C. Chen, W. Xu, G. Li, H. Qu, C. Ma, H. Zhang, E. Bahojb Noruzi, M. Cai, M. Wang, X. Hou and H. Li, *Chem. – Eur. J.*, 2024, **30**, e202303742.
180 W. Xu, G. Li, H. Qu, C. Ma, H. Zhang, J. Cheng and H. Li, *ACS Nano*, 2023, **17**, 19305–19312.
181 T.-N. Gao, S. Huang, R. Nooijen, Y. Zhu, G. Kociok-Koehn, T. Stuerzer, G. Li, J. H. Bitter, G. I. J. Salentijn, B. Chen, F. M. Miloserdov and H. Zuilhof, *Angew. Chem., Int. Ed.*, 2024, **63**, e202403474.
182 J. Chen, Y. Zhang, Y. Chai, Z. Meng, Y. Zhang, L. Chen, D. Quan, Y. Wang, Q. Meng and C. Li, *Chem. Sci.*, 2021, **12**, 5202–5208.
183 A. Nazarova, P. Padnya, A. Khannanov, A. Khabibrakhmanova, P. Zelenikhin and I. Stoikov, *Int. J. Mol. Sci.*, 2023, **24**, 8357.
184 S. Zhou, W. Li, Q. Zhao, H. Dong, Y. Wang, F. Lu, J. Zhao, S. Liu, H. Chen, L. Wang, W. Liu, M. Zhang and S. Chen, *ACS Appl. Mater. Interfaces*, 2021, **13**, 58291–58300.
185 S. Zhou, Y. Chen, J. Xu, Y. Yin, J. Yu, W. Liu, S. Chen and L. Wang, *J. Mater. Chem. B*, 2023, **11**, 2706–2713.
186 X. Zhang, Q. Cheng, L. Li, L. Shangguan, C. Li, S. Li, F. Huang, J. Zhang and R. Wang, *Theranostics*, 2019, **9**, 3107–3121.
187 Y. Chai, L. Chen, Y. Zhang, L. Zhao, Z. Meng, J. Chen, C. Li and Q. Meng, *Chin. Chem. Lett.*, 2022, **33**, 3003–3006.
188 Q. Zhao, J. Zhu, Y. Chen, H. Dong, S. Zhou, Y. Yin, Q. Cai, S. Chen, C. Chen and L. Wang, *J. Hazard. Mater.*, 2024, **469**, 133875.
189 D. N. Shurpik, O. A. Mostovaya, D. A. Sevastyanov, O. A. Lenina, A. S. Sapunova, A. D. Voloshina, K. A. Petrov, I. V. Kovyazina, P. J. Cragg and I. I. Stoikov, *Org. Biomol. Chem.*, 2019, **17**, 9951–9959.
190 S. Valimaki, N. K. Beyeh, V. Linko, R. H. A. Ras and M. A. Kostiainen, *Nanoscale*, 2018, **10**, 14022–14030.
191 E. Subakaeva, P. Zelenikhin, E. Sokolova, A. Pergat, Y. Aleksandrova, D. Shurpik and I. Stoikov, *Pharmaceutics*, 2023, **15**, 2660.
192 K. Atacan, N. Güy, A. B. Semerci, E. Yemisci, A. N. Kursunlu and M. Ozmen, *J. Mol. Struct.*, 2023, **1289**, 135905.
193 S. Guo, Q. Huang, Y. Chen, J. Wei, J. Zheng, L. Wang, Y. Wang and R. Wang, *Angew. Chem., Int. Ed.*, 2021, **60**, 618–623.
194 Y. I. Aleksandrova, D. N. Shurpik, V. A. Nazmutdinova, P. V. Zelenikhin, E. V. Subakaeva, E. A. Sokolova, Y. O. Leonteva, A. V. Mironova, A. R. Kayumov, V. S. Petrovskii, I. I. Potemkin and I. I. Stoikov, *ACS Appl. Mater. Interfaces*, 2024, **16**, 17163–17181.
195 R. Joseph, A. Naugolny, M. Feldman, I. M. Herzog, M. Fridman and Y. Cohen, *J. Am. Chem. Soc.*, 2016, **138**, 754–757.
196 R. Joseph, D. Kaizerman, I. M. Herzog, M. Hadar, M. Feldman, M. Fridman and Y. Cohen, *Chem. Commun.*, 2016, **52**, 10656–10659.
197 D. Kaizerman-Kane, M. Hadar, R. Joseph, D. Logviniuk, Y. Zafrani, M. Fridman and Y. Cohen, *ACS Infect. Dis.*, 2021, **7**, 579–585.
198 C. Jonkergouw, N. K. Beyeh, E. Osmekhina, K. Leskinen, S. M. Taimoory, D. Fedorov, E. Anaya-Plaza, M. A. Kostiainen, J. F. Trant, R. H. A. Ras, P. Saavalainen and M. B. Linder, *Nat. Commun.*, 2023, **14**, 2141.
199 G. Ping, Y. Wang, L. Shen, Y. Wang, X. Hu, J. Chen, B. Hu, L. Cui, Q. Meng and C. Li, *Chem. Commun.*, 2017, **53**, 7381–7384.
200 L. Gao, M. Li, S. Ehrmann, Z. Tu and R. Haag, *Angew. Chem., Int. Ed.*, 2019, **58**, 3645–3649.
201 H. Wang, Y. Wang, W. Xu, H. Zhang, J. Lv, X. Wang, Z. Zheng, Y. Zhao, L. Yu, Q. Yuan, L. Yu, B. Zheng and L. Gao, *ACS Appl. Mater. Interfaces*, 2023, **15**, 54266–54279.
202 L. Barbera, D. Franco, L. M. De Plano, G. Gattuso, S. P. P. Guglielmino, G. Lentini, N. Manganaro, N. Marino, S. Pappalardo, M. F. Parisi, F. Puntoriero, I. Pisagatti and A. Notti, *Org. Biomol. Chem.*, 2017, **15**, 3192–3195.
203 L. Xia, J. Tian, T. Yue, H. Cao, J. Chu, H. Cai and W. Zhang, *Adv. Healthcare Mater.*, 2021, **11**, e2102015.
204 T. Yue, L. Xia, J. Tian, B. Huang, C. Chen, H. Cao and W. Zhang, *Chem. Commun.*, 2022, **58**, 2991–2994.
205 X. Tian, S. Li, K. Velmurugan, Z. Bai, Q. Liu, K. Wang, M. Zuo and X.-Y. Hu, *Mater. Chem. Front.*, 2023, **7**, 2484–2492.
206 J. Wang, F. Li, Z. Xu, M. Zang, S. Liu, T. Li, J. Xu, H. Sun, S. Yu and J. Liu, *Chem. Eng. J.*, 2022, **444**, 136620.
207 G. Xu, P. Yang, Y. Zhang, L. Sun, X. Hu, W. Zhang, Y. Tu, Y. Tian, A. Li, X. Xie and X. Gu, *Chemosphere*, 2023, **341**, 140056.
208 Y. Huang, Y. Yang, B. Liang, S. Lu, X. Yuan, Z. Jia, J. Liu and Y. Liu, *ACS Appl. Mater. Interfaces*, 2023, **15**, 16448–16459.
209 J.-Y. Chen, W.-W. Haoyang, M. Zhang, G. Wu, Z.-T. Li and J.-L. Hou, *Faraday Discuss.*, 2018, **209**, 149–159.
210 Y. Chang, J. Y. Chen, J. Yang, T. Lin, L. Zeng, J. F. Xu, J. L. Hou and X. Zhang, *ACS Appl. Mater. Interfaces*, 2019, **11**, 38497–38502.
211 T. Duran, M. A. Karaselek, S. Kuccukturk, A. N. Kursunlu and M. Ozmen, *J. Biomol. Struct. Dyn.*, 2024, DOI: **10.1080/07391102.2024.2331629**.
212 J. Chen, H. Ni, Z. Meng, J. Wang, X. Huang, Y. Dong, C. Sun, Y. Zhang, L. Cui, J. Li, X. Jia, Q. Meng and C. Li, *Nat. Commun.*, 2019, **10**, 3546.
213 Y. Liu, X. Chen, J. Ding, L. Yu, D. Ma and J. Ding, *ACS Omega*, 2017, **2**, 5283–5288.
214 L. Shangguan, Q. Chen, B. Shi and F. Huang, *Chem. Commun.*, 2017, **53**, 9749–9752.
215 B. Li, Z. Meng, Q. Li, X. Huang, Z. Kang, H. Dong, J. Chen, J. Sun, Y. Dong, J. Li, X. Jia, J. L. Sessler, Q. Meng and C. Li, *Chem. Sci.*, 2017, **8**, 4458–4464.
216 Q. Hao, Y. Chen, Z. Huang, J. F. Xu, Z. Sun and X. Zhang, *ACS Appl. Mater. Interfaces*, 2018, **10**, 5365–5372.
217 J. Yang, D. Dai, L. Ma and Y.-W. Yang, *Chin. Chem. Lett.*, 2021, **32**, 729–734.
218 J. Chen, Y. Zhang, Y. Zhang, L. Zhao, L. Chen, Y. Chai, Z. Meng, X. Jia, Q. Meng and C. Li, *Chin. Chem. Lett.*, 2021, **32**, 3034–3038.

219 J. L. Zhang, X. W. Zhang, B. Yuan, H. Zhang, X. Z. Wang, H. Wang and H. W. Zhao, *ACS Omega*, 2024, **9**, 11829–11835.
220 N. J. Wheate, K. A. Dickson, R. R. Kim, A. Nematollahi, R. B. Macquart, V. Kayser, G. Yu, W. B. Church and D. J. Marsh, *J. Pharm. Sci.*, 2016, **105**, 3615–3625.
221 K. Yang, J. Wen, S. Chao, J. Liu, K. Yang, Y. Pei and Z. Pei, *Chem. Commun.*, 2018, **54**, 5911–5914.
222 L. Shao, Y. Pan, B. Hua, S. Xu, G. Yu, M. Wang, B. Liu and F. Huang, *Angew. Chem., Int. Ed.*, 2020, **59**, 11779–11783.
223 B. Lu, Y. Huang, H. Quan, J. Xia, J. Wang, Y. Ding, Y. Wang and Y. Yao, *ACS Macro Lett.*, 2023, **12**, 1365–1371.
224 K. Zhong, Z. Zhang, W. Cheng, G. Liu, X. Zhang, J. Zhang, S. Sun and B. Wang, *Adv. Healthcare Mater.*, 2024, **13**, e2302495.
225 X. Yang, B. Wu, J. Zhou, H. Lu, H. Zhang, F. Huang and H. Wang, *Nano Lett.*, 2022, **22**, 7588–7596.
226 B. Huang, P. Wang, Y. Ouyang, R. Pang, S. Liu, C. Hong, S. Ma, Y. Gao, J. Tian and W. Zhang, *ACS Appl. Mater. Interfaces*, 2020, **12**, 41038–41046.
227 X. Y. Hu, L. Gao, S. Mosel, M. Ehlers, E. Zellermann, H. Jiang, S. K. Knauer, L. Wang and C. Schmuck, *Small*, 2018, **14**, e1803952.
228 X. Liu, J. Liu, Q. Xu, W. Tao, X. Xie, C. Meng, Q. Zhou, Y. Zhang and Y. Ling, *J. Colloid Interface Sci.*, 2023, **648**, 994–1005.
229 Y. Chang, C. Hou, J. Ren, X. Xin, Y. Pei, Y. Lu, S. Cao and Z. Pei, *Chem. Commun.*, 2016, **52**, 9578–9581.
230 K. Yang, Y. Chang, J. Wen, Y. Lu, Y. Pei, S. Cao, F. Wang and Z. Pei, *Chem. Mater.*, 2016, **28**, 1990–1993.
231 Y. Lu, C. Hou, J. Ren, K. Yang, Y. Chang, Y. Pei, H. Dong and Z. Pei, *Int. J. Nanomed.*, 2019, **14**, 3525–3532.
232 S. Guo, T. Liang, Y. Song, M. Cheng, X.-Y. Hu, J.-J. Zhu and L. Wang, *Polym. Chem.*, 2017, **8**, 5718–5725.
233 X. Liu, J. Liu, C. Meng, P. Zhu, X. Liu, J. Qian, S. Ling, Y. Zhang and Y. Ling, *ACS Appl. Mater. Interfaces*, 2021, **13**, 53574–53585.
234 G. Yu, J. Zhou, J. Shen, G. Tang and F. Huang, *Chem. Sci.*, 2016, **7**, 4073–4078.
235 Z. Shen, N. Ma, C. Hou, X. Chen, S. Chao, Y. Pei and Z. Pei, *Colloids Surf., A*, 2022, **648**, 129262.
236 W. Zhou, S. Chen, Y. Ouyang, B. Huang, H. Zhang, W. Zhang and J. Tian, *Chem. Sci.*, 2023, **14**, 11481–11489.
237 D. Liu, J. Du, S. Qi, M. Li, J. Wang, M. Liu, X. Du, X. Wang, B. Ren, D. Wu and J. Shen, *Mater. Chem. Front.*, 2021, **5**, 1418–1427.
238 Q. Duan, Y. Cao, Y. Li, X. Hu, T. Xiao, C. Lin, Y. Pan and L. Wang, *J. Am. Chem. Soc.*, 2013, **135**, 10542–10549.
239 L. B. Meng, W. Zhang, D. Li, Y. Li, X. Y. Hu, L. Wang and G. Li, *Chem. Commun.*, 2015, **51**, 14381–14384.
240 L. Rui, Y. Xue, Y. Wang, Y. Gao and W. Zhang, *Chem. Commun.*, 2017, **53**, 3126–3129.
241 Q. Wang, P. Zhang, J. Xu, B. Xia, L. Tian, J. Chen, J. Li, F. Lu, Q. Shen, X. Lu, W. Huang and Q. Fan, *ACS Appl. Bio Mater.*, 2018, **1**, 70–78.
242 Z. Wang, Y. Wang, X. Sun, J. Zhou, X. Chen, J. Xi, L. Fan, J. Han and R. Guo, *Small*, 2022, **18**, e2200588.
243 Y. Wang, J. Du, Y. Wang, Q. Jin and J. Ji, *Chem. Commun.*, 2015, **51**, 2999–3002.
244 J. Chen, Y. Zhang, Z. Meng, L. Guo, X. Yuan, Y. Zhang, Y. Chai, J. L. Sessler, Q. Meng and C. Li, *Chem. Sci.*, 2020, **11**, 6275–6282.
245 G. Sun, M. Zuo, Z. Xu, K. Wang, L. Wang and X. Y. Hu, *ACS Appl. Bio Mater.*, 2022, **5**, 3320–3328.
246 Y. Chang, K. Yang, P. Wei, S. Huang, Y. Pei, W. Zhao and Z. Pei, *Angew. Chem., Int. Ed.*, 2014, **53**, 13126–13130.
247 Y. Liu, S. Jiang, W. Mao, P. Li, F. Zhou and D. Ma, *Chin. Chem. Lett.*, 2022, **33**, 209–212.
248 L. Liu, Q. Zhou, Q. He, W. Duan and Y. Huang, *Front. Chem.*, 2021, **9**, 661143.
249 X. Li, Q. Zhou, W. Duan, Y. Huang and L. Liu, *Supramol. Chem.*, 2024, **34**, 239–246.
250 X. Guan, F. Meng, H. Tan, X. Wang, J. Li, J. Wei, J. Ouyang and N. Na, *Chem. Sci.*, 2022, **13**, 8657–8666.
251 H. Liu, J. Yang, X. Yan, C. Li, M. Elsabahy, L. Chen, Y. W. Yang and H. Gao, *J. Mater. Chem. B*, 2021, **9**, 9594–9605.
252 Y. Bai, X. Li, M. Li, Q. Shang, J. Yang, L. Fan and W. Tian, *J. Mater. Chem. B*, 2022, **10**, 4952–4958.
253 X. Tian, M. Zuo, P. Niu, K. Velmurugan, K. Wang, Y. Zhao, L. Wang and X. Y. Hu, *ACS Appl. Mater. Interfaces*, 2021, **13**, 37466–37474.
254 S. Chao, Z. Shen, B. Li, Y. Pei and Z. Pei, *Chem. Commun.*, 2023, **59**, 3455–3458.
255 Y. Yin, P. Sun, H. Dong, Y. Chen, S. Chen and L. Wang, *Chin. Chem. Lett.*, 2023, **34**, 108594.
256 W. Shao, X. Liu, G. Sun, X. Y. Hu, J. J. Zhu and L. Wang, *Chem. Commun.*, 2018, **54**, 9462–9465.
257 G. Sun, Z. He, M. Hao, Z. Xu, X. Y. Hu, J. J. Zhu and L. Wang, *Chem. Commun.*, 2019, **55**, 10892–10895.
258 S. Chao, X. Lv, N. Ma, Z. Shen, F. Zhang, Y. Pei and Z. Pei, *Chem. Commun.*, 2020, **56**, 8861–8864.
259 Y. Bai, X. Li, S. Song, J. Yang, X. Liu and Z. Chen, *Nano Res.*, 2023, **16**, 9921–9929.
260 Z. Shen, N. Ma, F. Wang, J. Ren, C. Hou, S. Chao, Y. Pei and Z. Pei, *Chin. Chem. Lett.*, 2022, **33**, 4563–4566.
261 G. Yu, W. Yu, Z. Mao, C. Gao and F. Huang, *Small*, 2015, **11**, 919–925.
262 J. Chen, Y. Zhang, L. Zhao, Y. Zhang, L. Chen, M. Ma, X. Du, Z. Meng, C. Li and Q. Meng, *ACS Appl. Mater. Interfaces*, 2021, **13**, 53564–53573.
263 Y. Cao, X. Zou, S. Xiong, Y. Li, Y. Shen, X. Hu and L. Wang, *Chin. J. Chem.*, 2015, **33**, 329–334.
264 Y. Cao, Y. Li, X.-Y. Hu, X. Zou, S. Xiong, C. Lin and L. Wang, *Chem. Mater.*, 2015, **27**, 1110–1119.
265 X. Wu, Y. Li, C. Lin, X. Y. Hu and L. Wang, *Chem. Commun.*, 2015, **51**, 6832–6835.
266 X. Liu, K. Jia, Y. Wang, W. Shao, C. Yao, L. Peng, D. Zhang, X. Y. Hu and L. Wang, *ACS Appl. Mater. Interfaces*, 2017, **9**, 4843–4850.
267 Y. Bai, C. Liu, J. Yang, C. Liu, Q. Shang and W. Tian, *Colloids Surf., B*, 2022, **217**, 112606.
268 J. Zhou, H. Xu, Z. Tong, Y. Yang and G. Jiang, *Mater. Sci. Eng., C*, 2018, **89**, 237–244.

269 D. Xia, L. Shangguan, M. Xue and B. Shi, *New J. Chem.*, 2016, **40**, 9890–9894.
270 X. Y. Hu, K. Jia, Y. Cao, Y. Li, S. Qin, F. Zhou, C. Lin, D. Zhang and L. Wang, *Chem. – Eur. J.*, 2015, **21**, 1208–1220.
271 Z. Tong, J. Zhou, R. Huang, J. Zhou, R. Zhang, W. Zhuo and G. Jiang, *J. Polym. Sci., Part A: Polym. Chem.*, 2017, **55**, 2477–2482.
272 Y. Ding, C. Wang, Y. Ma, L. Zhu, B. Lu, Y. Wang, J. Wang, T. Chen, C. M. Dong and Y. Yao, *Acta Biomater.*, 2022, **143**, 381–391.
273 Y. Ding, W. Yu, R. Shen, X. Zheng, H. Zheng, Y. Yao, Y. Zhang, C. Du and H. Yi, *Adv. Healthcare Mater.*, 2024, **13**, e2303308.
274 J. Zhong, Q. Tang, Y. Ju, Y. Lin, X. Bai, J. Zhou, H. Luo, Z. Lei and Z. Tong, *J. Biomater. Sci., Polym. Ed.*, 2019, **30**, 202–214.
275 J. Zhou, J. Gu, X. Sun, Q. Ye, X. Wu, J. Xi, J. Han and Y. Liu, *Adv. Sci.*, 2024, **11**, e2308493.
276 X. Chen, Z. Wang, X. Sun, Y. Han, Y. Huang, J. Xi, X. Bian, J. Han and R. Guo, *Chem. Eng. J.*, 2021, **403**, 126423.
277 X. Min, F. Yi, X.-L. Han, M. Li, Q. Gao, X. Liang, Z. Chen, Y. Sun and Y. Liu, *Chem. Eng. J.*, 2022, **432**, 134327.
278 Y. Zhang, Y. Wang, T. Chen, Y. Han, C. Yan, J. Wang, B. Lu, L. Ma, Y. Ding and Y. Yao, *Chem. Commun.*, 2023, **59**, 8266–8269.
279 H. Quan, Y. Huang, J. Xia, J. Yang, B. Lu, P. Liu and Y. Yao, *ChemBioChem*, 2023, **24**, e202300461.
280 Z. Shen, S. Chao, B. Li, C. Hu, Y. Pei and Z. Pei, *Colloids Surf., A*, 2024, **700**, 134781.
281 Y. Wang, Y. Wen, Y. Qu, Z. Pei and Y. Pei, *J. Colloid Interface Sci.*, 2022, **615**, 386–394.
282 X. Li, J. Han, J. Qin, M. Sun, J. Wu, L. Lei, J. Li, L. Fang and Y. W. Yang, *Chem. Commun.*, 2019, **55**, 14099–14102.
283 J. Li, B. Hu, Z. Chen, J. Li, W. Jin, Y. Wang, Y. Wan, Y. Lv, Y. Pei, H. Liu and Z. Pei, *Chem. Sci.*, 2024, **15**, 765–777.
284 E. C. S. Santos, T. C. Dos Santos, T. S. Fernandes, F. L. Jorge, V. Nascimento, V. G. C. Madriaga, P. S. Cordeiro, N. R. Checca, N. M. Da Costa, L. F. R. Pinto and C. M. Ronconi, *J. Mater. Chem. B*, 2020, **8**, 703–714.
285 X. Huang, S. Wu, X. Ke, X. Li and X. Du, *ACS Appl. Mater. Interfaces*, 2017, **9**, 19638–19645.
286 X. Huang and X. Du, *ACS Appl. Mater. Interfaces*, 2014, **6**, 20430–20436.
287 C. Ding, Y. Liu, T. Wang and J. Fu, *J. Mater. Chem. B*, 2016, **4**, 2819–2827.
288 Y. Yao, Y. Wang, R. Zhao, L. Shao, R. Tang and F. Huang, *J. Mater. Chem. B*, 2016, **4**, 2691–2696.
289 C. Ding, L. Tong and J. Fu, *Chem. – Eur. J.*, 2017, **23**, 15041–15045.
290 J. Ahn, H. Jin, J. Park, B. Lee, M. Ok, J. H. Lee, J. Bae and J. H. Jung, *Part. Part. Syst. Charact.*, 2020, **37**, 2000136.
291 J. Yang, D. Dai, X. Lou, L. Ma, B. Wang and Y. W. Yang, *Theranostics*, 2020, **10**, 615–629.
292 X. Wang, L. L. Tan, X. Li, N. Song, Z. Li, J. N. Hu, Y. M. Cheng, Y. Wang and Y. W. Yang, *Chem. Commun.*, 2016, **52**, 13775–13778.
293 Y. Qu, W. Jin, Y. Wan, Z. Pei and Y. Pei, *Chin. Chem. Lett.*, 2024, **35**, 108493.
294 K. Yang, K. Yang, S. Chao, J. Wen, Y. Pei and Z. Pei, *Chem. Commun.*, 2018, **54**, 9817–9820.
295 C. Hu, Y. Yu, S. Chao, H. Zhu, Y. Pei, L. Chen and Z. Pei, *Molecules*, 2021, **26**, 3878.
296 L. L. Tan, H. Li, Y. C. Qiu, D. X. Chen, X. Wang, R. Y. Pan, Y. Wang, S. X. Zhang, B. Wang and Y. W. Yang, *Chem. Sci.*, 2015, **6**, 1640–1644.
297 L. L. Tan, H. Li, Y. Zhou, Y. Zhang, X. Feng, B. Wang and Y. W. Yang, *Small*, 2015, **11**, 3807–3813.
298 L. L. Tan, N. Song, S. X. Zhang, H. Li, B. Wang and Y. W. Yang, *J. Mater. Chem. B*, 2016, **4**, 135–140.
299 M. X. Wu, H. J. Yan, J. Gao, Y. Cheng, J. Yang, J. R. Wu, B. J. Gong, H. Y. Zhang and Y. W. Yang, *ACS Appl. Mater. Interfaces*, 2018, **10**, 34655–34663.
300 M. X. Wu, J. Gao, F. Wang, J. Yang, N. Song, X. Jin, P. Mi, J. Tian, J. Luo, F. Liang and Y. W. Yang, *Small*, 2018, **14**, e1704440.
301 N. Song, Z. Zhang, P. Liu, D. Dai, C. Chen, Y. Li, L. Wang, T. Han, Y. W. Yang, D. Wang and B. Z. Tang, *Adv. Funct. Mater.*, 2021, **31**, 2009924.
302 J. Jiang, Z. Su, Q. He, W. Duan, Y. Huang and L. Liu, *Chem. – Eur. J.*, 2024, **30**, e202400007.
303 Q. L. Li, Y. Sun, L. Ren, X. Wang, C. Wang, L. Li, Y. W. Yang, X. Yu and J. Yu, *ACS Appl. Mater. Interfaces*, 2018, **10**, 29314–29324.
304 M. Cen, Y. Ding, J. Wang, X. Yuan, B. Lu, Y. Wang and Y. Yao, *ACS Macro Lett.*, 2020, **9**, 1558–1562.
305 C. P. Li, Y. X. Lu, C. T. Zi, Y. T. Zhao, H. Zhao and Y. P. Zhang, *Int. J. Mol. Sci.*, 2020, **21**, 4979.
306 T. Fernandes, E. Santos, V. Madriaga, I. Bessa, V. Nascimento, F. Garcia and C. Ronconi, *J. Braz. Chem. Soc*, 2019, **30**, 2452–2463.
307 X. Wu, J. Yang, J. Xing, Y. Lyu, R. Zou, X. Wang, J. Yao, D. Zhang, D. Qi, G. Shao, A. Wu and J. Li, *J. Mater. Chem. B*, 2023, **11**, 4855–4864.
308 P. V. Skvortsova, D. A. Faizullin, E. A. Ermakova, D. N. Shurpik, N. E. Gogoleva, Y. V. Gogolev, S. A. Ziganshina, I. I. Stoikov, Y. F. Zuev and B. I. Khairutdinov, *J. Mol. Liq.*, 2020, **319**, 114178.
309 L. S. Yakimova, A. R. Nugmanova, O. A. Mostovaya, A. A. Vavilova, D. N. Shurpik, T. A. Mukhametzyanov and I. I. Stoikov, *Nanomaterials*, 2020, **10**, 777.
310 X. Y. Hu, M. Ehlers, T. Wang, E. Zellermann, S. Mosel, H. Jiang, J. E. Ostwaldt, S. K. Knauer, L. Wang and C. Schmuck, *Chem. – Eur. J.*, 2018, **24**, 9754–9759.
311 K. Wang, M. Zuo, T. Zhang, H. Yue and X.-Y. Hu, *Chin. Chem. Lett.*, 2023, **34**, 107848.
312 Q. Li, D. Ma, Y.-Y. Liu, H. Wang, W. Zhou, D.-W. Zhang and Z.-T. Li, *Org. Chem. Front.*, 2024, **11**, 3019–3025.
313 A. L. Barran-Berdon, M. Martinez-Negro, L. Garcia-Rio, O. Domenech, C. Tros de Ilarduya, E. Aicart and E. Junquera, *J. Mater. Chem. B*, 2017, **5**, 3122–3131.
314 S. Guo, Q. Huang, J. Wei, S. Wang, Y. Wang, L. Wang and R. Wang, *Nano Today*, 2022, **43**, 101396.

315 V. Sultanaev, L. Yakimova, A. Nazarova, I. Sedov, O. Mostovaya, T. Mukhametzyanov, D. Davletshin, D. Takuntseva, E. Gilyazova, E. Bulatov and I. Stoikov, *J. Mater. Chem. B*, 2024, **12**, 3103–3114.
316 G. Li, W. Gong, L. Yang, M. Cheng, H. Yan, J. Quan, F. Zhang, Z. Lu and H. Li, *Bioconjugate Chem.*, 2022, **33**, 2237–2244.
317 H. Yan, J. Ma, F. Zhu, J. Quan, M. K. Dhinakaran and H. Li, *Chem. - Asian J.*, 2020, **15**, 1025–1029.
318 H. Zhu, J. Liu, B. Shi, H. Wang, Z. Mao, T. Shan and F. Huang, *Mater. Chem. Front.*, 2018, **2**, 1475–1480.
319 D. G. Liz, A. M. Manfredi, M. Medeiros, R. Montecinos, B. Gómez-González, L. Garcia-Rio and F. Nome, *Chem. Commun.*, 2016, **52**, 3167–3170.
320 E. H. Wanderlind, D. G. Liz, A. P. Gerola, R. F. Affeldt, V. Nascimento, L. C. Bretanha, R. Montecinos, L. Garcia-Rio, H. D. Fiedler and F. Nome, *ACS Catal.*, 2018, **8**, 3343–3347.
321 N. Cheng, Y. Chen, X. Wu and Y. Liu, *Chem. Commun.*, 2018, **54**, 6284–6287.
322 C. Park, E. S. Jeong, K. J. Lee, H. R. Moon and K. T. Kim, *Chem. - Asian J.*, 2014, **9**, 2654.
323 M. Zeng, K. Chen, J. Tan, J. Zhang and Y. Wei, *Front. Chem*, 2018, **6**, DOI: **10.3389/fchem.2018.00457**.
324 Y. Sun, F. Guo, T. Zuo, J. Hua and G. Diao, *Nat. Commun.*, 2016, **7**, 12042.
325 Z. Ye, Z. J. Yan, C. Zhang, J. L. Hou, S. Yue and L. Xiao, *Nano Lett.*, 2021, **21**, 10494–10500.
326 Z. Jia, R. Tang, X. Yuan, H. Zhu, J. Guo, Y. Chen, Y. Yang, B. Liang, S. Lu, D. Cao and J. Liu, *Small*, 2023, **19**, 2302176.
327 X. Yuan, R. Tang, Z. Jia, Y. Chen, J. Liu and Y. Liu, *Chem. Eng. J.*, 2023, **464**, 142679.
328 M. Zuo, W. Qian, Z. Xu, W. Shao, X. Y. Hu, D. Zhang, J. Jiang, X. Sun and L. Wang, *Small*, 2018, **14**, e1801942.
329 Q. Huan, T. Lin, Y.-H. Fu and J.-L. Hou, *Chin. Chem. Lett.*, 2024, **35**, 108566.
330 Y.-H. Fu, Y.-F. Hu, T. Lin, G.-W. Zhuang, Y.-L. Wang, W.-X. Chen, Z.-T. Li and J.-L. Hou, *Nat. Chem.*, 2024, **16**, 1418–1426.
331 Q. Xiao, D. Guan, Y.-H. Fu, T. Fan, L. Zhang, Z.-T. Li, Y. Zhang, Y. Wang and J.-L. Hou, *J. Am. Chem. Soc.*, 2024, **146**, 22869–22873.